LINEAR STABILITY OF ELECTRON-FLOW HYDRODYNAMICS IN UNGATED SEMICONDUCTORS

A Dissertation

Submitted to the Graduate School
of the University of Notre Dame
in Partial Fulfillment of the Requirements
for the Degree of

Doctor of Philosophy

by

Williams R. Calderón Muñoz

Mihir Sen, Director

Graduate Program in Aerospace and Mechanical Engineering
Notre Dame, Indiana
April 2009

LINEAR STABILITY OF ELECTRON-FLOW HYDRODYNAMICS IN UNGATED SEMICONDUCTORS

Abstract

by

Williams R. Calderón Muñoz

Semiconductors play an important role in modern electronic technology. They are present in most sensing and transduction applications, satisfying requirements such as compactness, tunability and portability. It is known that any fluctuation in electron density inside a semiconductor produces acceleration or deceleration of the electrons that generates electromagnetic radiation. For this reason, in recent years this has been proposed as a source of radiation for what is called the 'THz gap' in the electromagnetic spectrum. Radiation sources at this frequency range can provide an improvement over current techniques in bioimaging and sensing due to advantages such as non-ionizability and easy absorption by water. An understanding of how electron-flow instabilities occur and the parameters that affect them is needed to determine if semiconductors can be used as THz radiation sources.

The main motivation of this work is to analyze from a hydrodynamic perspective the conditions under which instabilities occur in electron flow in ungated semiconductors. A continuum description of the electron flow is presented. The governing equations include Gauss' law, the mass, momentum and energy conservation equations for electrons and a constitutive equation for energy flux in

the lattice. Linear stability analysis was used to study the instabilities of the steady-state solution of this system of equations.

Three configurations were analyzed. The first is one-dimensional, with a mathematical model that is thermally uncoupled in that it does not consider electron-lattice interactions, and it is assumed that the lattice and electron temperatures are not affected by the electron flow. The second configuration is two-dimensional, but still thermally uncoupled. The third is a thermally-coupled one-dimensional analysis in which electron-lattice interactions exist, and the lattice and electron temperatures are dependent variables. The driving force in all cases is due to an imposed external electric field.

Stability analysis in the thermally-uncoupled configurations showed that the instability spectrum becomes denser when the configuration goes from one to two dimensions. The uncoupled system becomes more unstable when the applied voltage increases. Changes in the material parameters such as doping density and length of the semiconductor can also affect stability. In general, the thermally-coupled configuration does not become unstable with higher applied voltages. However, it does if electronic heat conduction and energy loss from electrons to the lattice through scattering are neglected. Therefore, control of these phenomena is crucial for the generation of instabilities in semiconductors. Applied voltage and room temperature can determine suitable operating conditions for THz electromagnetic sources based on semiconductors.

To my Family

CONTENTS

FIGURES

TABLES

ACKNOWLEDGMENTS

I would like to preface this work with the most interesting phrase I have read lately.

'The reasonable man adapts himself to the world; the unreasonable one persists in trying to adapt the world to himself. Therefore all progress depends on the unreasonable man' G. Bernard Shaw.

This phrase describes one of the main features that every researcher should have, persistence. Being persistent is likely one of the hardest things to accomplish for most of the people. This is not something that anybody can learn in a class, but with initiative, attitude and curiosity the persistence reveals by itself.

I would like to acknowledge my family for its support throughout this process, which began a long time ago in a very small city called Los Andes in the central part of Chile.

I would also like to acknowledge The University of Notre Dame for the great opportunity of being a graduate student and to my advisor, Dr. Mihir Sen, and my co-advisor, Dr. Debdeep Jena for their advices and suggestions, with whom this work would no have been possible.

Finally, I would like to thank the Universidad de Chile and CONICYT-Chile for their support, which allowed me to pursue my Ph.D. studies and work.

SYMBOLS

e	electron charge
k_B	Boltzmann's constant
$E, \vec{\mathcal{E}}$	electric field
$\mathcal{E}_j$	j-component of electric field
$\vec{B}$	magnetic field
B_k	k-component of magnetic field
F	external force used in Appendix A
F_i	i-component of external force
L	length of semiconductor
H	height of semiconductor
R	aspect ratio of semiconductor $(= H/L)$
$\vec{k}$	wavenumber vector
$k, k_x, k_{x,j}$	x-component of wavenumber
$k_y, k_{y,m}$	y-component of wavenumber
k_{xi}	imaginary part of k_x
k_{yi}	imaginary part of k_y
m_e	electron effective mass
n	charge density
E	electron energy used in Appendix A and B

E_n	electron energy density ($= n\langle E \rangle$)
$\vec{p}$	electron momentum
p_j	j-component of electron momentum
p_n	electron momentum density
p_{nj}	j-component of electron momentum density
k_d	degree of freedom
n_0	charge density at $x = 0$ for all y
N_D	doping concentration
m, p	natural number
m^c	critical mode
a	parameter used in Chapter 3 ($= -\alpha/(2\gamma^2)\,(2\gamma\omega/\sqrt{\alpha} + 1)$)
b	parameter used in Chapter 3 ($= \alpha/(2\gamma^2)\sqrt{4\gamma^2 - 1}$)
b'	parameter used in Chapter 3 ($= \alpha/(2\gamma^2)\sqrt{1 - 4\gamma^2}$)
y_m	real number ($= \pm(\pi/2)(4m \pm 1)$)
r	real number ($= \sqrt{\alpha}/(2\gamma)(-1 \pm \sqrt{1 - 4\gamma^2}$)
t	time
$\vec{v}$	electron velocity vector
u	longitudinal electron velocity
v	transversal electron velocity
v_i	i-component of velocity
v_i^d	i-component of drift velocity
v_i^{th}	i-component of thermal velocity
v_p	phase velocity
v_g	group velocity
V	voltage

V_0	voltage at $x = 0$ for all y
W	Lambert W-function
x	longitudinal coordinate
x_j	j-component of position
y	transversal coordinate
z	perpendicular coordinate to xy-plane
z_*	complex number
K_{r_k}	parameter used in Chapter 2
K_c	parameter used in Chapter 2
r_k	parameter used in Chapter 2
g	parameter used in Chapter 2
C_{LO}	heat capacity for longitudinal optical phonons
C_A	heat capacity for acoustic phonons
C_L	heat capacity for the lattice
k_e	electron thermal conductivity
k_A	acoustic phonon thermal conductivity
k_L	lattice thermal conductivity
T_e	electron temperature
T_{LO}	longitudinal optical phonon temperature
T_A	acoustic phonon temperature
T_L	lattice temperature
T_1, T_2, T_3	temperature boundary conditions defined in Chapter 5
T_{room}	room temperature
q_i	i-component of electron heat flux
q_{Ai}	i-component of acoustic phonon heat flux

q_e	electron temperature gradient
q_L	lattice temperature gradient
E_0	electric field at $x = 0$
u_0	electron velocity at $x = 0$
q_{e0}	electron temperature gradient at $x = 0$
q_{L0}	lattice temperature gradient at $x = 0$
f	distribution function of particles defined in the infinitesimal volume $dx_1dx_2dx_3dv_1dv_2dv_3$ at time t
dx_i	infinitesimal variation of position in x_i-direction, $i = 1, 2, 3$
dv_i	infinitesimal variation of velocity in x_i-direction, $i = 1, 2, 3$
dV	fixed differential control volume $(= dx_1dx_2dx_3)$
M	mass $(= nm_edV)$
$\mathbf{J}, \mathbf{J}_s$	square matrix defined in Chapter 5
$\mathbf{P}, \mathbf{P}_s$	square matrix defined in Chapter 5
$\mathbf{Y}, \mathbf{Y}_s$	vector defined in Chapter 5
$\mathbf{A}$	square matrix defined in Chapter 5
a_{ij}	coefficient (i, j) of matrix A
A, B, C, D	coefficients used in Chapters 3 and 4
A_f, B_f, C_f, D_f, g_f	functions used in Chapter 3
A_i	coefficients used in Chapter 5 with $i = 1$ and 2
B_i	coefficients used in Chapter 5 with $i = 1, 2$ and 3
C_i	coefficients used in Chapter 5 with $i = 1, 2, 3, 4, 5, 6, 7$ and 8
D_i	coefficients used in Chapter 5 with $i = 1, 2, 3, 4, 5, 6$ and 7
E_i	coefficients used in Chapter 5 with $i = 1, 2, 3, 4$ and 5
Z_i	coefficients used in Chapter 5 with $i = 1, 2, 3$ and 4

Greek symbols

α	non-dimensional parameter $(= eN_D L^2/V_0\epsilon_s)$
γ	non-dimensional parameter $(= \sqrt{\tau_p^2 e^2 N_D/\epsilon_s m_e})$
γ_{pn}	non-dimensional parameter $(= \sqrt{m_e \mu_{no}^2 N_D/\epsilon_s})$
γ_E	non-dimensional parameter $(= \sqrt{\tau_E^2 e^2 N_D/m_e\epsilon_s})$
β	non-dimensional parameter $(= k_B T_{room}/eV_0)$
σ	non-dimensional parameter $(= (k_e/N_D k_B L^2)\sqrt{m_e L^2/eV_0})$
θ_1	non-dimensional parameter $(= (k_L/L^2 C_L)\sqrt{m_e L^2/eV_0})$
θ_2	non-dimensional parameter $(= (3N_D k_B/2\tau_E C_L)\sqrt{m_e L^2/eV_0})$
ϵ_s	permittivity
τ_p	momentum relaxation time
τ_{e-LO}	energy relaxation time for electron-optical phonon interactions
τ_{LO-A}	energy relaxation time for optical-acoustic phonons interactions
τ_E	energy relaxation time
ω	temporal eigenmode $(= \omega_r + i\omega_i)$
ω_r	temporal eigenmode real component
ω_i	temporal eigenmode imaginary component
ω_1, ω_2	temporal eigemodes defined in Chapter 5
ω_p	plasma frequency
μ	electron mobility
μ_{no}	electron low field mobility

μ_{cr}	critical electron mobility defined in Chapter 3
ϕ_i	coefficients used in Chapter 5 with $i = 1, 2$ and 3
η_i	coefficients used in Chapter 5 with $i = 1, 2$ and 3
δ_{ij}	Kronecker delta
ε_{ikj}	permutation symbol

Other symbols

$'$	perturbation
*	dimensional quantity
$\overline{(\quad)}$	steady state
$\widehat{(\quad)}$	amplitude
$\widetilde{(\quad)}$	one-variable function
$\langle(\quad)\rangle$	average in the velocity space

CHAPTER 1

INTRODUCTION

1.1 Motivation and objectives

Thermal management and transduction applications of solid state devices have become a key issue in a world where technology advances play an important role in the economy. The requirement of high-speed devices combined with a strong scale-down in the size of the devices make thermal dissipation a complex issue in their performance. Transduction devices are required to detect or emit desired signal frequencies in a wide range of subsystems and components. Several examples can be cited here to illustrate the range in which these issues or applications are involved: sensing of chemical and biological systems, imaging, and the telecommunications and semiconductor industry. Most of them have in common the fact that they involve highly complex process which makes difficult their modeling. An important range of frequencies in the transduction applications of solid state devices is terahertz. Since it is dificult to produce, it is called terahertz gap. Many interesting applications can be useful in this range that makes it a cutting edge research topic in semiconductor devices. For instance, most of the chemical and biological reactions are characterized in the range of THz frequencies. Therefore, to analyze with more accuracy these kind of reactions, every change in the whole process needs to be captured. Due to this, the charged-particle interactions in

semiconductors and its possible applications need to be understood. Therefore, modeling of electron transport is very important for this purpose. Among the physical models describing the transport of electrons and phonons is the classical hydrodynamic model. It has its origin in the Boltzmann Transport Equation, which governs the evolution of a particle distribution function in space and time. Essentially, the Boltzmann Transport Equation is a particle number balance equation. Considering the electrons as the particles of interest, the moments of this equation represent the hydrodynamic model of electron transport, which enforces the conservation of charge, momentum, and energy instead of detailed knowledge of the electron distribution function. Due to its similarity with compressible flow in fluids, hydrodynamic models provide a wide supply of theoretical and computational tools that may be applied to electron flow. Taking into account that the hydrodynamic model itself is a nonlinear set of equations that is difficult to treat, and the fact that it is also very important to know about the dynamics behind of this set of equations, a linearized analytical approach emerges as an important tool to understand this system. Considering all these ideas, the research work proposed here intends to study the hydrodynamic stability of the transport of electrons in ungated semiconductors by using the hydrodynamic model and constitutive equations to capture the thermal interactions which are present in this process. More technically, the objective is to do the linear stability analysis of the hydrodynamic model of the electron flow in the transport of electrons through the semiconductor. The main purpose is to determine, either analytically or numerically, the eigenfunctions and eigenvalues of the linearized dynamical system which determine the stability of the system.

1.2 Review of hydrodynamic stability analysis

Originally, hydrodynamic stability is concerned with the study of the transition from laminar to turbulent motions of fluids or to determine the stability and instability of the fluids. In general terms, stability can be defined as the quality of being immune to small disturbances or perturbations. Stability in mechanical or electrical systems with only a few degrees of freedom can be studied by using mathematical tools. However, in the case of continuous media in which the basic equations take the form of nonlinear partial differential equations, the number of degrees of freedom is infinite and to determine their stability becomes more difficult. In spite of more complications, linearization approximations and extensions of the theory developed with discrete systems are used to understand such systems. The major contributions to the study of hydrodynamic stability can be found in the theoretical papers of Helmholtz (1821-1894), combined with efforts of Reynolds (1842-1912), Kelvin (1824-1907) and Rayleigh (1842-1919), among others. This last is considered the founder of the theory of hydrodynamical stability, who between 1878 and 1917 published a great number of papers on this subject. Around 1907 there were the first intuitions about the existence of a critical Reynolds number to explain the problem of turbulence. In addition to the works of Prandtl (1875-1953), the first confirmation of linear theory by experiments was done by Taylor (1886-1975) in his work on vortices between concentric rotating cylinders. Lin (1916-) improved the mathematical procedures and laid the foundations for a general expansion of stability analysis. At that time the stability of Poiseuille flows had become a particularly controversial issue and Lin put it in order by his newer and more general analysis. The results of Lin were found to be correct by using a digital computer. Experimental results of Schubauer and

Skramstad [1] helped clarify that the critical Reynolds number marked only the threshold of 'sinuous' motion and not that of turbulence. At that point, experimental results and theory agreed as far as eigenfunctions and eigenvalues were concerned. Around 1955, three main categories of manifestations of instability in a continuous medium were formulated: first, oscillations in parallel flows, channel flows and boundary layers; second, boundary layers along curved walls and third, Bénard cells and convective instabilities, cases where the mean flow is zero. Basic flow is defined by the set of fields that need to be specified at each point and time, for instance velocity and temperature. From the physical point of view, we want to know if the basic flow can be observed or not. If a small disturbance is introduced, this may either die away, persists as a disturbance of similar magnitude or grows so much that the basic flow becomes a different flow pattern. Stability problems can be found in many fields such as mechanics, electronics, aeronautical engineering, economics, etc. Lately, stability analysis has become very important to understand some phenomena in magnetohydrodynamics and plasma physics [2–4].

1.3 Review of electron flow in semiconductors

The main focus of current and previous work has been the study of electron transport to improve the electronic performance and applications of semiconductor materials. Due to the complexity of the involved processes, there are several ways to investigate the phenomena.

In recent years, there has been considerable interest in the study of heat generation and transport in semiconductors such as GaAs, Si and electronic devices as metal semiconductor field effect transistors and metal-oxide semiconductor field

effect transistors [5–9], due to the non-equilibrium nature of hot electrons, optical phonons, and acoustic phonons [10–12]. Hydrodynamic models have played an important role as a tool to simulate electron transport in semiconductor devices [13–23]. At the same time, other simulation techniques such as the Monte Carlo method, the Finite Volume method applied to the Boltzmann Transport Equation, and Molecular Dynamics have been used to model phonon propagation and to determine thermal conductivity in films [24–26]. On the other hand, sub-micrometer scale temperature measurement techniques such as Atomic Force Microscopy and Scanning Thermal Microscopy have given relevant experimental data [27]. A nonlocal formulation has been developed to study problems where the phonon mean free path is comparable to the domain dimensions [28, 29]. Simulations of electron transport in two-dimensional metal-semiconductor field effect transistor devices show how dependent it is on thermal effects [30–32]. In addition to this, different approaches such as hole dynamics in p-SiGe quantum-cascade structures using Monte Carlo simulations [33], and responses in field-effect transistors to perturbations such as external magnetic field and so on, have been studied [34–36].

Thermal transport is a key issue in electronic performance. The mechanism of thermal transport in microscale solid thin film of semiconductors is as follows. Heat conduction in crystalline materials occurs due to lattice vibrations, which are called phonons. These are responsible for the heat transport. Phonons are produced primarily by collisions between electrons and atoms in the lattice structure of the semiconductor. They travel through space and engage in interactions with one another, which is called phonon-phonon interaction, and with impurities, defects, electrons and geometric boundaries. As a definition, the average distance

that a phonon travels before it interacts with another phonon is its mean free path. The drift or ballistic movement of phonons results in a deviation from thermodynamic equilibrium. Otherwise, phonon-phonon scattering helps restore thermodynamic equilibrium. Regarding scattering events, there are two situations which are necessary to emphasize. First, if the characteristic size of a solid material is much larger than the mean free path of the phonons in the semiconductor, the number of scattering events is large and local thermodynamic equilibrium is restored. Second, if the characteristic dimension of the medium is significantly smaller than the mean free path of the phonons, the number of scattering events is too small and thermodynamic equilibrium may not exist in the material [10, 23, 37–40].

The thermal transport in low-dimensional nanostructured materials [41], such as nanowires and so on, is different than it is in bulk materials [42]. Phonon modes and thermal conductivities in SiGe nanocrystals and monocrystalline silicon films have been studied as well [43, 44]. Monte Carlo simulations in single crystalline Si nanowires shows a dependence between phonon transport and Umklapp (U) scattering probability [45]. Theoretical predictions for the thermal conductivity and its temperature dependence have been investigated in Si and Ge nanowires and metal non-metal interfaces [46, 47]. In addition, detailed reviews reporting current important and relevant techniques in nanoscale thermal transport have been published [48, 49].

Existence of solution and well-posedness analysis for the hydrodynamic model for semiconductors has been analyzed for specific boundary conditions [50–54]. In parallel with this, theoretical studies using hydrodynamic models have showed similarities between electron transport and fluid flow, for instance in topics such as electron vortices [55], steady shock waves and subsonic flow [51, 53, 56, 57],

and turbulent flow [58].

The nature of charged-particle interactions is extremely important in solid state devices. Electric and magnetic properties of ionized gas are governed by the behavior of electrons in the gas [59]. A non-uniform distribution of charged particles under external fields can show a wide variety of oscillations. As a result, the increasing necessity of compact, tunable and small solid-state THz sources for the detection of chemical reactions, characterization of chemical and biological systems, applications in imaging, radio astronomy and industry, makes the study of charged-particle interactions in semiconductors a more important issue. This fact has motivated a number of theoretical and experimental work. A number of solid-state devices are being currently explored for filling the so-called 'THz-gap' - both narrow and broadband electromagnetic wave emitters spanning the frequency range from 300 GHz to 3 THz (corresponding to wavelengths from 100 μm to 1 mm). Though non-solid state sources such as free-electron lasers [60] and relativistic electron accelerators [61] exist for this purpose, compact solid-state sources offer the unique advantage of portability, and the possibility of coupling with Integrated Circuits. Optical devices such as quantum-cascade lasers are approaching this gap from the high-frequency regime [62]. However, the operation of these lasers is limited to cryogenic temperatures. On the other hand, high-speed electronic transistors are rapidly advancing to fill the THz gap from the low-frequency end [63]. The switching speeds of ultrascaled transistors, however, are limited by transit-time effects and parasitics. Switching speed in such transistors is approaching the 1 THz mark, indicating that a room-temperature all-electronic THz emitter is possible in the near future.

In 1993, Dyakonov and Shur [64] proposed that the current flow in a two-

dimensional electron gas channel in traditional high-electron mobility transistors can become inherently unstable under certain bias conditions [64–67]. This instability stems from the fluid-like flow of electrons in the two-dimensional electron gas, which can result in the formation of plasma waves, much like the formation of waves on the surface of shallow water. Using a gradual channel approximation for the relationship between the gate potential and the local channel charge, they showed that plasma waves could be generated. Spatial and time dependent instabilities in one-dimensional electron flow have been described analytically by using the hydrodynamic model [68]. Microscopically-bounded plasma due to current-driven plasma instability has been report in lower-dimensional solid-state systems [69]. A close analogy of this hydrodynamic model with shallow-water equations was obtained [70, 71]. Subsequently, Dyakonov and Shur [72, 73] have also shown that current instabilities and plasma waves can be generated in an ungated two-dimensional electron layer. A hydrodynamic model applied to a two-dimensional electron plasma in a field effect transistor showed a nonlinear dynamic response and how the boundary conditions are determinant in the nonlinear effects [74]. Transit-time effects in plasma instability are related to the electron drift across the high field region in high electron mobility transistors [75]. Plasma oscillations in both gated two-dimensional electron layers and stripes in high electron mobility transistors have been recently analyzed [76, 77]. Instabilities in multilayered semiconductor structures have been studied numerically and theorically [78]. Drift wave instabilities in semiconductor electron-hole plasma have been reported [79]. The proposal for the all-electronic plasma-wave THz emitter has inspired a number of experimental efforts. Experimental technique using two-color diode laser and its limitations have been described [80]. Sub-THz and THz radiation in

silicon field effect transistors and deep submicron gate length high electron mobility transistors due to plasma waves have recently been claimed to be observed [81, 82]. Theoretical and experimental studies have showed nonresonant and resonant detection of THz radiation in both Si metal-oxide semiconductor field effect transistors and gated two-dimensional structures such as GaAs high electron mobility transistors [83, 84]. Under special conditions, a nanometer field effect transistor made of InGaAs/InAlAs can also produce THz emission [85, 86]. New techniques and algorithms to determine the radiation spectrum of THz sources have been analyzed [87].

Thus a large body of not only experimental but also theoretical work exists. This last has been primarily based on the solutions of the hydrodynamic transport equations of field effect transistors. The problems that have received most attention are those for which the electrostatic part (governed by Poisson's equation) relating the charge to the electrostatic potential yields an analytically tractable solution. For example, in [64], the capacitor approximation greatly simplifies the system of transport equations by relating the charge in the channel linearly to the gate voltage. However, the complete solution of the hydrodynamic transport equations has not been analyzed analytically for a general charge distribution. Taking in consideration the fact that the hydrodynamic model for semiconductors is a quasi-linear elliptic-parabolic-hyperbolic system of equations [50], the purpose of this work is to present either an analytical or numerical formalism for the treatment of instabilities in one-dimensional and two-dimensional current flow in ungated semiconductors in three cases: one-dimensional and two-dimensional without thermal coupling, and one-dimensional with thermal coupling. A perturbation treatment of the hydrodynamic transport equations is expected to yield a

broadband spectrum of collective plasma excitations and their frequencies.

1.4 Modeling techniques

There have been several techniques used to study electron flow in semiconductors from the theoretical point of view. Among these methods we can mention Monte Carlo, Finite Volume and Molecular Dynamics applied to the Boltzmann's equation. The solution of the Boltzmann's equation gives the evolution in time of the distribution in space and velocity of electrons inside the semiconductor. Knowledge about dependent variables such as voltage, electron velocity, electron density, electron temperature and lattice temperature play a fundamental role in device design and therefore they are more interesting from an engineering point of view. That has supported the use of hydrodynamic models as a useful technique to study and characterize the evolution of electron flow in semiconductors through these dependent variables. However, this model is a nonlinear set of partial differential equations. Due to that, a linearized analysis is useful to get information about the instabilities in the electron flow in semiconductors. In analogy to fluid mechanics, the techniques and tools from theory of hydrodynamic stability can be used to analyze the linear stability of the steady-state flow of electrons in semiconductors. It is important to emphasize that a linear stability analysis is an useful approach to get the frequencies of the instabilities and does not provide the saturated behavior of the instabilities present in the nonlinear system.

1.5 Problem definition

An ungated semiconductor is a semiconductor bar under a one-dimensional electric field through two metallic contacts at both edges, the source and the drain.

This configuration was chosen to understand the necessary conditions to generate and support instabilities, specially in the electron density, since it is known that these are responsible for the acceleration and deceleration of the electrons inside the semiconductor and that implies the generation of electromagnetic radiation. By using the hydrodynamic model, we study linear stability with two different approximations in the modeling, thermally uncoupled and thermally coupled. The thermally uncoupled model neglects the electron temperature and lattice temperature, and just considers changes and perturbations in voltage, electron density and electron velocity. The thermal energy of the electron remains uncoupled from its momentum. The thermally coupled model considers the electron and lattice energies, and changes and perturbations in voltage, electron density, electron velocity, electron temperature and lattice temperature are allowed. Both models are nonlinear.

CHAPTER 2

GOVERNING EQUATIONS

The proposed problem consists in studying the linear stability of the electron transport in an ungated semiconductor by using a hydrodynamic model. Three cases are considered: one-dimensional and two-dimensional electron transport without thermal coupling, and one-dimensional electron transport with thermal coupling. The schematics for both one-dimensional and two-dimensional configurations are in Figs. 3.1 and 4.1.

2.1 Governing equations: a general description

Currently, it is possible to divide the mathematical models for semiconductors into three categories: drift-diffusion, Boltzmann, and quasi-hydrodynamic models. The hydrodynamic model has been developed from Boltzmann's equation and takes an intermediate role between the drift-diffusion and Boltzmann's models. The main problem for any model is the description of non-equilibrium and non-local processes that are taking place in the different transfer phenomena. The hydrodynamic balance equations take the form of continuity equations for the carrier density, the mean momentum density, and the mean energy density. Hydrodynamic balance equations for n, $\vec{p}$, and E (moments of the Boltzmann equation) are obtained by multiplying the Boltzmann Transport equation by appropriate

powers of v_j and integrating over the velocity space as shown in Appendix A. These equations can also be obtained by doing the mass, momentum and energy balances over a control volume as shown in Appendix B. Since the dispersion relation for transverse optical phonons (TO), for instance in GaAs, is practically constant [40], that means the group velocity is ~ 0, just the longitudinal optical (LO) and acoustic phonons (A) must be taken in account for heat transfer purposes. The general form of the governing equations [23, 40] is:

$$\text{Gauss} \quad \frac{\partial^2 V^*}{\partial x_i^* \partial x_i^*} = -\frac{e}{\epsilon_s}\left(N_D - n^*\right), \tag{2.1a}$$

$$\text{Continuity} \quad \frac{\partial n^*}{\partial t^*} + \frac{\partial (v_i^* n^*)}{\partial x_i^*} = 0, \tag{2.1b}$$

$$\text{Momentum} \quad \frac{\partial v_j^*}{\partial t^*} + v_i^* \frac{\partial v_j^*}{\partial x_i^*} = -\frac{e}{m_e}(\varepsilon_{ikj} v_i^* B_k^* - \frac{\partial V^*}{\partial x_j^*}) - \frac{1}{n^* m_e}\frac{\partial (n^* k_B T_e^*)}{\partial x_j^*} - \frac{v_j^*}{\tau_p}, \tag{2.1c}$$

$$\text{Electron energy} \quad \frac{\partial T_e^*}{\partial t^*} + v_i^* \frac{\partial T_e^*}{\partial x_i^*} = -\frac{2}{3} T_e^* \frac{\partial v_i^*}{\partial x_i^*} + \frac{2}{3 n^* k_B}\frac{\partial}{\partial x_i^*}\left(k_e \frac{\partial T_e^*}{\partial x_i^*}\right) - \frac{T_e^* - T_L^*}{\tau_E} + \frac{2 m_e (v_i^* v_i^*)}{3 k_B \tau_p}\left(1 - \frac{\tau_p}{2\tau_E}\right), \tag{2.1d}$$

$$\text{LO phonon energy} \quad C_{LO}\frac{\partial T_{LO}^*}{\partial t^*} = \frac{3 n^* k_B}{2}\left(\frac{T_e^* - T_{LO}^*}{\tau_{e-LO}}\right) + \frac{n^* m_e}{2\tau_{e-LO}}\left(v_i^* v_i^*\right) - C_{LO}\left(\frac{T_{LO}^* - T_A^*}{\tau_{LO-A}}\right), \tag{2.1e}$$

$$\text{A phonon energy} \quad C_A \frac{\partial T_A^*}{\partial t^*} = \frac{\partial}{\partial x_i^*}\left(k_A \frac{\partial T_A^*}{\partial x_i^*}\right) + C_{LO}\left(\frac{T_{LO}^* - T_A^*}{\tau_{LO-A}}\right), \tag{2.1f}$$

where V^* is the voltage, e is the electron charge, ϵ_s is the dielectric constant of the semiconductor, m_e is the effective electron mass, B^* is an applied magnetic field, n^* is the electron concentration, v_j^* is the electron drift velocity, k_B is the Boltzmann constant, k_e is the electronic thermal conductivity, k_A is the acoustic

phonon thermal conductivity (lattice), T_e^* is the electron temperature, T_L^* is the lattice temperature, T_{LO}^* is the optical phonon temperature, T_A^* is the acoustic phonon temperature (lattice temperature), τ_p is the momentum relaxation time, τ_{e-LO} is the electron energy relaxation time for the electron-longitudinal optical phonon scattering, τ_E is the energy relaxation time, τ_{e-A} is the electron energy relaxation time for the electron-acoustic phonon scattering, τ_{LO-A} is the energy relaxation time for the optical phonon-acoustic phonon scattering, and C_{LO} and C_A are the heat capacity for longitudinal optical and acoustic phonons.

In the transport of electrons, they may switch between different valleys and bands inside the semiconductor due to electron-electron, electron-hole, electron-photon or electron-phonon interactions. That produces both a generation rate and a recombination rate of particles in each valley, that together correspond to the recombination-generation rate. For each valley this rate may be nonzero, but if all valleys and bands are considered simultaneously, it should be zero because the mass or charge must be conserved [22]. Phonons are defined as a quantum of lattice vibrational energy. In the hydrodynamic model, phonons are viewed as a wave packet with particlelike properties. Lattice thermal conductivity is explained by phonon interactions. Detailed expressions for k_e and k_A [10, 23, 37, 88–90] are,

$$k_e = K_{r_k} k_B^2 n^* T_e^* \frac{\tau_p}{m_e}, \tag{2.2a}$$

$$k_A = \frac{K_c}{T_A^{*g}}, \tag{2.2b}$$

where $K_{r_k} = (2.5 + r_k)$, r_k denotes the dominant scattering process, and K_c is a constant that fits experimental results. For instance, $r_k = -1/2$ for acoustic-mode scattering and $r_k = 3/2$ for scattering by ionized impurities, $g \sim 1.2$ and $K_c \sim 4 \times 10^4 \mathrm{W\ K^{g-1} m^{-1}}$ for $N_D = 3 \times 10^{17} \mathrm{cm}^3$. The momentum relaxation time

can be expressed as [91]

$$\tau_p = \frac{m_e \mu_{no}}{e} \frac{T_L^*}{T_e^*}, \tag{2.3}$$

where μ_{no} is the low field mobility. Substituting Eq. (2.3) into Eq. (2.2a), the electronic thermal conductivity becomes

$$k_e = K_{r_k} k_B^2 n^* T_L^* \frac{\mu_{no}}{m_e}. \tag{2.4}$$

2.2 Boundary conditions

A general set of boundary conditions for the two-dimensional case are

$$V^*(0, y^*, t^*) = -V_0, \tag{2.5a}$$

$$V^*(L, y^*, t^*) = 0, \tag{2.5b}$$

$$n^*(0, y^*, t^*) = n_0, \tag{2.5c}$$

$$v^*(x^*, 0, t^*) = 0, \tag{2.5d}$$

$$v^*(x^*, H, t^*) = 0, \tag{2.5e}$$

$$\frac{\partial V^*}{\partial y^*}(x^*, 0, t^*) = 0, \tag{2.5f}$$

$$\frac{\partial V^*}{\partial y^*}(x^*, H, t^*) = 0, \tag{2.5g}$$

$$\int_0^L \int_0^H n^*(x^*, y^*, t^*) dx^* dy^* = N_D L H, \tag{2.5h}$$

$$T_e^*(0, y^*, t^*) = T_1, \tag{2.5i}$$

$$\frac{\partial T_e^*}{\partial x^*}(L, y^*, t^*) = 0, \tag{2.5j}$$

$$\frac{\partial T_e^*}{\partial y^*}(x^*, 0, t^*) = 0, \tag{2.5k}$$

$$\frac{\partial T_e^*}{\partial y^*}(x^*, H, t^*) = 0, \tag{2.5l}$$

$$T_A^*(0, y^*, t^*) = T_2, \tag{2.5m}$$

$$T_A^*(L, y^*, t^*) = T_3, \tag{2.5n}$$

$$\frac{\partial T_A^*}{\partial y^*}(x^*, 0, t^*) = 0, \tag{2.5o}$$

$$\frac{\partial T_A^*}{\partial y^*}(x^*, H, t^*) = 0. \tag{2.5p}$$

These boundary conditions establish an imposed external electric field through the semiconductor in the x-direction, a fixed electron density at the source, zero electron flow through the horizontal walls (two-dimensional configuration only), adiabatic horizontal walls (electrons and lattice), fixed electron and lattice temperatures at the source, fixed lattice temperature and adiabatic condition for the electron temperature at the drain. With these conditions, the main flow is in the x-direction. The one-dimensional case has no velocity and electric field in the y-direction and boundary conditions at $y = 0$ and $y = H$ do not apply.

2.3 Nondimensionalization

For convenience, dimensionless hydrodynamic transport equations are used. Dependent and independent variables are nondimensionalized. As consequence of this process, dimensionless groups are found and their influence in the tunable parameters is shown for each problem in the following Chapters.

CHAPTER 3

ONE-DIMENSIONAL ANALYSIS WITHOUT THERMAL COUPLING

In this Chapter we perform a linear stability analysis of the one-dimensional hydrodynamic model without thermal coupling in order to study the response of electron flow to small perturbations.

3.1 Mathematical model

We consider a doped semiconductor of one-dimensional geometry as shown in Fig. 3.1. Current is driven through the device by a voltage difference between the two contacts at $x = 0, L$. The coordinate x is in the direction of the electron flow, and t is time. In this work, we assume the simplest case of instabilities, where all transverse fluctuations in the (y, z) plane are neglected, similar to the plane-wave approximation in the propagation of electromagnetic waves. In bulk semiconductors, this forms a subspace of collective excitations, whereas for charge flow in quantum wires, fluctuations in the transverse direction are not allowed. As in previous analyses, we will also neglect the generation of heat due to interaction between electrons and phonons. This can be experimentally realized if the transport in the semiconductor is ballistic, and the voltage drops occur only at the contacts.

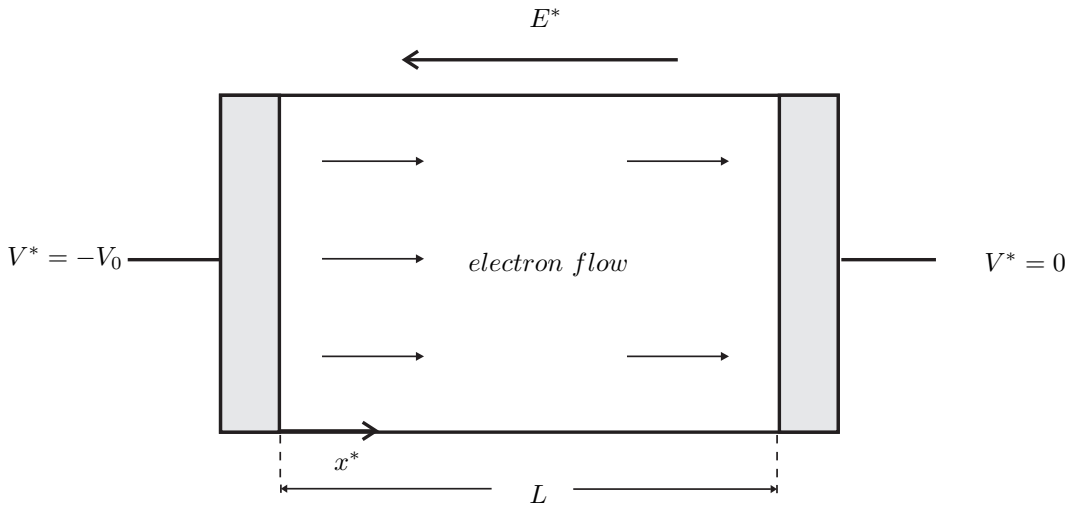

Figure 3.1. Schematic of one-dimensional semiconductor material.

The one-dimensional hydrodynamic equations for electron flow are [40]

$$\frac{\partial V^*}{\partial x^*} + E^* = 0, \tag{3.1a}$$

$$\frac{\partial E^*}{\partial x^*} + \frac{e}{\epsilon_s}\left(n^* - N_D\right) = 0, \tag{3.1b}$$

$$\frac{\partial n^*}{\partial t^*} + \frac{\partial (u^* n^*)}{\partial x^*} = 0, \tag{3.1c}$$

$$\frac{\partial u^*}{\partial t^*} + u^* \frac{\partial u^*}{\partial x^*} + \frac{e}{m_e} E^* + \frac{u^*}{\tau_p} = 0, \tag{3.1d}$$

where $V^*(x^*, t^*)$ is the voltage, $E^*(x^*, t^*)$ is the electric field, $n^*(x^*, t^*)$ is the charge density, and $u^*(x^*, t^*)$ is the average electron velocity. The system parameters are the doping concentration N_D, the permittivity ϵ_s, the charge of an electron e, its effective mass m_e, and the momentum relaxation time τ_p. Here, the Poisson equation Eq. (3.1b), the continuity equation Eq. (3.1c), and the momentum conservation equation Eq. (3.1d) are effectively decoupled from the energy conservation equations by choosing the length of the semiconductor layer to be less than a mean free path of electrons (i.e., weak elastic scattering in the ballistic regime).

The voltage at both ends and the charge density at $x^* = 0$ are prescribed boundary conditions. The physical realization is an ohmic contact at $x^* = 0$, which does not allow any perturbations in the majority carrier density due to an infinitely high surface recombination velocity. The carrier density at the right contact is allowed perturbations, but across the whole semiconductor layer, charge neutrality is enforced at all times. This form of a contact can be achieved, for example, by an inductive boundary condition, as in [64]. Charge neutrality of the semiconductor layer also implies the absence of space charge injection effects. Then, we must have $\int_0^L n^*(x^*, t^*)\, dx^* = N_D L$, where L is the length of the device,

which can be put in terms of the electric field E using Eq. (3.1b).

Thus the boundary conditions are

$$V^*(0,t^*) = -V_0, \quad V(L,t^*) = 0, \quad n^*(0,t^*) = n_0, \quad E^*(0,t^*) = E^*(L,t^*).$$

For convenience, the hydrodynamic transport equations are non-dimensionalized. Writing $V = V^*/V_0$, $n = n^*/N_D$, $x = x^*/L$, $u = u^*\sqrt{m_e/eV_0}$, and $t = t^*\sqrt{eV_0/m_eL^2}$, the dimensionless versions of Eq. (3.1) is

$$\frac{\partial V}{\partial x} + E = 0, \tag{3.2a}$$

$$\frac{\partial E}{\partial x} + \alpha\,(n-1) = 0, \tag{3.2b}$$

$$\frac{\partial n}{\partial t} + \frac{\partial (un)}{\partial x} = 0, \tag{3.2c}$$

$$\frac{\partial u}{\partial t} + u\frac{\partial u}{\partial x} + E + \frac{\sqrt{\alpha}}{\gamma}u = 0, \tag{3.2d}$$

where the dimensionless groups are $\alpha = eN_DL^2/V_0\epsilon_s$ and $\gamma = \sqrt{\tau_p^2e^2N_D/\epsilon_sm_e} = \omega_p\tau_p$, where $\omega_p = \sqrt{e^2N_D/\epsilon_sm_e}$ is identified as the fundamental plasma frequency of the free electrons in the semiconductor. The electron Reynolds number in terms of the dimensionless groups is $R_e = \gamma^2/\alpha$ [11]. The dimensionless parameter γ can be expected to play a major role in any phenomena related to collective excitations of the electron gas, as will be seen later. The only electrically tunable parameter is α, which is inversely proportional to the applied bias V_0. The dimensionless boundary conditions are

$$V(0,t) = -1, \quad V(1,t) = 0, \quad n(0,t) = 1, \quad E(0,t) = E(1,t).$$

By choosing an ohmic contact, we clamp the value to $n_0 = N_D$, the free electron

density at the left contact, at all times.

3.2 One-dimensional electron flow

The steady-state solution of Eq. (3.2) that satisfies the boundary conditions is

$$\overline{E}(x) = -1, \quad \overline{V}(x) = x - 1, \quad \overline{n}(x) = 1, \quad \overline{u}(x) = \frac{\gamma}{\sqrt{\alpha}} \ .$$

where $\overline{(\quad)}$ indicates time-independence. The steady state solution captures the drift flow, with the dimensional form of the electron concentration and velocity given by $n^*(x^*) = N_D$, and $u^*(x^*) = (e\tau_p/m_e) \times (V_0/L)$ for all x^*. Any instabilities that exist are due to time-dependent fluctuations to this steady state.

Applying small perturbations of the form

$$E = \overline{E} + E'(x,t), \quad V = \overline{V} + V'(x,t), \quad n = \overline{n} + n'(x,t), \quad u = \overline{u} + u'(x,t), \tag{3.3}$$

substituting in Eq. (3.2) and linearizing, we get

$$\frac{\partial V'}{\partial x} + E' = 0, \tag{3.4a}$$

$$\frac{\partial E'}{\partial x} + \alpha n' = 0, \tag{3.4b}$$

$$\frac{\partial n'}{\partial t} + \frac{\gamma}{\sqrt{\alpha}} \frac{\partial n'}{\partial x} + \frac{\partial u'}{\partial x} = 0, \tag{3.4c}$$

$$\frac{\partial u'}{\partial t} + \frac{\gamma}{\sqrt{\alpha}} \frac{\partial u'}{\partial x} + E' + \frac{\sqrt{\alpha}}{\gamma} u' = 0. \tag{3.4d}$$

The boundary conditions on the perturbations are

$$V'(0,t) = 0, \quad V'(1,t) = 0, \quad n'(0,t) = 0, \quad E'(0,t) = E'(1,t). \tag{3.5}$$

Using normal modes of the form

$$\begin{Bmatrix} V' \\ E' \\ n' \\ u' \end{Bmatrix} = \begin{Bmatrix} \widehat{V} \\ \widehat{E} \\ \widehat{n} \\ \widehat{u} \end{Bmatrix} e^{kx+\omega t},$$

where the wavenumber k, the frequency ω, and the amplitudes denoted by $\widehat{\ }$ are all complex, Eq. (3.4) becomes

$$\begin{bmatrix} k & 1 & 0 & 0 \\ 0 & k & \alpha & 0 \\ 0 & 0 & \omega + k\gamma/\sqrt{\alpha} & k \\ 0 & 1 & 0 & \omega + k\gamma/\sqrt{\alpha} + \sqrt{\alpha}/\gamma \end{bmatrix} \begin{Bmatrix} \widehat{V} \\ \widehat{E} \\ \widehat{n} \\ \widehat{v} \end{Bmatrix} = \begin{Bmatrix} 0 \\ 0 \\ 0 \\ 0 \end{Bmatrix}.$$

For a non-trivial solution, the determinant should vanish, so that the characteristic polynomial is given by

$$-k\left[k\left(\omega + \frac{\gamma}{\sqrt{\alpha}}k\right)\left(\omega + \frac{\gamma}{\sqrt{\alpha}}k + \frac{\sqrt{\alpha}}{\gamma}\right) + \alpha k\right] = 0. \tag{3.6}$$

A critical value of the electron mobility defines two distinct phases of the collective excitations possible in the electron system. This critical mobility is defined by

$$\mu_{cr} = \frac{1}{2}\sqrt{\frac{\epsilon_s}{m_e N_D}}. \tag{3.7}$$

It is equivalent to satisfy the critical condition $\tau_p = 1/2\omega_p$. If the mobility of electrons is higher than the critical value, the condition $4\gamma^2 > 1$ is obtained, and vice versa. For most semiconductors, this critical mobility is in the range of $1 - 10$

$\mathrm{cm}^2/(\mathrm{V\ s})$, and therefore the condition $4\gamma^2 > 1$ is achievable in reasonably clean semiconductors doped to a nominal level $N_D \sim 10^{17}/\mathrm{cm}^3$.

3.2.1 For $4\gamma^2 > 1$

The four roots of Eq. (3.6) are $k_{1,2} = 0$ and $k_{3,4} = a \pm ib$, where

$$a = -\frac{\alpha}{2\gamma^2}\left(\frac{2\gamma\omega}{\sqrt{\alpha}} + 1\right), \tag{3.8a}$$

$$b = \frac{\alpha}{2\gamma^2}\sqrt{4\gamma^2 - 1}. \tag{3.8b}$$

Then we can write the amplitudes of the perturbations as

$$V' = \left[A + Bx + Ce^{(a+ib)x} + De^{(a-ib)x}\right] e^{\omega t}, \tag{3.9a}$$

$$E' = \left[-B - C(a+ib)e^{(a+ib)x} - D(a-ib)e^{(a-ib)x}\right] e^{\omega t}, \tag{3.9b}$$

$$n' = \left[\frac{1}{\alpha}(C(a+ib)^2 e^{(a+ib)x} + D(a-ib)^2 e^{(a-ib)x})\right] e^{\omega t}, \tag{3.9c}$$

$$\begin{aligned} u' = \frac{\gamma}{\omega\gamma + \sqrt{\alpha}}\Bigg[&(a+ib)Ce^{(a+ib)x}\left\{\frac{\gamma\omega(a+ib)}{\alpha^{3/2}} + \frac{\gamma^2(a+ib)^2}{\alpha^2} + 1\right\} \\ &+(a-ib)De^{(a-ib)x}\left\{\frac{\gamma\omega(a-ib)}{\alpha^{3/2}} + \frac{\gamma^2(a-ib)^2}{\alpha^2} + 1\right\} + B\Bigg] e^{\omega t}. \end{aligned} \tag{3.9d}$$

The boundary conditions, Eq. (3.5), can be written as

$$\begin{bmatrix} 1 & 0 & 1 & 1 \\ 1 & 1 & e^{a+ib} & e^{a-ib} \\ 0 & 0 & (a+ib)^2 & (a-ib)^2 \\ 0 & 0 & (a+ib)(1-e^{a+ib}) & (a-ib)(1-e^{a-ib}) \end{bmatrix} \begin{Bmatrix} A \\ B \\ C \\ D \end{Bmatrix} = \begin{Bmatrix} 0 \\ 0 \\ 0 \\ 0 \end{Bmatrix}.$$

For a non-trivial solution the determinant must vanish, which gives

$$(a+ib)(1-e^{a-ib})-(a-ib)(1-e^{a+ib})=0,$$

from which the condition

$$e^{a-b\cot b}(a-b\cot b)=-\frac{be^{-b\cot b}}{\sin b}$$

is obtained. This can be written as

$$W\left(-\frac{be^{-b\cot b}}{\sin b}\right)=a-b\cot b.$$

where the Lambert W-function is defined as the solution of $W(z_*)e^{W(z_*)}=z_*$ [92, 93]. Finally, substituting a from Eq. (3.8a), we get

$$\omega=-\frac{\gamma}{\sqrt{\alpha}}\left[\frac{\alpha}{2\gamma^2}+b\cot b+W\left(-\frac{be^{-b\cot b}}{\sin b}\right)\right]. \tag{3.10}$$

$W(z_*)$ has an infinite number of complex values even for real z_* (as it is here), so that ω also has an infinite number of values corresponding to the branches of the function. We can split the complex frequency into its real and imaginary parts as $\omega=\omega_r+i\omega_i$, and then normalize them using $\omega_p=\sqrt{\alpha}$ (a physical meaning for ω_p is given in Section 3.3.2). Positive ω_r represents unstable, growing exponentials in time in Eq. (3.9), whereas ω_i is the frequency of oscillation. A portion of the ω-spectra for three different values of α is shown in Fig. 3.2. The complex frequencies shift to the left and the oscillations become more stable as α is increased; this corresponds to a decrease in the applied voltage. The distribution of electron density perturbation $n'(x,t)$ for $\alpha=10$ and for an unstable eigenvalue

at different instants in time within the first period of oscillation is shown in Fig. 3.3. The behavior is that of a wave that is growing in time. The corresponding unstable behavior of the small signal voltage $V'(x,t)$, electric field $E'(x,t)$, electron density $n'(x,t)$ and velocity $u'(x,t)$ at $x = 0.5$ are shown in Fig. 3.4; again the variables are seen to be growing in time.

Thus the hydrodynamic instability of electron flow in an ungated doped bulk semiconductor exhibits a broadband spectrum, which can be tuned from the damped stable oscillations (for $\omega_r < 0$) to growing, unstable ones (for $\omega_r > 0$) by increasing the applied bias. These collective oscillations of the electron density will lead to broadband radiation at those frequencies. With appropriate cavity design, the energy in selected modes can be enhanced at the expense of others, similar to what is done in [64].

The low-mobility cases exhibit similar behavior, the major difference being that higher voltages are necessary to achieve undamped plasma oscillations.

3.2.2 For $4\gamma^2 = 1$

Eq. (3.6) now has two pairs of repeated roots. Instead of Eq. (3.10), we have

$$\omega = -\frac{\gamma}{\sqrt{\alpha}}\left[\frac{\alpha}{2\gamma^2} + 1 + W\left(-e^{-1}\right)\right].$$

The ω-spectra for three different values of α are shown in Fig. 3.5. Again, the tendency is to move toward greater stability as α is increased. For $\alpha = 1$, the spatial distribution of the electron density $n'(x,t)$ at an unstable eigenvalue and its evolution in time within the first period of oscillation is shown in Fig. 3.6. It describes a wave that is growing in time. However, as is clear from a comparison of Figs. 3.5 and 3.2, the hydrodynamic instability is damped strongly, and larger

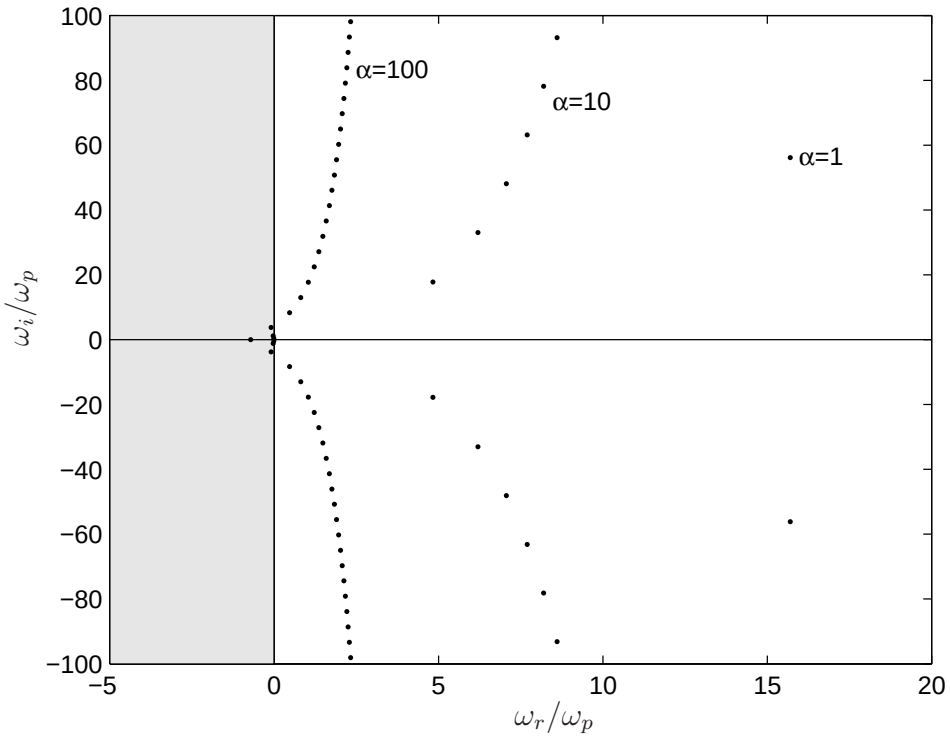

Figure 3.2. ω-spectra for $\gamma = 20$.

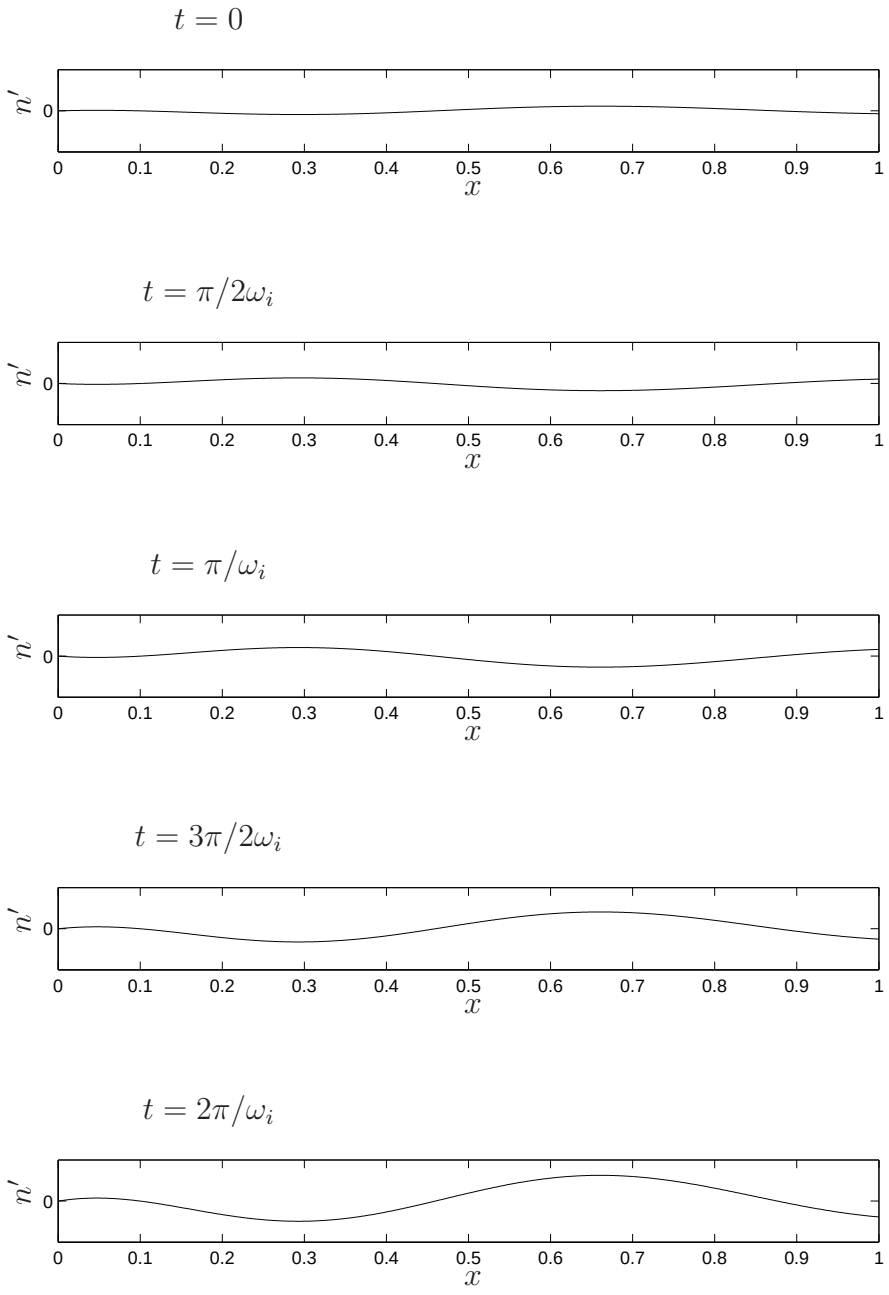

Figure 3.3. Spatial distribution of electron density $n'(x,t)$ in arbitrary scale for $\alpha = 10$ and $\gamma = 20$ at $\omega_i \sim 20\omega_p$.

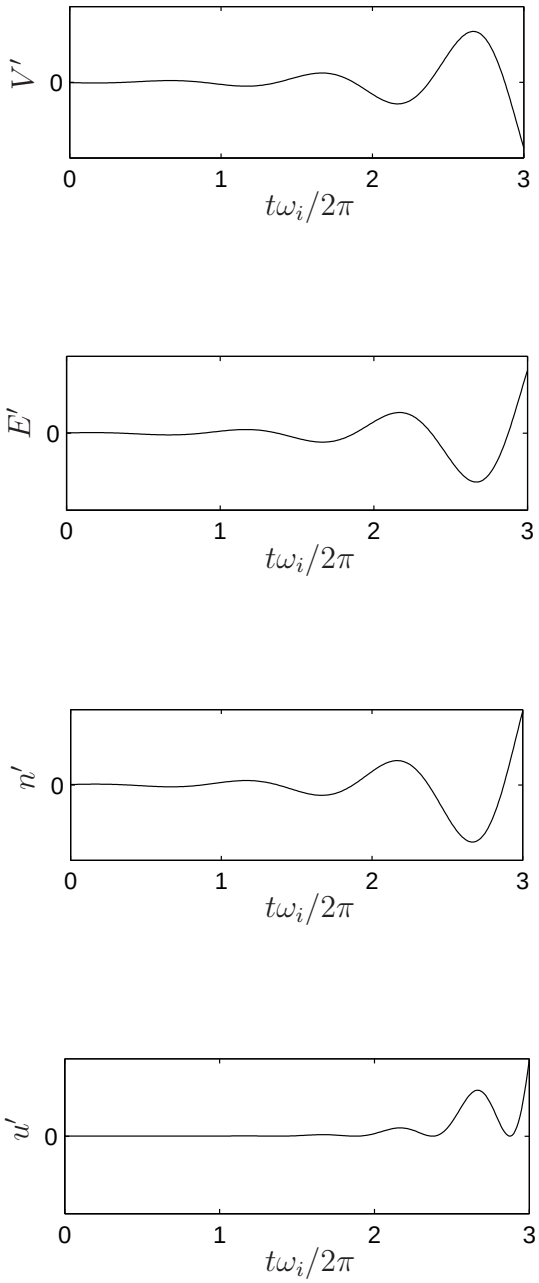

Figure 3.4. Time variation of voltage $V'(x,t)$, electric field $E'(x,t)$, electron density $n'(x,t)$ and electron velocity $u'(x,t)$ in arbitrary scale at $x = 0.5$ for $\alpha = 10$ and $\gamma = 20$ with $\omega_i \sim 20\omega_p$.

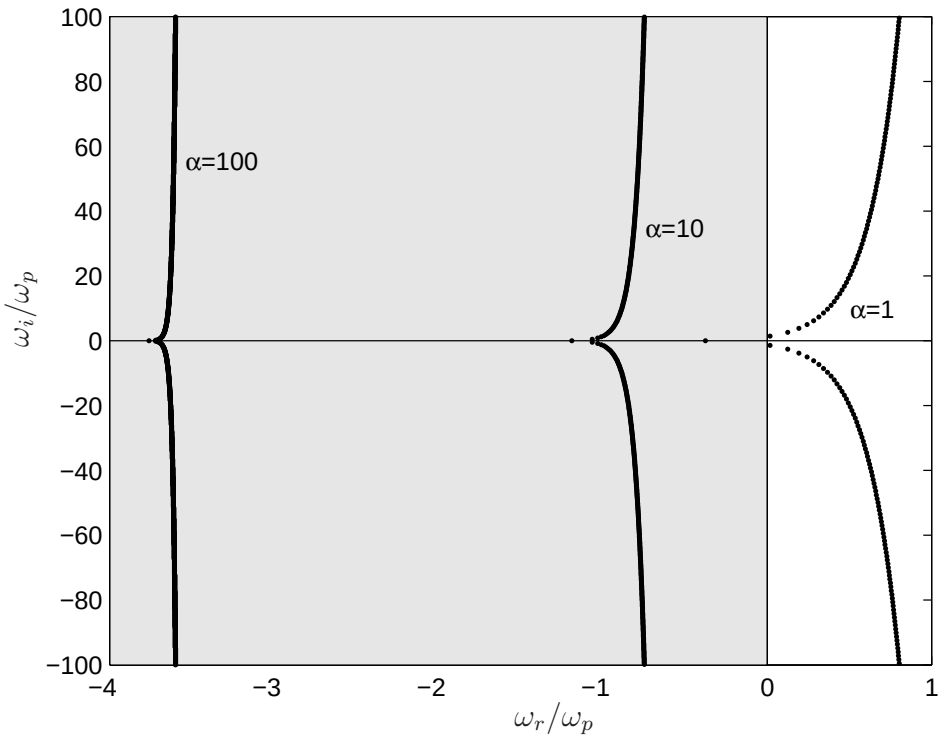

Figure 3.5. ω-spectra for $\gamma = 1/2$.

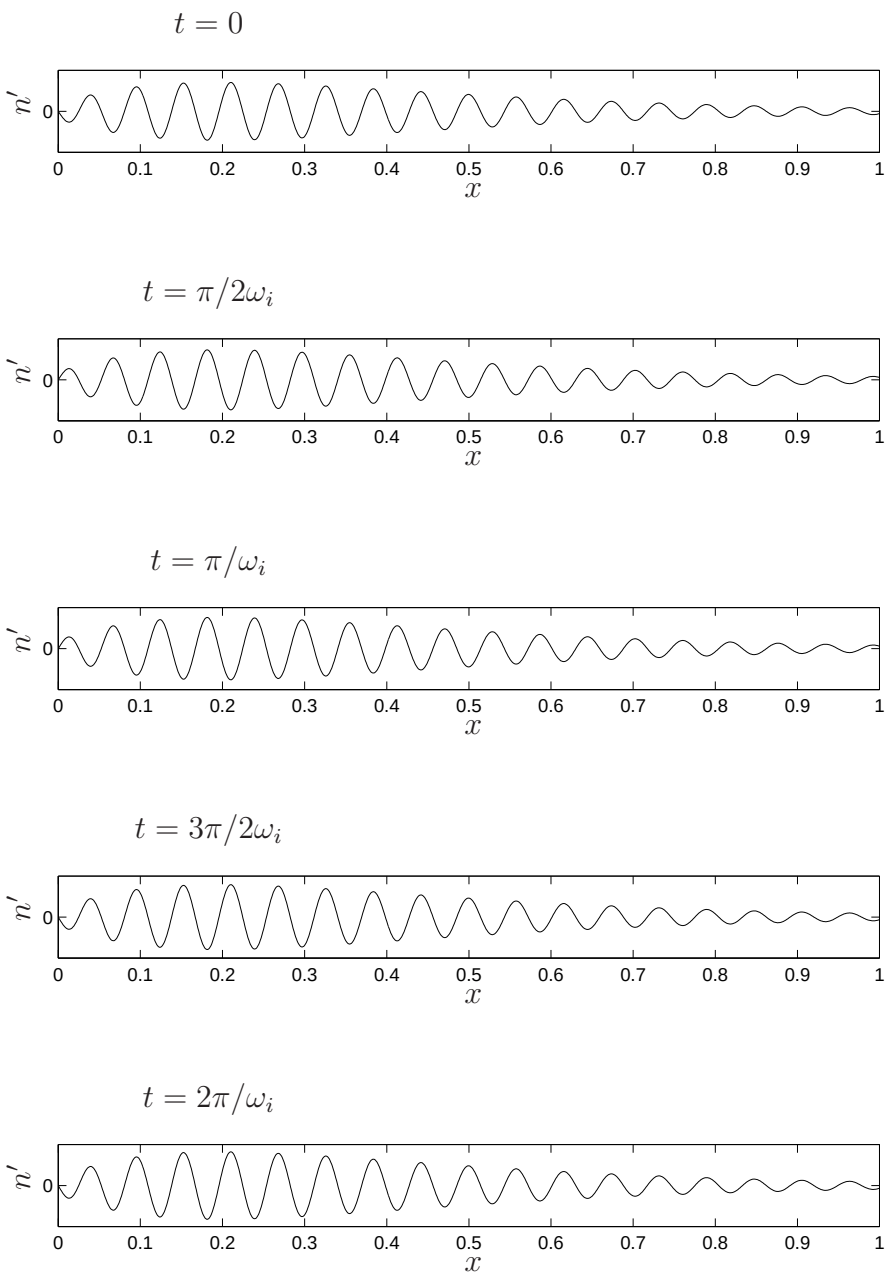

Figure 3.6. Spatial distribution of electron density $n'(x,t)$ in arbitrary scale for $\alpha = 1$ and $\gamma = 1/2$ at $\omega_i \sim 20\omega_p$.

voltages are now necessary to achieve growing unstable oscillations with $\omega_r > 0$.

3.2.3 For $4\gamma^2 < 1$

The roots of Eq. (3.6) are now all real. The analysis of Section 3.2.1 still holds as long as it is remembered that b is imaginary. On writing $b = ib'$ where $b' = \alpha\sqrt{1-4\gamma^2}/2\gamma^2$ is now real, Eq. (3.10) becomes

$$\omega = -\frac{\gamma}{\sqrt{\alpha}}\left[\frac{\alpha}{2\gamma^2} + b'\coth b' + W\left(-\frac{b'e^{-b'\coth b'}}{\sinh b'}\right)\right].$$

The complex values of ω for three different values of α are shown in Fig. 3.7. As before, stability is increased on increasing α. For $\alpha = 1$, the spatial distribution of the electron density $n'(x,t)$ at an unstable eigenvalue and its evolution in time within the first period of oscillation is shown in Fig. 3.8. A growing wave-like behavior is also observed here.

3.2.4 Phase and group velocities

The constant b in Eq. (3.8b) is real, but a in (3.8a) is complex, so that

$$a = -\frac{\alpha}{2\gamma^2}\left[\left(\frac{2\gamma\omega_r}{\sqrt{\alpha}} + 1\right) + i\ \frac{2\gamma\omega_i}{\sqrt{\alpha}}\right].$$

where ω_i is the frequency of oscillation of the wave. The wave number $k = a + ib$ can also be separated into its real and imaginary parts as

$$k = -\frac{\alpha}{2\gamma^2}\left[\left(\frac{2\gamma\omega_r}{\sqrt{\alpha}} + 1\right) + i\left(\frac{2\gamma\omega_i}{\sqrt{\alpha}} + \sqrt{4\gamma^2 - 1}\right)\right],$$

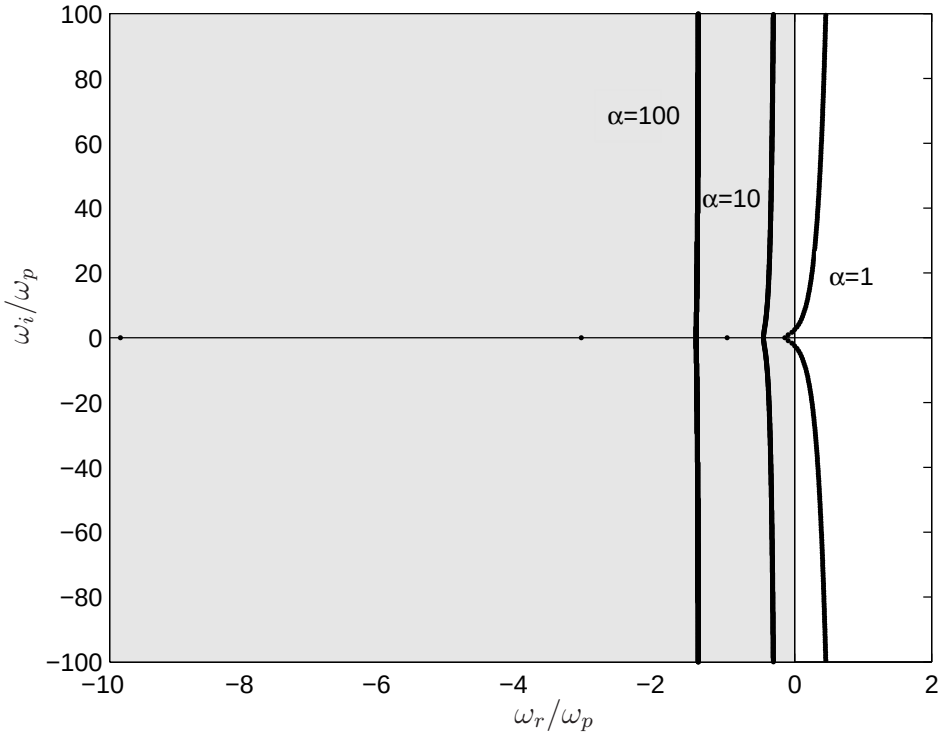

Figure 3.7. ω-spectra for $\gamma = 1/3$.

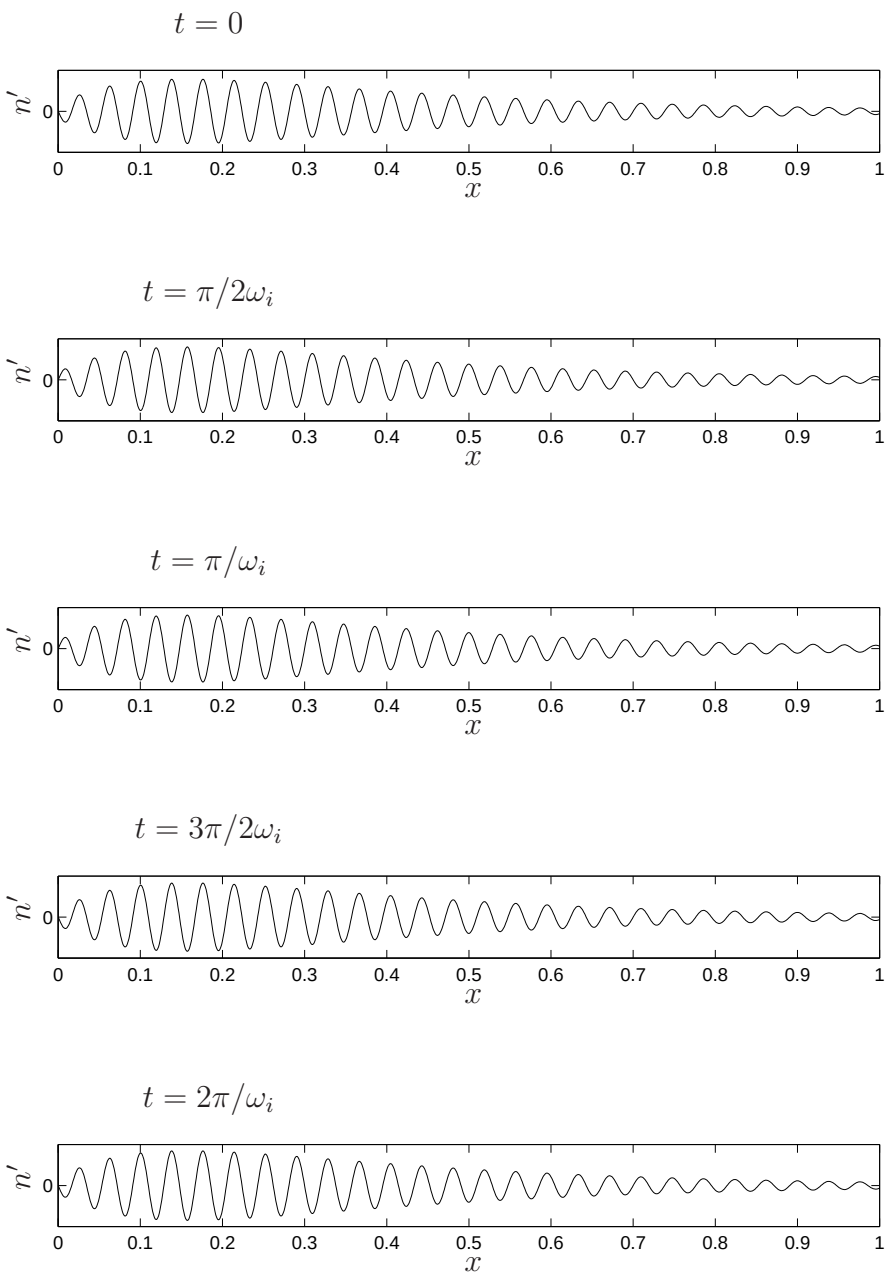

Figure 3.8. Spatial distribution of electron density $n'(x,t)$ in arbitrary scale for $\alpha = 1$ and $\gamma = 1/3$ at $\omega_i \sim 20\omega_p$.

where the imaginary part is the wave number of the spatial oscillations. From this dispersion relation, the phase and group velocities can be deduced to be

$$\begin{aligned} v_p &= \frac{\gamma}{\sqrt{\alpha}} \frac{2\gamma\omega_i}{2\gamma\omega_i + \sqrt{\alpha\,(4\gamma^2 - 1)}}, \\ v_g &= \frac{\gamma}{\sqrt{\alpha}}, \end{aligned}$$

respectively. Waves running in both $+x$ and $-x$ directions are possible. Since the magnitude of the group velocity of the plasma excitation is found to be exactly the same as the steady state electron velocity, it indicates that the fluctuation rides on the steady state velocity, and in a stationary rest-frame, the effective plasma velocity is $v_g \pm \overline{u} = 0$ & $2\gamma/\sqrt{\alpha}$, meaning the 'rightgoing' plasma wave is twice as fast as the steady state flow, and there are no left going waves.

3.3 Special cases

3.3.1 Asymptotic approximation

The Lambert W-function can be approximated for values of ω around the origin such that the ratio between the real and imaginary component is much less than one. In this case, Eq. (3.10) becomes

$$\omega = -\frac{\gamma}{\sqrt{\alpha}} \left[\frac{\alpha}{2\gamma^2} + b \cot b + \log\left(-\frac{b e^{-b\cot b}}{y_m \sin b} \right) + i y_m \right],$$

where $y_m = \pm(\pi/2)(4m \pm 1)$ (keeping the argument of the log function positive) and $m = 1, 2, 3, \ldots$.

3.3.2 Zero electron flow

A possible dimensionless steady-state solution of Eq. (3.2) is $\overline{E} = 0$, $\overline{V} =$ constant, $\overline{v} = 0$, and $\overline{n} = 1$. For small perturbations, as in Eq. (3.3), we have upon linearization

$$\begin{aligned}
\frac{\partial V'}{\partial x} + E' &= 0, \\
\frac{\partial E'}{\partial x} + \alpha n' &= 0, \\
\frac{\partial n'}{\partial t} + \frac{\partial u'}{\partial x} &= 0, \\
\frac{\partial u'}{\partial t} + E' + \frac{\sqrt{\alpha}}{\gamma} u' &= 0.
\end{aligned}$$

It is possible to reduce the equations to a single fourth-order equation

$$\frac{\partial^4 V'}{\partial t^2 \partial x^2} + \frac{\sqrt{\alpha}}{\gamma} \frac{\partial^3 V'}{\partial t \partial x^2} + \alpha \frac{\partial^2 V'}{\partial x^2} = 0.$$

This can be solved by writing it first as

$$\frac{\partial^2}{\partial x^2} \left[\frac{\partial^2 V'}{\partial t^2} + \frac{\sqrt{\alpha}}{\gamma} \frac{\partial V'}{\partial t} + \alpha V' \right] = 0,$$

and then integrating twice w.r.t. x to get

$$\frac{\partial^2 V'}{\partial t^2} + \frac{\sqrt{\alpha}}{\gamma} \frac{\partial V'}{\partial t} + \alpha V' = A_f(t) x + B_f(t).$$

The homogeneous part of the temporal solution is obtained as usual by setting $V' \sim e^{rt}$, where

$$r = \frac{\sqrt{\alpha}}{2\gamma} \left[-1 \pm \sqrt{1 - 4\gamma^2} \right].$$

Damped oscillatory solutions are possible if $4\gamma^2 > 1$. The solution then takes the form

$$V'(x,t) = e^{-t\sqrt{\alpha}/2\gamma}\left[C_f(x)\sin\omega t + D_f(x)\cos\omega t\right] + g_f(x,t)$$

where

$$\omega = \frac{\sqrt{\alpha}}{2\gamma}\sqrt{4\gamma^2 - 1},$$

and g_f is the particular solution corresponding to $A_f(t)x + B_f(t)$. If the momentum relaxation time $\tau_p \to \infty$, then $\gamma \to \infty$ also, so that damped oscillations at the plasma frequency $\omega_p = \sqrt{\alpha}$ may occur.

3.4 Conclusions

In summary, a perturbative formalism for studying instabilities in the hydrodynamic model of carrier flow in semiconductors is presented. The treatment allows an analytic evaluation of plasma oscillation modes in a generic semiconductor. The eigenvalue spectrum indicates that there is an unstable region which depends strongly on the applied voltage; the spectrum becomes more stable as the applied voltage decreases. Considering GaAs with an electron effective mass $m = 6.6\%$ of the free electron mass, $\epsilon_s = 12.5\epsilon_0$, $L = 100$ nm, $N_D = 5 \times 10^{17}$ cm^{-3}, $\tau_p = 0.4$ ps, and $V_0 = 1$ V gives $\alpha = 7.072$, $\gamma = 17.365$ and $Re = 42.639$. The corresponding plasma frequency is $\omega_p = \sqrt{e^2 N_D/\epsilon_s m_e}$ =6.9 THz. Eigenvalues around the origin with positive real parts thus have frequencies of the order of terahertz, so that the ungated semiconductor could be a possible source of radiation in this frequency range. The major result is that a broadband spectrum of eigenvalues tunable by the applied voltage results due to the instabilities, and these frequencies can be analytically evaluated for general boundary conditions using the perturbative

formalism presented. The formalism presented should prove useful in the analysis and design of plasma-wave instability based THz sources in the future.

CHAPTER 4

TWO-DIMENSIONAL ANALYSIS WITHOUT THERMAL COUPLING

In this Chapter we perform a linear stability analysis of the two-dimensional model without thermal coupling in order to study the response of electron flow to small perturbations and differences in the spectrum with the one-dimensional model described in Chapter 3.

4.1 Mathematical model

The problem is defined by a doped two-dimensional semiconductor as shown in Fig. 4.1. The driving force through the device is given by an electric field due to a voltage difference between the two contacts at $x^* = 0$ and $x^* = L$. x^* and y^* are the Cartesian coordinates and t^* is the time. In general, the electric field has also a component out of the (x^*, y^*) plane. Due to an imposed electric field in the x^*-direction and a two-dimensional semiconductor, the (y^*, z^*) plane describes an equipotential area. We are interested in capturing instabilities in the (x^*, y^*) plane, neglecting variations in the direction normal to the paper. Electron-lattice interactions are neglected, which implies that the heat generation sources due to electron transport in the semiconductor are not taken into account. Under these assumptions, the two-dimensional hydrodynamic equations for electron flow are [40]

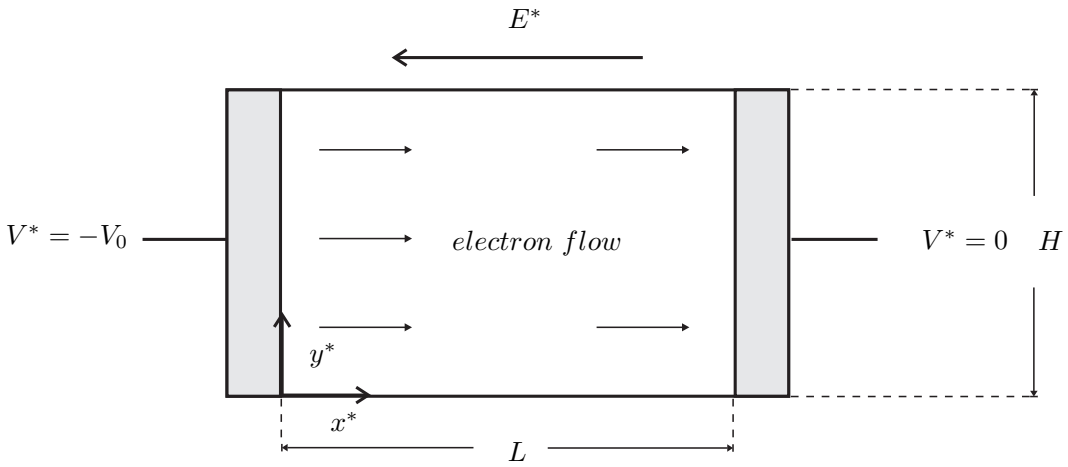

Figure 4.1. Schematic of two-dimensional semiconductor material.

$$\frac{\partial^2 V^*}{\partial x^{*2}} + \frac{\partial^2 V^*}{\partial y^{*2}} - \frac{e}{\epsilon_s}(n^* - N_D) = 0, \tag{4.1a}$$

$$\frac{\partial n^*}{\partial t^*} + \frac{\partial (u^* n^*)}{\partial x^*} + \frac{\partial (v^* n^*)}{\partial y^*} = 0, \tag{4.1b}$$

$$\frac{\partial u^*}{\partial t^*} + u^* \frac{\partial u^*}{\partial x^*} + v^* \frac{\partial u^*}{\partial y^*} - \frac{e}{m_e}\frac{\partial V^*}{\partial x^*} + \frac{u^*}{\tau_p} = 0, \tag{4.1c}$$

$$\frac{\partial v^*}{\partial t^*} + u^* \frac{\partial v^*}{\partial x^*} + v^* \frac{\partial v^*}{\partial y^*} - \frac{e}{m_e}\frac{\partial V^*}{\partial y^*} + \frac{v^*}{\tau_p} = 0, \tag{4.1d}$$

where $V^*(x^*, y^*, t^*)$ is the voltage, $n^*(x^*, y^*, t^*)$ is the charge density, $u^*(x^*, y^*, t^*)$ and $v^*(x^*, y^*, t^*)$ are the drift electron velocities in the x^* and y^* directions respectively. The system of Eqs. (4.1) includes Gauss's law Eq. (4.1a), the continuity equation Eq. (4.1b) and the momentum conservation equations in the x^* and y^* directions Eqs. (4.1c) and (4.1d). The system parameters are the doping concentration N_D, the permittivity ϵ_s, the charge of an electron e, its effective mass m_e, and the momentum relaxation time τ_p. The boundary conditions impose a voltage gradient along x^*-direction, a fixed charge density at $x^* = 0$, a constant charge in the semiconductor as a whole, and charge reflexion along the edges $y^* = 0$ and $y^* = H$. This is made by imposing an ohmic contact between the semiconductor and the metal at $x^* = 0$ and an inductive boundary condition at $x^* = L$ as explained in Section 3.1 [68]. Then, the boundary conditions are

$$V^*(0, y^*, t^*) = -V_0, \quad V^*(L, y^*, t^*) = 0, \quad n^*(0, y^*, t^*) = n_0, \tag{4.2a}$$

$$v^*(x^*, 0, t^*) = 0, \quad v^*(x^*, H, t^*) = 0, \quad \frac{\partial V^*}{\partial y^*}(x^*, 0, t^*) = 0, \quad \frac{\partial V^*}{\partial y^*}(x^*, H, t^*) = 0. \tag{4.2b}$$

In addition, the charge neutrality condition is

$$\int_0^L \int_0^H n^*(x^*, y^*, t^*) dx^* dy^* = N_D L H. \tag{4.3}$$

For convenience, the governing equations can be non-dimensionalized. Defining the aspect ratio as $R = H/L$ and writing V, n, x, u ans t as in Section 3.1, and $y = y^*/H$, $v = v^*\sqrt{m_e/eV_0}$, the non-dimensional version of Eq. (4.1) is

$$\frac{\partial^2 V}{\partial x^2} + \frac{1}{R^2}\frac{\partial^2 V}{\partial y^2} - \alpha\,(n-1) = 0, \tag{4.4a}$$

$$\frac{\partial n}{\partial t} + \frac{\partial (un)}{\partial x} + \frac{1}{R}\frac{\partial (vn)}{\partial y} = 0, \tag{4.4b}$$

$$\frac{\partial u}{\partial t} + u\frac{\partial u}{\partial x} + \frac{1}{R}v\frac{\partial u}{\partial y} - \frac{\partial V}{\partial x} + \frac{\sqrt{\alpha}}{\gamma}u = 0, \tag{4.4c}$$

$$\frac{\partial v}{\partial t} + u\frac{\partial v}{\partial x} + \frac{1}{R}v\frac{\partial v}{\partial y} - \frac{1}{R}\frac{\partial V}{\partial y} + \frac{\sqrt{\alpha}}{\gamma}v = 0. \tag{4.4d}$$

The dimensionless parametric groups are $\alpha = eN_D L^2/V_0\epsilon_s$, $\gamma = \sqrt{\tau_p^2 e^2 N_D/\epsilon_s m_e} = \omega_p\tau_p$, and $\omega_p = \sqrt{e^2 N_D/\epsilon_s m_e}$, which is the fundamental plasma frequency of free electrons in the semiconductor. α is the only tunable parameter and it is inversely proportional to the applied bias V_0; γ captures the phenomena related to collective excitations of the electron gas. The non-dimensional boundary and charge neutrality conditions are

$$V(0,y,t) = -1, \quad V(1,y,t) = 0, \quad n(0,y,t) = 1, \tag{4.5a}$$

$$v(x,0,t) = 0, \quad v(x,1,t) = 0, \tag{4.5b}$$

$$\frac{\partial V}{\partial y}(x,0,t) = 0, \quad \frac{\partial V}{\partial y}(x,1,t) = 0, \tag{4.5c}$$

$$\int_0^1 \int_0^1 n(x,y,t) dx\, dy = 1. \tag{4.5d}$$

The charge neutrality condition Eq. (4.5d) can be rewritten by integrating Eq. (4.4a) in the xy-plane to give

$$\int_0^1 \left(\frac{\partial V}{\partial x}(1,y,t) - \frac{\partial V}{\partial x}(0,y,t)\right) dy + \int_0^1 \left(\frac{\partial V}{\partial y}(x,1,t) - \frac{\partial V}{\partial y}(x,0,t)\right) dx = 0. \quad (4.6)$$

Substituting Eqs. (4.5c) into Eq. (4.6), we get

$$\int_0^1 \left(\frac{\partial V}{\partial x}(1,y,t) - \frac{\partial V}{\partial x}(0,y,t)\right) dy = 0. \quad (4.7)$$

4.2 Two-dimensional electron flow

The steady-state solution of Eqs. (4.4) satisfying the boundary conditions in Eqs. (4.5) is

$$\overline{V}(x,y) = x - 1, \quad \overline{n}(x,y) = 1, \quad \overline{u}(x,y) = \frac{\gamma}{\sqrt{\alpha}}, \quad \overline{v}(x,y) = 0, \quad (4.8)$$

where $\overline{(\quad)}$ indicates time-independence. The steady-state solution captures the drift flow, and the electron velocity is independent of position. The electron density and electric field are also independent of position, since the potential varies linearly [94, 95]. In dimensional form the electron concentration is $\overline{n}^*(x^*, y^*) = N_D$, which is the doping density of the semiconductor, and the electron velocity is $\overline{u}^*(x^*, y^*) = (e\tau_p/m_e)(V_0/L) = \mu E^*$ where μ is the electron mobility and E^* is the electric field. Any instabilities that may exist are due to the growth of fluctuations from this steady state.

Applying small perturbations to the time-independent solution, we have $V = \overline{V}(x,y) + V'(x,y,t)$, $n = \overline{n}(x,y) + n'(x,y,t)$, $u = \overline{u}(x,y) + u'(x,y,t)$ and $v =$

$\overline{v}(x,y) + v'(x,y,t)$. Substituting in Eq. (4.4) and linearizing, we get

$$\frac{\partial^2 V'}{\partial x^2} + \frac{1}{R^2}\frac{\partial^2 V'}{\partial y^2} - \alpha n' = 0, \tag{4.9a}$$

$$\frac{\partial n'}{\partial t} + \frac{\gamma}{\sqrt{\alpha}}\frac{\partial n'}{\partial x} + \frac{\partial u'}{\partial x} + \frac{1}{R}\frac{\partial v'}{\partial y} = 0, \tag{4.9b}$$

$$\frac{\partial u'}{\partial t} + \frac{\gamma}{\sqrt{\alpha}}\frac{\partial u'}{\partial x} - \frac{\partial V'}{\partial x} + \frac{\sqrt{\alpha}}{\gamma}u' = 0, \tag{4.9c}$$

$$\frac{\partial v'}{\partial t} + \frac{\gamma}{\sqrt{\alpha}}\frac{\partial v'}{\partial x} - \frac{1}{R}\frac{\partial V'}{\partial y} + \frac{\sqrt{\alpha}}{\gamma}v' = 0. \tag{4.9d}$$

The perturbation in the electron density is in the (x^*, y^*) plane as well as perpendicular to it. Since this perturbation is small, any variation of the electric field perpendicular to the (x^*, y^*) plane is small in magnitude and can be neglected if it is compared to the steady-state electric field and its perturbations in the (x^*, y^*) plane. Due to this, Eq. (4.9a) does not consider the out of the plane voltage perturbation. The actual three-dimensional voltage perturbation has been calculated [72].

The boundary and charge neutrality conditions on the perturbations are

$$V'(0,y,t) = 0, \quad V'(1,y,t) = 0, \quad n'(0,y,t) = 0, \tag{4.10a}$$

$$v'(x,0,t) = 0, \quad v'(x,1,t) = 0, \tag{4.10b}$$

$$\frac{\partial V'}{\partial y}(x,0,t) = 0, \quad \frac{\partial V'}{\partial y}(x,1,t) = 0, \tag{4.10c}$$

$$\int_0^1 \left(\frac{\partial V'}{\partial x}(1,y,t) - \frac{\partial V'}{\partial x}(0,y,t) \right) dy = 0. \tag{4.10d}$$

Using normal modes of the form

$$\{V'\ n'\ u'\ v'\}^T = \left\{ \widetilde{V}(y)\ \widetilde{n}(y)\ \widetilde{u}(y)\ \widetilde{v}(y) \right\}^T \exp\left(k_x x + \omega t\right), \tag{4.11}$$

where the wavenumber vector $\vec{k} = k_x\mathbf{i}+k_y\mathbf{j}$, the frequency is ω, and the amplitudes denoted by $\widetilde{\ }$ are all complex. Therefore, Eqs. (4.9) become

$$\frac{d^2\widetilde{V}}{dy^2} + {k_x}^2 R^2 \widetilde{V} - \alpha R^2 \widetilde{n} = 0, \tag{4.12a}$$

$$\frac{d\widetilde{v}}{dy} + R\left(\omega + k_x \frac{\gamma}{\sqrt{\alpha}}\right)\widetilde{n} + k_x R\widetilde{u} = 0, \tag{4.12b}$$

$$k_x \widetilde{V} - \left(\omega + k_x \frac{\gamma}{\sqrt{\alpha}} + \frac{\sqrt{\alpha}}{\gamma}\right)\widetilde{u} = 0, \tag{4.12c}$$

$$\frac{d\widetilde{V}}{dy} - R\left(\omega + k_x \frac{\gamma}{\sqrt{\alpha}} + \frac{\sqrt{\alpha}}{\gamma}\right)\widetilde{v} = 0. \tag{4.12d}$$

If $(\omega + k_x\gamma/\sqrt{\alpha} + \sqrt{\alpha}/\gamma) = 0$, then Eq. (4.12a) and (4.12c) give $\widetilde{V} = \widetilde{n} = 0$, which is not of interest, so we will assume that $(\omega + k_x\gamma/\sqrt{\alpha} + \sqrt{\alpha}/\gamma) \neq 0$. By differentiating (4.12d), the system of equations can be reduced to

$$\frac{d\widetilde{V}^2}{dy^2} - k_y^2 \widetilde{V} = 0, \tag{4.13}$$

with

$$k_y^2 = -k_x^2 R^2. \tag{4.14}$$

By using Eq. (4.12d) with the boundary conditions in Eqs. (4.10b) and (4.10c) we get

$$\frac{d\widetilde{V}}{dy}(0) = 0, \quad \frac{d\widetilde{V}}{dy}(1) = 0. \tag{4.15}$$

The general solution for Eq. (4.13) is

$$\widetilde{V} = C_1 \exp(k_y y) + C_2 \exp(-k_y y). \tag{4.16}$$

By applying the boundary conditions (4.15), this takes the form

$$\widetilde{V} = D\cosh(k_{y,m}y), \tag{4.17}$$

with $k_{y,m} = \pm i2\pi m$. Therefore, the general solution can be written as

$$\widetilde{V} = \sum_{m=0}^{\infty} D_m \cos(ik_{y,m}y). \tag{4.18}$$

It is easy to show that the proposed solution in Eq. (4.11) can satisfy the boundary conditions in Eqs. (4.10a) and (4.10d) independently of the value of k_y. Re-writing

$$\left\{\widetilde{V}\ \widetilde{n}\ \widetilde{u}\ \widetilde{v}\right\}^T = \left\{\widehat{V}\ \widehat{n}\ \widehat{u}\ \widehat{v}\right\}^T \exp\left(k_y y\right),$$

where the amplitudes denoted by $\widehat{\ }$ are also all complex, Eq. (4.9) becomes

$$\begin{bmatrix} -k_x^2 - k_y^2/R^2 & \alpha & 0 & 0 \\ 0 & \omega + k_x\gamma/\sqrt{\alpha} & k_x & k_y/R \\ -k_x & 0 & \omega + k_x\gamma/\sqrt{\alpha} + \sqrt{\alpha}/\gamma & 0 \\ -k_y/R & 0 & 0 & \omega + k_x\gamma/\sqrt{\alpha} + \sqrt{\alpha}/\gamma \end{bmatrix} \begin{Bmatrix} \widehat{V} \\ \widehat{n} \\ \widehat{u} \\ \widehat{v} \end{Bmatrix} = \begin{Bmatrix} 0 \\ 0 \\ 0 \\ 0 \end{Bmatrix}.$$

For a non-trivial solution, the determinant should vanish, so that the characteristic equation is

$$-(k_x^2R^2 + k_y^2)(\omega\sqrt{\alpha}\gamma + \gamma^2 k_x + \alpha)\left[\left(\omega + \frac{\gamma}{\sqrt{\alpha}}k_x\right)\left(\omega + \frac{\gamma}{\sqrt{\alpha}}k_x + \frac{\sqrt{\alpha}}{\gamma}\right) + \alpha\right] = 0. \tag{4.19}$$

The roots of Eq. (4.19) are

$$k_{x,1} = i\frac{k_y}{R}, \quad k_{x,2} = -i\frac{k_y}{R}, \quad k_{x,3} = a + ib, \quad k_{x,4} = a - ib, \tag{4.20}$$

where $a = -(\alpha/2\gamma^2)(2\gamma\omega/\sqrt{\alpha}+1)$ and $b = (\alpha/2\gamma^2)\sqrt{4\gamma^2-1}$. Since $k_{y,m} = \pm i2\pi m$, we have two cases.

4.2.1 $m \neq 0$

Now there are oscillations in both x and y directions. The modes in the x-direction are described in Eq. (4.20) and the modes in the y-direction are $k_{y,m} = \pm i2\pi m$. We can write the amplitudes of the perturbations as

$$
\begin{aligned}
V' &= \left[Ae^{ik_{y,m}x/R} + Be^{-ik_{y,m}x/R} + Ce^{k_{x,3}x} + De^{k_{x,4}x}\right] e^{k_y y+\omega t},\\
\frac{\partial V'}{\partial x} &= \left[Ai\frac{ik_{y,m}}{R}e^{ik_{y,m}x/R} - Bi\frac{k_{y,m}}{R}e^{-ik_{y,m}x/R} + Ck_{x,3}e^{k_{x,3}x} + Dk_{x,4}e^{k_{x,4}x}\right] e^{k_y y+\omega t},\\
n' &= \frac{1}{\alpha}\left[Ce^{k_{x,3}x}\left(k_{x,3}^2 + \frac{k_{y,m}^2}{R^2}\right) + De^{k_{x,4}x}\left(k_{x,4}^2 + \frac{k_{y,m}^2}{R^2}\right)\right] e^{k_y y+\omega t}.
\end{aligned}
$$

The boundary conditions in Eqs. (4.10a) and (4.10d) can be written as

$$
\begin{bmatrix}
1 & 1 & 1 & 1\\
e^{ik_{y,m}/R} & e^{-ik_{y,m}/R} & e^{k_{x,3}} & e^{k_{x,4}}\\
0 & 0 & k_{x,3}^2 + k_{y,m}^2/R^2 & k_{x,4}^2 + k_{y,m}^2/R^2\\
i\frac{k_{y,m}}{R}(1-e^{ik_{y,m}/R}) & -i\frac{k_{y,m}}{R}(1-e^{-ik_{y,m}/R}) & k_{x,3}(1-e^{k_{x,3}}) & k_{x,4}(1-e^{k_{x,4}})
\end{bmatrix}
\begin{Bmatrix} A\\ B\\ C\\ D \end{Bmatrix} = \begin{Bmatrix} 0\\ 0\\ 0\\ 0 \end{Bmatrix}.
$$

For a non-trivial solution the determinant must vanish, which gives

$$
\begin{aligned}
&\left((a+ib)^2 + \frac{k_{y,m}^2}{R^2}\right)\left[(a-ib)(1-e^{a-ib})\left(e^{-ik_{y,m}/R} - e^{ik_{y,m}/R}\right)\right.\\
&+i\frac{k_{y,m}}{R}\left(e^{a-ib} - e^{-ik_{y,m}/R}\right)\left(1-e^{ik_{y,m}/R}\right)\\
&\left.+i\frac{k_{y,m}}{R}\left(e^{a-ib} - e^{ik_{y,m}/R}\right)\left(1-e^{-ik_{y,m}/R}\right)\right]\\
&-\left((a-ib)^2 + \frac{k_{y,m}^2}{R^2}\right)\left[(a+ib)(1-e^{a+ib})\left(e^{-ik_{y,m}/R} - e^{ik_{y,m}/R}\right)\right.\\
&\left.+i\frac{k_{y,m}}{R}\left(e^{a+ib} - e^{-ik_{y,m}/R}\right)\left(1-e^{ik_{y,m}/R}\right)\right.
\end{aligned}
$$

$$+i\frac{k_{y,m}}{R}\left(e^{a+ib}-e^{ik_{y,m}/R}\right)\left(1-e^{-ik_{y,m}/R}\right)\Bigg]=0. \tag{4.21}$$

Eq. (4.21) is satisfied by

$$a+ib=\pm i\frac{k_{y,m}}{R},\quad a-ib=\pm i\frac{k_{y,m}}{R}.$$

If $b=\pm 2\pi p$, with p being a natural number, Eq. (4.21) is also satisfied by $a=0$. Due to the complexity of Eq. (4.21) other solutions may be possible, in which case the spectrum may include additional temporal modes. b may be real, zero, or imaginary if $4\gamma^2$ is grater than, equal to, or less than unity.

4.2.1.1 For $4\gamma^2 > 1$

The solution for ω is

$$\omega_m=\frac{\sqrt{\alpha}}{2\gamma}\left[\pm\frac{4\gamma^2\pi m}{\alpha R}-1\pm i\sqrt{4\gamma^2-1}\right], \tag{4.22}$$

which indicates temporal modes that are either growing or decaying with an oscillatory component. Also, if $b=\pm 2\pi p$, the temporal mode is $\omega=-\sqrt{\alpha}/2\gamma$.

4.2.1.2 For $4\gamma^2 \leq 1$

Now

$$\omega_m=\frac{\sqrt{\alpha}}{2\gamma}\left[\pm\frac{4\gamma^2\pi m}{\alpha R}-1\pm\sqrt{1-4\gamma^2}\right]. \tag{4.23}$$

In addition to this, if $b=\pm i2\pi p$, the temporal mode is $\omega=-\sqrt{\alpha}/2\gamma$. For $4\gamma^2\leq 1$, the temporal modes ω are real and therefore the evolution in time is either growing or decaying without oscillations. Furthermore, a and b are real, which implies no spatial oscillations. From the non-linear nature of the problem, the growth must

TABLE 4.1

TEMPORAL EIGENMODES

Condition	ω
$4\gamma^2 > 1$	$\omega = -\frac{\gamma}{\sqrt{\alpha}}\left[\frac{\alpha}{2\gamma^2} + b\cot b + W\left(-\frac{be^{-b\cot b}}{\sin b}\right)\right]$
$4\gamma^2 = 1$	$\omega = -\frac{\gamma}{\sqrt{\alpha}}\left[\frac{\alpha}{2\gamma^2} + 1 + W\left(-e^{-1}\right)\right]$
$4\gamma^2 < 1$	$\omega = -\frac{\gamma}{\sqrt{\alpha}}\left[\frac{\alpha}{2\gamma^2} + b'\coth b' + W\left(-\frac{b'e^{-b'\coth b'}}{\sinh b'}\right)\right]$

have an upper limit, though the linear analysis does not give this value.

4.2.2 $m = 0$

This represents oscillations only along the x-direction. That is the one-dimensional uncoupled problem and a complete treatment of this has been described in Chapter 3 and also in [68]. The temporal modes are described by Lambert W functions[1]. There are three operating conditions which can be determined by the value of $4\gamma^2$. This also defines the nature of the spatial modes in the x-direction: no oscillations (purely real), constant amplitude oscillations (purely imaginary) and oscillations with spatial growth or decay (complex). By requiring a non-trivial solution over a wave-like solution for the perturbed system, the temporal modes are obtained. The solutions of Eq. (4.21) are in Table 4.1, where $b' = (\alpha\sqrt{1-4\gamma^2})/2\gamma^2$.

[1]The Lambert W-function is defined as the solution of the equation $W(z_*)e^{W(z_*)} = z_*$.

4.3 Discussion

4.3.1 Spectrum of eigenmodes

The spectrum presents both stable and unstable regions. It is tunable mainly through the applied voltage, but the aspect ratio R can also determine instability when we have spatial oscillations along the y-direction, i.e. if $k_{y,m} \neq 0$. Since $k_{y,m}$ is purely imaginary, we get oscillations along the y-direction with a constant amplitude in space. The number of oscillatory spatial modes over a range of spatial mode amplitudes is independent of the value of the oscillatory component for $k_{y,m} = 0$. Otherwise, for $k_{y,m} \neq 0$ this number presents two delta functions at $\omega_i = \pm\sqrt{\omega_p - 1/4\tau_p^2}$. Taking $4\gamma^2 > 1$, the spectrum for GaAs is shown in Fig. 4.2.

4.3.2 Aspect ratio dependency

We are interested in imaginary components of the temporal modes ω, which describe the oscillatory behavior in time. Given an aspect ratio R, there is a critical positive mode above which the system is unstable. From Eq. (4.22), the critical positive mode is

$$m^c = \frac{\alpha R}{4\gamma^2 \pi}. \tag{4.24}$$

Moreover, this critical mode can be written in terms of the plasma frequency as

$$m^c = \frac{\alpha R}{4\pi(\omega_p \tau_p)^2}. \tag{4.25}$$

It can also be written as

$$m^c = \frac{1}{\overline{u}^*}\left(\frac{H}{4\pi\tau_p}\right). \tag{4.26}$$

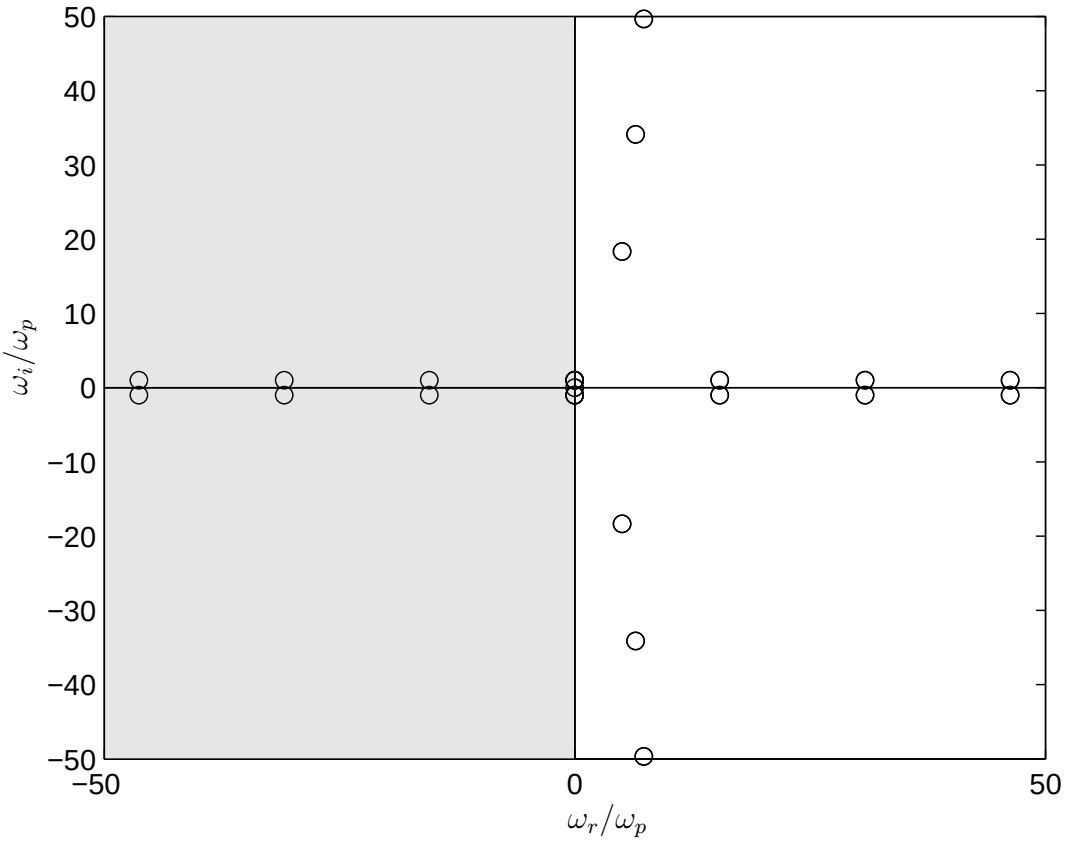

Figure 4.2. Spectrum of eigenvalues for GaAs semiconductor where effective mass of electron = 6.6% of its actual mass, $\epsilon_s = 113.28 \times 10^{-12}$ $C^2/(m^2\ N)$, $L = 100$ nm, $n_0 = 5 \times 10^{17}$ cm^{-3}, $N_D = 5 \times 10^{17}$ cm^{-3}, $\tau_p = 0.4 \times 10^{-12}$ s and $V_0 = 1$ V, which gives $\alpha = 7.072$, $\gamma = 17.365$ and $\omega_p = 43.41 \times 10^{12}$ s^{-1}. The shaded area represents the stable region and the unshaded the unstable.

As an example, choosing $\alpha = 10$, $\gamma = 1$ and $R = 1$ we get $m^c \sim 0.8$, therefore $m \geq 1$ guaranties an unstable regime. As is shown in in Fig. 4.3, which describes the evolution of electron density and electric field through the first period of oscillations in time for a configuration with $R = 0.5$, the first unstable mode is $m = 1$. When $R = 1$, the first unstable mode is $m = 1$ and the evolution of electron density and electric field are shown in Fig. 4.4. Otherwise, when $R = 2$ the first unstable mode is $m = 2$ as is shown in Fig. 4.5. It illustrates how the first unstable mode is determined by R. The magnitude of the oscillatory components of the spectrum for $k_{y,m} \neq 0$ is $\sqrt{\omega_p^2 - 1/4\tau_p^2}$. It depends only on material parameters through γ and τ_p, and tends to the plasma frequency ω_p in the ballistic limit $\tau_p \to \infty$. This limit is reached when there is a very low electron-impurity scattering.

4.3.3 Dispersion relation

By definition, the dispersion relation provides a relationship between the oscillatory component of the temporal modes, ω_i, and the oscillatory component of the spatial modes, k_{xi} and k_{y_i}. Many situations of physical interest may have multiple and discrete roots of ω_i. In the proposed problem, the relation can be obtained from Eq. (4.19).

For $4\gamma^2 > 1$, the dispersion relation takes the form

$$\frac{\alpha}{2\gamma^2}\left[-\frac{2\gamma\omega_i}{\sqrt{\alpha}} \pm \sqrt{4\gamma^2 - 1}\right] - k_{xi} = 0. \tag{4.27}$$

This linear relationship between ω_i and k_{xi} is two parallel lines as shown in Fig. 4.6. The values of ω_i are determined by Eq. (4.22) and the corresponding value

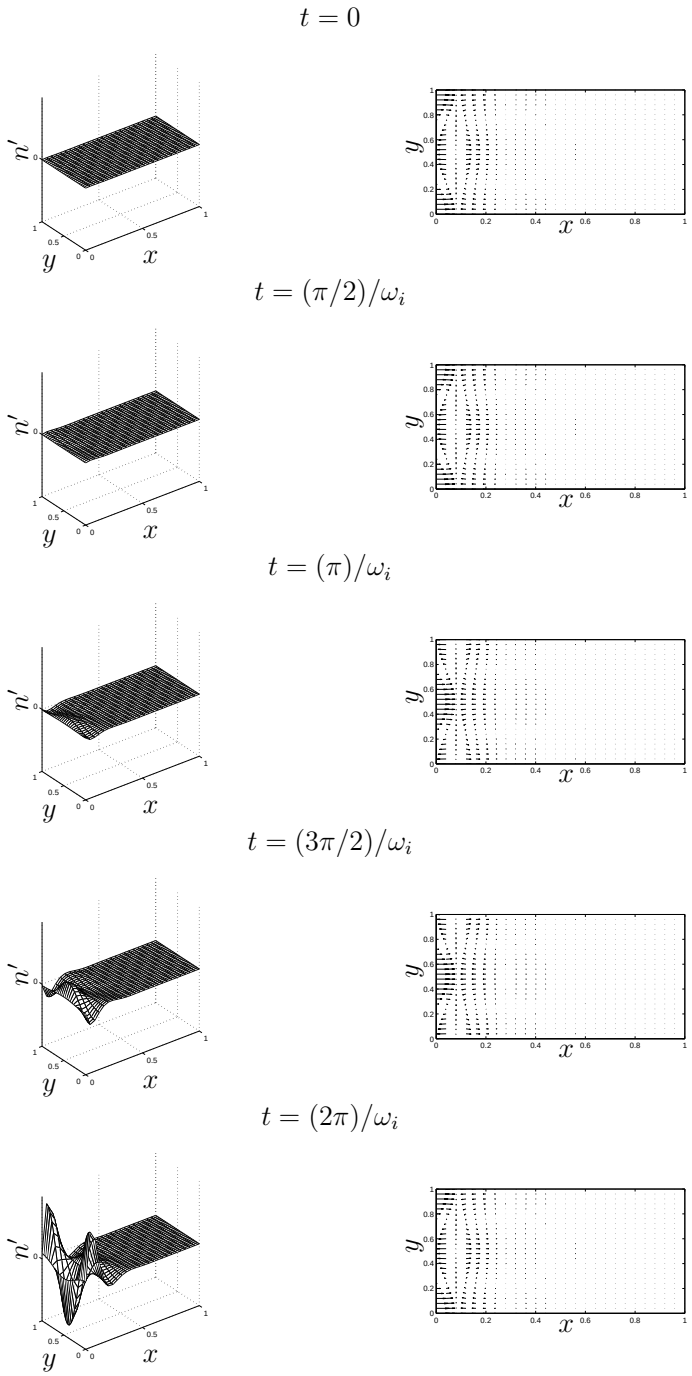

Figure 4.3. Electron density eigenfunction (left) and electric field (right) for $\alpha = 10$, $\gamma = 1$, $R = 0.5$ and $\omega_i \sim 0.87\omega_p$ (arbitrary scale) at the first unstable eigenmode $m = 1$.

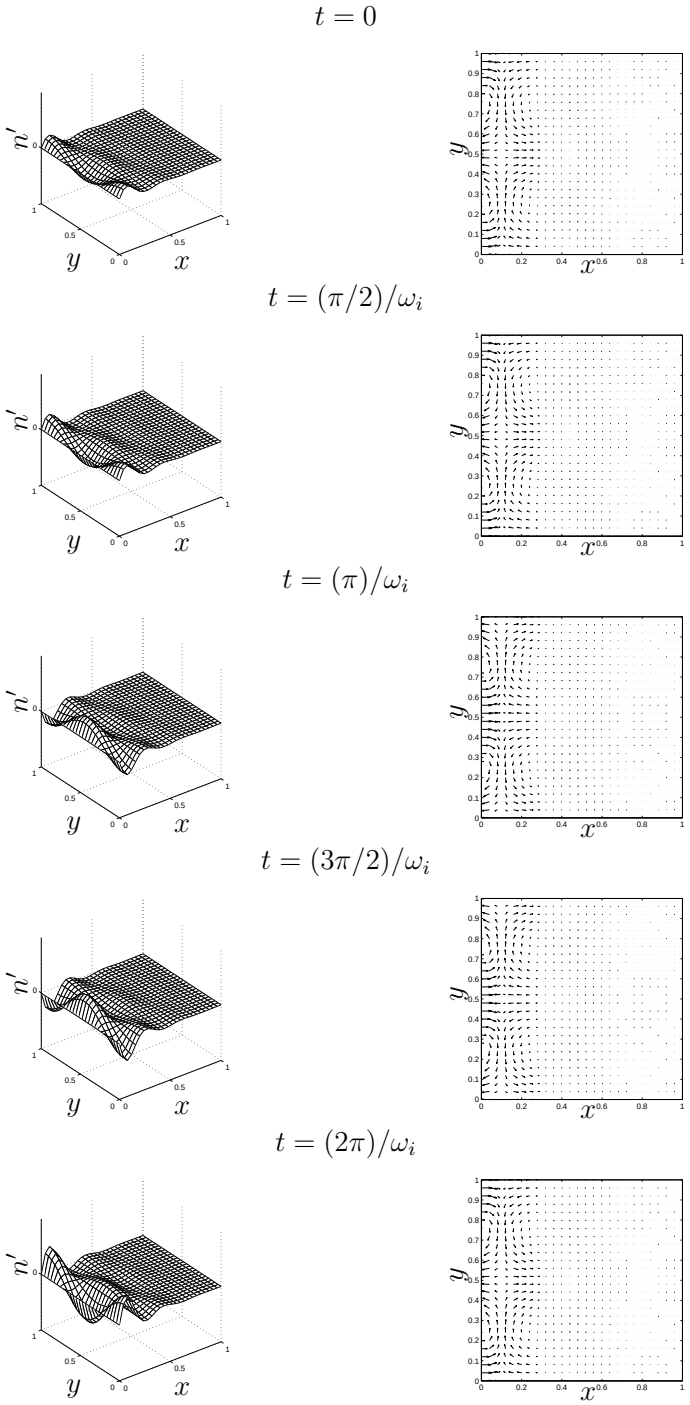

Figure 4.4. Electron density eigenfunction (left) and electric field (right) for $\alpha = 10$, $\gamma = 1$, $R = 1$ and $\omega_i \sim 0.87\omega_p$ (arbitrary scale) at the first unstable eigenmode $m = 1$.

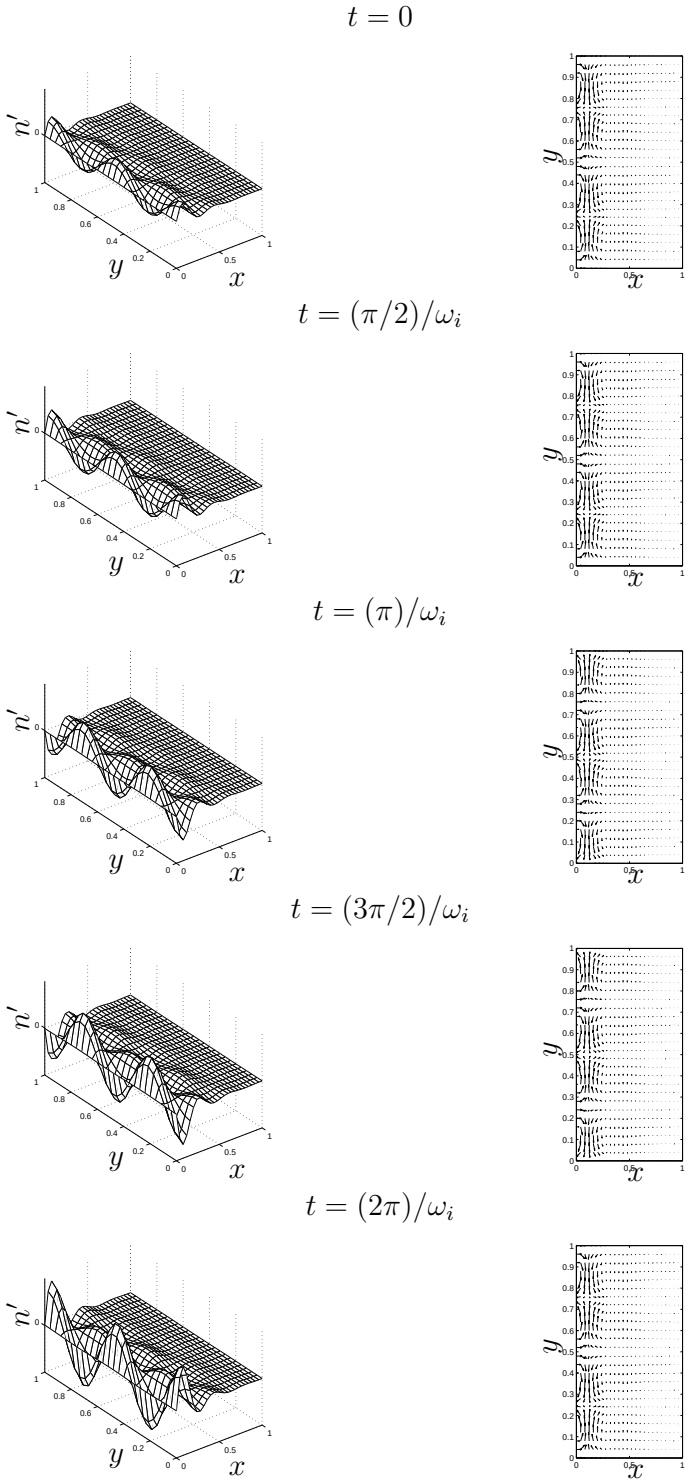

Figure 4.5. Electron density eigenfunction (left) and electric field (right) for $\alpha = 10$, $\gamma = 1$, $R = 2$ and $\omega_i \sim 0.87\omega_p$ (arbitrary scale) at the first unstable eigenmode $m = 2$.

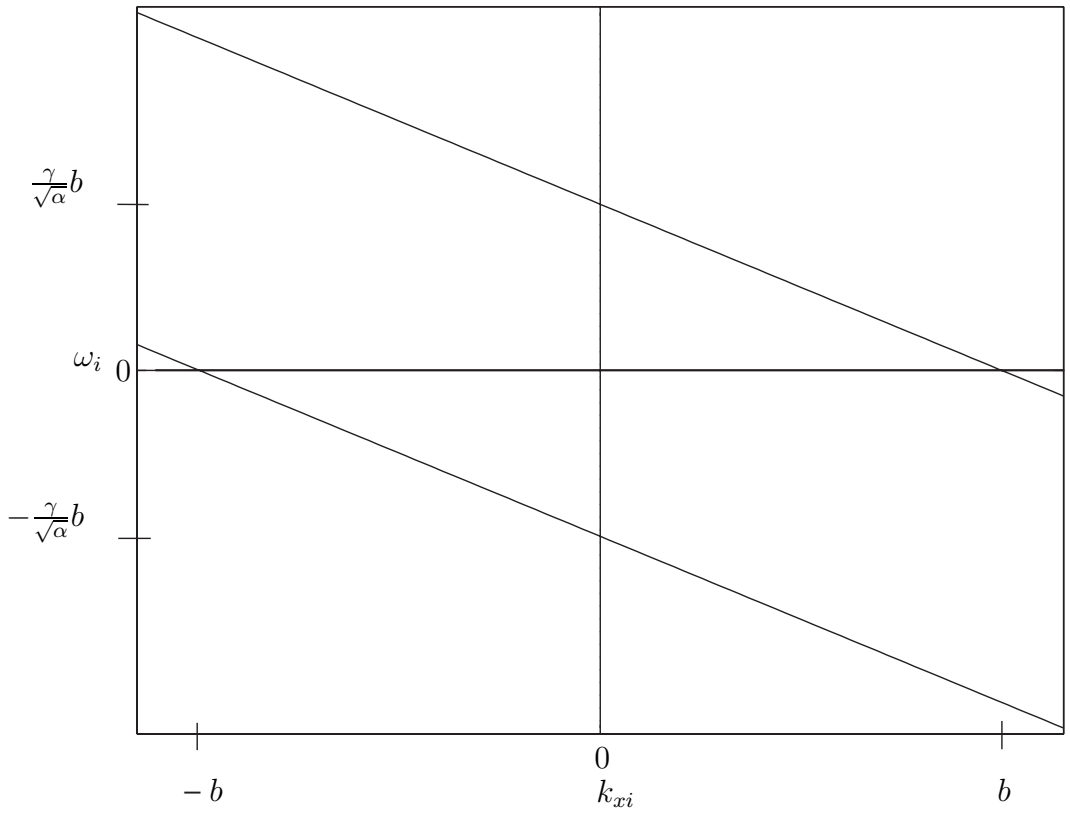

Figure 4.6. Dispersion relation for $4\gamma^2 > 1$.

in Table 4.1. From this, the phase and group velocities can be deduced to be

$$v_p = \frac{\gamma}{\sqrt{\alpha}} \frac{2\gamma\omega_i}{2\gamma\omega_i + \sqrt{\alpha(4\gamma^2 - 1)}}, \tag{4.28}$$

$$v_g = \frac{\gamma}{\sqrt{\alpha}}, \tag{4.29}$$

respectively.

For $4\gamma^2 \leq 1$, the expression for the dispersion relation is

$$\frac{\sqrt{\alpha}\omega_i}{\gamma} + k_{xi} = 0. \tag{4.30}$$

The relation is linear as in the previous case, but it is just one straight line crossing the origin, as shown in Fig. 4.7. This expression is just valid for $k_{y,m} = k_{y,0} = 0$ since $\omega_i \neq 0$, otherwise for $k_{y,m} \neq 0$, $\omega_i = 0$. From this, the phase and group velocities can be deduced to be

$$v_p = \frac{\gamma}{\sqrt{\alpha}}, \tag{4.31}$$

$$v_g = \frac{\gamma}{\sqrt{\alpha}}, \tag{4.32}$$

respectively. It can be noticed that the steady-state electron velocity in Eq. (4.8) and the group velocity of the instability waves are equal.

4.4 Conclusions

The instabilities in the hydrodynamic model of a two-dimensional electron flow in ungated semiconductors are analyzed. Analytical expressions for the spatial and

temporal plasma oscillation modes are derived. The spectrum of temporal modes

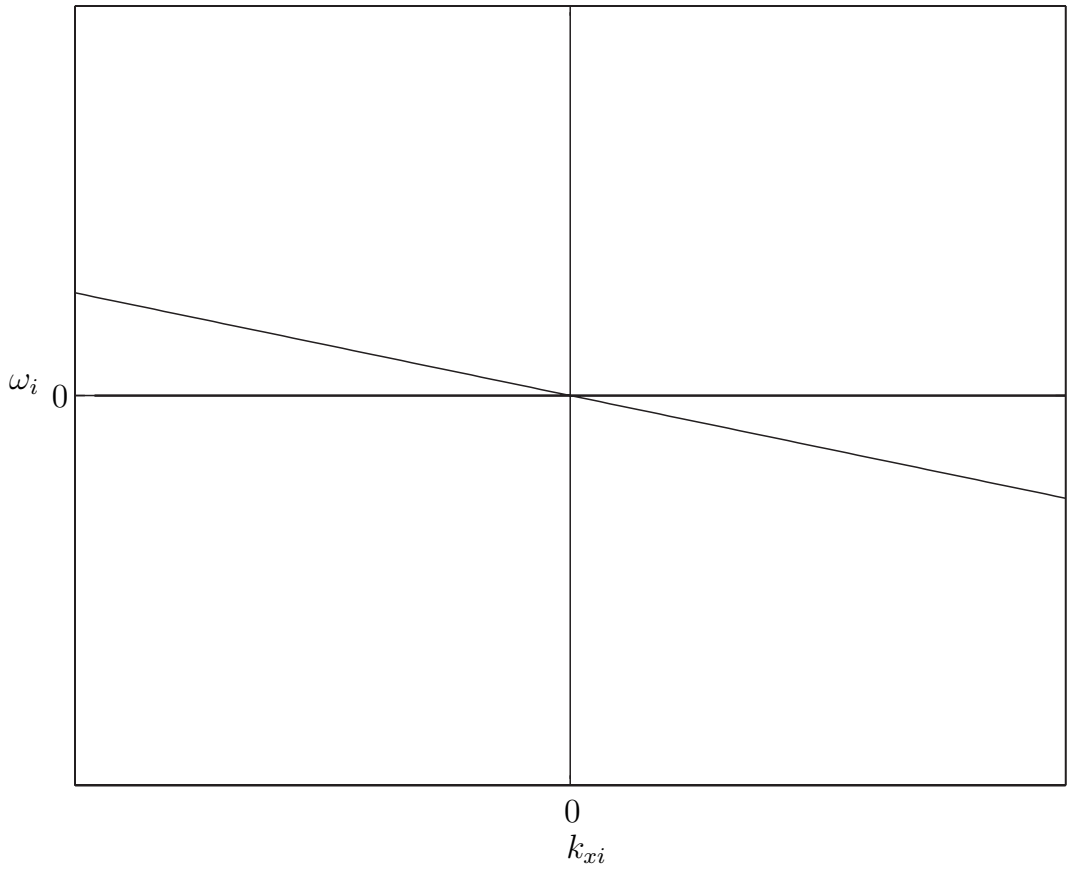

Figure 4.7. Dispersion relation for $4\gamma^2 \leq 1$.

shows a predominant unstable region, which depends strongly in the applied voltage through the semiconductor. As the applied voltage decreases, the spectrum is more stable. Also, the aspect ratio determines how unstable the temporal modes can be. As the aspect ratio decreases, the unstable modes become more unstable. The unstable region, which means temporal modes with positive real component, has oscillatory components able to describe terahertz frequencies under specific parameter values.

The spectrum of temporal modes and how they are determined by parameters such as the aspect ratio and the applied voltage, play a fundamental role in understanding and controlling the charged-particle interaction in solid state devices. Also, the spectrum of temporal modes gives the operating condition which can be obtained under the right set up of parameter such voltage and doping density, among others. All of this is very important to support semiconductors in a two-dimensional configuration (such as in a High Electron Mobility Transistor structure) as a radiative source. The theoretical formalism presented extends the earlier works on the subject by revealing a spectrum of both stable and unstable modes for plasma-mode oscillations, and presents a direct method for analyzing their dependence on the material and geometrical parameters of the device. This will prove to be valuable in the design process of compact electronic THz sources of the future.

CHAPTER 5

ONE-DIMENSIONAL ANALYSIS WITH THERMAL COUPLING

5.1 Introduction

In this Chapter we perform the linear stability analysis in three models: two-temperature, one-temperature with collision and one-temperature without collision. This is designed to determine the influence of heat conduction and energy loss due to scattering of the electrons on the stability of the electron flow in ungated semiconductors.

5.2 One-dimensional problem

There are several semiconductor geometries and operating conditions that can be modeled and studied in one dimension or in the predominant direction of electron transport. In the one-dimensional problem, the voltage drop, temperature changes and transport of electrons are just allowed along the x-direction. The variations in y and z are neglected. The schematic of the one-dimensional configuration is the same that was studied in the Chapter 3 and is shown in Fig. 3.1.

5.3 Two-temperature model

Here we consider the effects of heat conduction and energy loss due to the different scattering events present in the process of electron transport in the semiconductor. We consider the model described in Chapter 2 where the constitutive energy balance equations for the longitudinal optical and acoustic phonons are rewritten as the lattice energy conservation equation that relates the energy loss of the electrons with the lattice temperature due to collisions. The equations are taken from Section A.5.

5.3.1 Governing equations

The one-dimensional model equations [10, 22, 23, 40] with thermal coupling are

$$\text{Gauss} \quad \frac{\partial^2 V^*}{\partial x^{*2}} = -\frac{e}{\epsilon_s}\left(N_D - n^*\right), \tag{5.1a}$$

$$\text{Continuity} \quad \frac{\partial n^*}{\partial t^*} + \frac{\partial (u^* n^*)}{\partial x^*} = 0, \tag{5.1b}$$

$$\text{Momentum} \quad \frac{\partial u^*}{\partial t^*} + u^* \frac{\partial u^*}{\partial x^*} = \frac{e}{m_e}\frac{\partial V^*}{\partial x^*} - \frac{1}{n^* m_e}\frac{\partial (n^* k_B T_e^*)}{\partial x^*} - \frac{u^*}{\tau_p}, \tag{5.1c}$$

$$\begin{aligned}\text{Electron energy} \quad \frac{\partial T_e^*}{\partial t^*} + u^* \frac{\partial T_e^*}{\partial x^*} = &-\frac{2}{3} T_e^* \frac{\partial u^*}{\partial x^*} + \frac{2}{3 n^* k_B}\frac{\partial}{\partial x^*}\left(k_e \frac{\partial T_e^*}{\partial x^*}\right) \\ &- \frac{T_e^* - T_L^*}{\tau_E} + \frac{2 m_e (u^{*2})}{3 k_B \tau_p}\left(1 - \frac{\tau_p}{2\tau_E}\right),\end{aligned} \tag{5.1d}$$

$$\begin{aligned}\text{Lattice energy} \quad C_L \frac{\partial T_L^*}{\partial t^*} = &\frac{\partial}{\partial x^*}\left(k_L \frac{\partial T_L^*}{\partial x^*}\right) + \frac{3 n^* k_B}{2}\left(\frac{T_e^* - T_L^*}{\tau_E}\right) \\ &+ \frac{n^* m_e}{2\tau_E}\left(u^{*2}\right)\end{aligned} \tag{5.1e}$$

where $V^*(x^*, t^*)$ is the voltage, $n^*(x^*, t^*)$ is the electron concentration, $u^*(x^*, t^*)$ is the x-component electron drift velocity, $T_e^*(x^*, t^*)$ is the electron temperature,

$T_L^*(x^*, t^*)$ is the lattice temperature (acoustic phonon), e is the electron charge, ϵ_s is the permittivity of the semiconductor, N_D is the doping concentration, m_e is the effective electron mass k_B is the Boltzmann constant, k_e is the electronic thermal conductivity, k_L is the lattice thermal conductivity (acoustic phonon), τ_p is the momentum relaxation time, τ_E is the energy relaxation time and C_L is the heat capacity for lattice (acoustic phonon). In this analysis we consider k_e, k_L, τ_E and C_L as constant values. The momentum relaxation time, τ_p, is expressed as in Eq. (2.3).

5.3.2 Boundary conditions

The dimensional form of the boundary conditions to be considered is as follows

$$V^*(0, t^*) = -V_0, \quad V^*(L, t^*) = 0, \quad n^*(0, t^*) = n_0, \quad \frac{\partial V^*}{\partial x^*}(0, t^*) = \frac{\partial V^*}{\partial x^*}(L, t^*), \tag{5.2a}$$

$$T_e^*(0, t^*) = T_1, \tag{5.2b}$$

$$\frac{\partial T_e^*}{\partial x^*}(L, t^*) = 0, \tag{5.2c}$$

$$T_L^*(0, t^*) = T_2, \tag{5.2d}$$

$$T_L^*(L, t^*) = T_3. \tag{5.2e}$$

These conditions include an imposed external electric field, a constant electron density at the source, the charge neutrality condition through the semiconductor, a constant electron temperature at the source and an adiabatic condition at the drain, and an imposed lattice temperature at both the source and the drain.

5.3.3 non-dimensionalization

For convenience, dimensionless versions of the governing equations (5.1) are obtained. By writing V, n, x, u and t as in Section 3.1, and $T_e = (T_e^* - T_{room})k_B/eV_0$ and $T_L = (T_L^* - T_{room})k_B/eV_0$, the non-dimensional version of Eqs. (5.1) is

$$\frac{\partial^2 V}{\partial x^2} - \alpha\,(n-1) = 0, \tag{5.3a}$$

$$\frac{\partial n}{\partial t} + \frac{\partial (un)}{\partial x} = 0, \tag{5.3b}$$

$$\frac{\partial u}{\partial t} + u\frac{\partial u}{\partial x} - \frac{\partial V}{\partial x} + \frac{\beta}{n}\frac{\partial n}{\partial x} + \frac{\partial T_e}{\partial x} + \frac{T_e}{n}\frac{\partial n}{\partial x} + \left(\frac{T_e+\beta}{T_L+\beta}\right)\frac{\sqrt{\alpha}}{\gamma_{pn}}u = 0, \tag{5.3c}$$

$$\begin{aligned}\frac{\partial T_e}{\partial t} + u\frac{\partial T_e}{\partial x} + \frac{2}{3}\beta\frac{\partial u}{\partial x} + \frac{2}{3}T_e\frac{\partial u}{\partial x} - \frac{2}{3}\frac{\sigma}{n}\frac{\partial^2 T_e}{\partial x^2} + \frac{\sqrt{\alpha}}{\gamma_E}(T_e - T_L)\\ -\frac{2}{3}\left(\frac{T_e+\beta}{T_L+\beta}\right)\frac{\sqrt{\alpha}}{\gamma_{pn}}u^2 + \frac{1}{3}\frac{\sqrt{\alpha}}{\gamma_E}u^2 = 0,\end{aligned} \tag{5.3d}$$

$$\frac{\partial T_L}{\partial t} - \theta_1\frac{\partial^2 T_L}{\partial x^2} - \theta_2 n\left(T_e - T_L - \frac{1}{3}u^2\right) = 0, \tag{5.3e}$$

where the dimensionless parametric groups are $\alpha = eN_DL^2/V_0\epsilon_s$, $\beta = k_BT_{room}/eV_0$, $\sigma = (k_e/N_Dk_BL^2)\sqrt{m_eL^2/eV_0}$, $\gamma_{pn} = \sqrt{m_e\mu_{no}^2N_D/\epsilon_s}$, $\gamma_E = \sqrt{\tau_E^2e^2N_D/m_e\epsilon_s}$, $\theta_1 = (k_L/L^2C_L)\sqrt{m_eL^2/eV_0}$ and $\theta_2 = (3N_Dk_B/2\tau_EC_L)\sqrt{m_eL^2/eV_0}$. T_{room} is the room temperature.

The dimensionless version of boundary conditions in Eqs. (5.2) is as follows

$$V(0,t) = -1, \quad V(1,t) = 0, \quad n(0,t) = 1, \quad \frac{\partial V}{\partial x}(0,t) = \frac{\partial V}{\partial x}(1,t), \tag{5.4a}$$

$$T_e(0,t) = (T_1 - T_{room})k_B/eV_0, \tag{5.4b}$$

$$\frac{\partial T_e}{\partial x}(1,t) = 0, \tag{5.4c}$$

$$T_L(0,t) = (T_2 - T_{room})k_B/eV_0, \tag{5.4d}$$

$$T_L(1,t) = (T_3 - T_{room})k_B/eV_0. \tag{5.4e}$$

5.3.4 Steady-state solution

The steady-state version of the system of Eqs. (5.3) is as follows,

$$\frac{d^2\overline{V}}{dx^2} - \alpha\,(\overline{n} - 1) = 0, \tag{5.5a}$$

$$\frac{d(\overline{un})}{dx} = 0, \tag{5.5b}$$

$$\overline{u}\frac{d\overline{u}}{dx} - \frac{d\overline{V}}{dx} + \frac{\beta}{\overline{n}}\frac{d\overline{n}}{dx} + \frac{d\overline{T}_e}{dx} + \frac{\overline{T}_e}{\overline{n}}\frac{d\overline{n}}{dx} + \left(\frac{\overline{T}_e + \beta}{\overline{T}_L + \beta}\right)\frac{\sqrt{\alpha}}{\gamma_{pn}}\overline{u} = 0, \tag{5.5c}$$

$$\begin{aligned}\overline{u}\frac{\partial\overline{T}_e}{\partial x} + \frac{2}{3}\beta\frac{\partial\overline{u}}{\partial x} + \frac{2}{3}\overline{T}_e\frac{\partial\overline{u}}{\partial x} - \frac{2}{3}\frac{\sigma}{\overline{n}}\frac{\partial^2\overline{T}_e}{\partial x^2} + \frac{\sqrt{\alpha}}{\gamma_E}(\overline{T}_e - \overline{T}_L)\\ -\frac{2}{3}\left(\frac{\overline{T}_e + \beta}{\overline{T}_L + \beta}\right)\frac{\sqrt{\alpha}}{\gamma_{pn}}\overline{u}^2 + \frac{1}{3}\frac{\sqrt{\alpha}}{\gamma_E}\overline{u}^2 = 0,\end{aligned} \tag{5.5d}$$

$$\theta_1\frac{\partial^2\overline{T}_L}{\partial x^2} - \theta_2\overline{n}\left(\overline{T}_e - \overline{T}_L - \frac{1}{3}\overline{u}^2\right) = 0. \tag{5.5e}$$

Based on experimental results [94, 95], the voltage varies linearly with x and as consequence the electron density and electron velocity are constant. We solve numerically the system of Eqs. (5.5) for the electron velocity, the electron temperature and lattice temperature by using Mathematica. To do this, we consider the physical properties for GaAs shown in Table 5.1, the non-dimensional parameters in Table 5.2 and the following values for the temperature boundary conditions

$$T_1 = 2250 \text{ K},$$

$$T_2 = 301 \text{ K},$$

$$T_3 = 346 \text{ K}.$$

TABLE 5.1

PHYSICAL PROPERTIES FOR GaAs

Constant	*Value*
L	100 nm
e	$1.60218 \cdot 10^{-19}$ C
ϵ_s	$12.8 \cdot 8.85 \cdot 10^{-12}$ C^2/(N m^2)
k_B	$1.38066 \cdot 10^{-23}$ J/K
k_e	3 W/(m K)
k_L	42.61 W/(m K)
N_D	$5 \cdot 10^{17}$ cm^{-3}
m_e	$6.01 \cdot 10^{-32}$ kg
V_0	1.0 V
T_{room}	300 K
C_L	$8.73 \cdot 10^5$ J/(m^3 K)
τ_E	5 ps
μ_{no}	4500 cm^2/(V s)

TABLE 5.2

DIMENSIONLESS PARAMETERS FOR GaAs

Parameter	*Value*
α	7.072
γ_{pn}	7.331
γ_E	217.057
β	0.026
σ	2.662
θ_1	$2.989 \cdot 10^{-4}$
θ_2	$1.453 \cdot 10^{-7}$

The analytical solutions for $\overline{V}$, $\overline{n}$ and $\overline{u}$ are detailed in Eqs. (5.6) and are shown in Figs. 5.1, 5.2 and 5.3, and their dimensional versions in Figs. 5.6, 5.7 and 5.8, respectively. The numerical solutions for $\overline{T}_e$ and $\overline{T}_L$ are shown in Figs. 5.4 and 5.5, and their dimensional versions in Figs. 5.9 and 5.10, respectively.

The solutions for $\overline{V}$, $\overline{n}$ and $\overline{u}$ are

$$\overline{V}(x) = x - 1, \tag{5.6a}$$

$$\overline{n}(x) = 1, \tag{5.6b}$$

$$\overline{u}(x) = \frac{1}{3}. \tag{5.6c}$$

Therefore, the solutions for $\overline{V}^*$, $\overline{n}^*$ and $\overline{u}^*$ are

$$\overline{V}^*(x^*) = \left(\frac{x^*}{L} - 1\right) V_0, \tag{5.7a}$$

$$\overline{n}^*(x^*) = N_D, \tag{5.7b}$$

$$\overline{u}^*(x^*) = \frac{1}{3}\sqrt{\frac{eV_0}{m_e}}. \tag{5.7c}$$

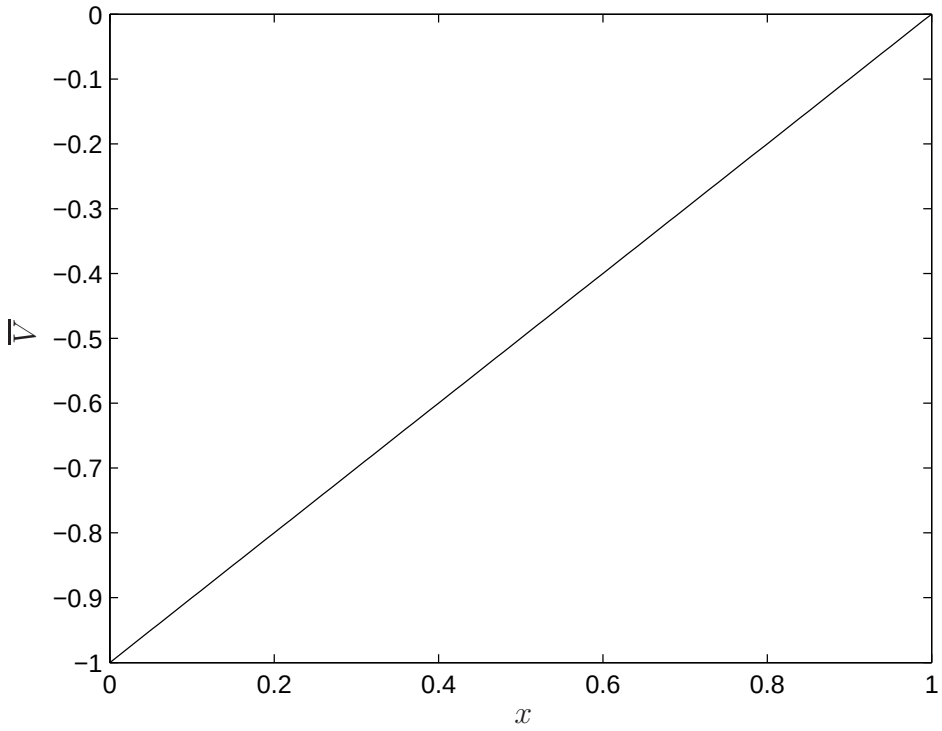

Figure 5.1. Two-temperature model; non-dimensional voltage distribution.

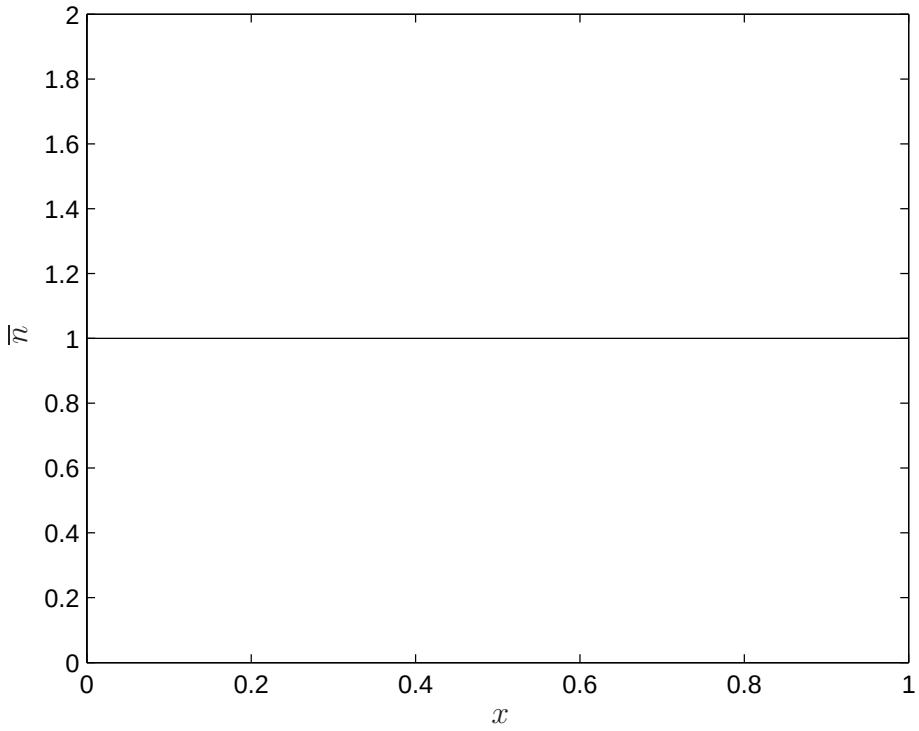

Figure 5.2. Two-temperature model; non-dimensional electron density distribution.

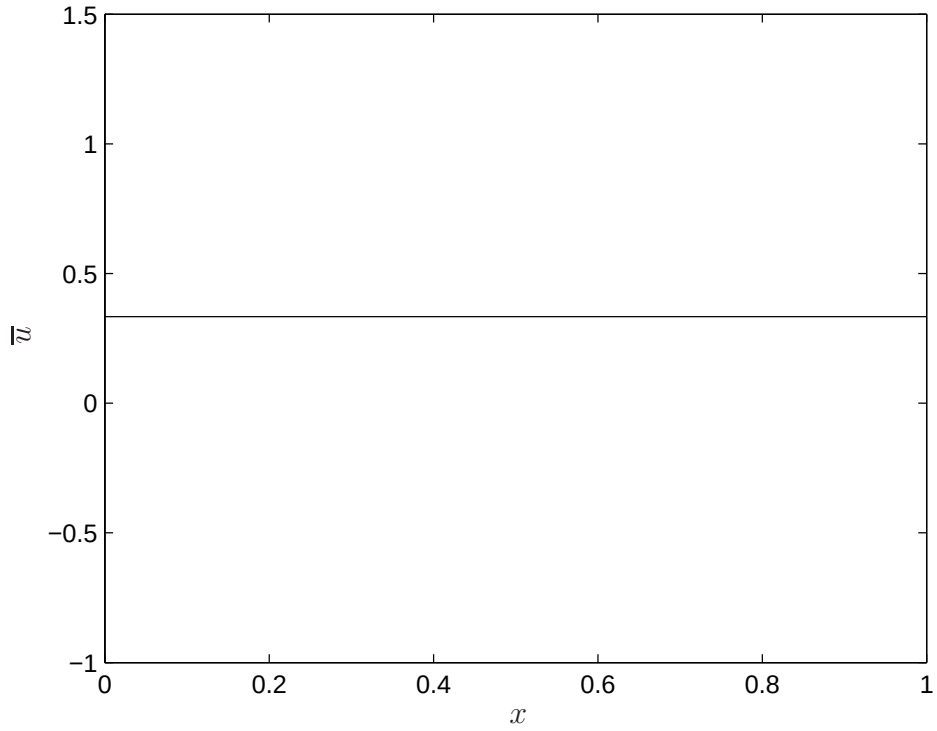

Figure 5.3. Two-temperature model; non-dimensional electron velocity distribution.

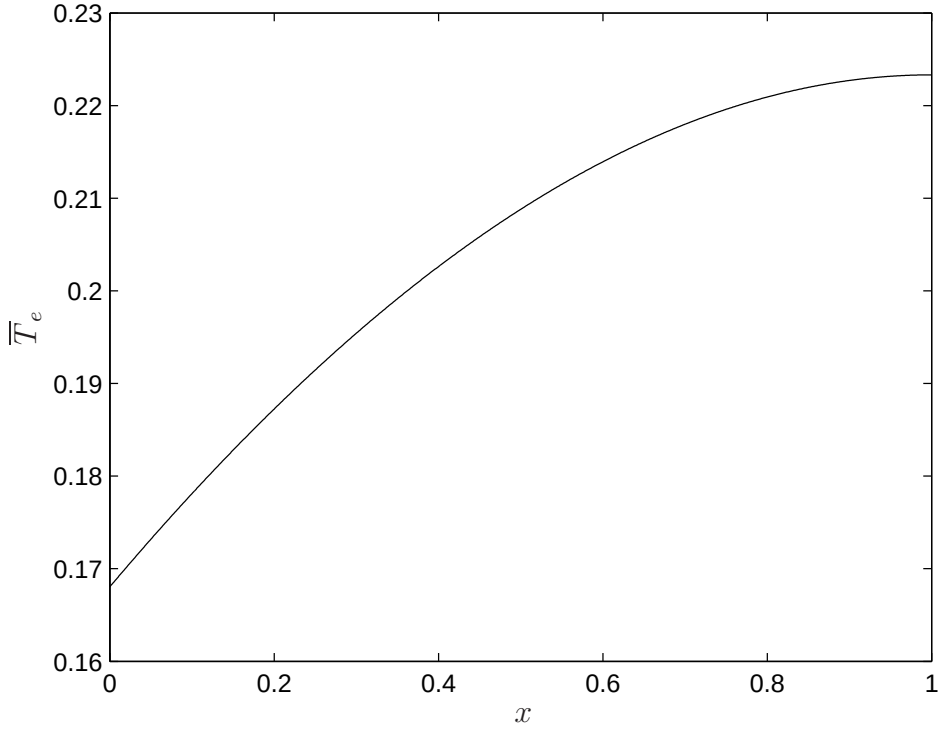

Figure 5.4. Two-temperature model; non-dimensional electron temperature distribution.

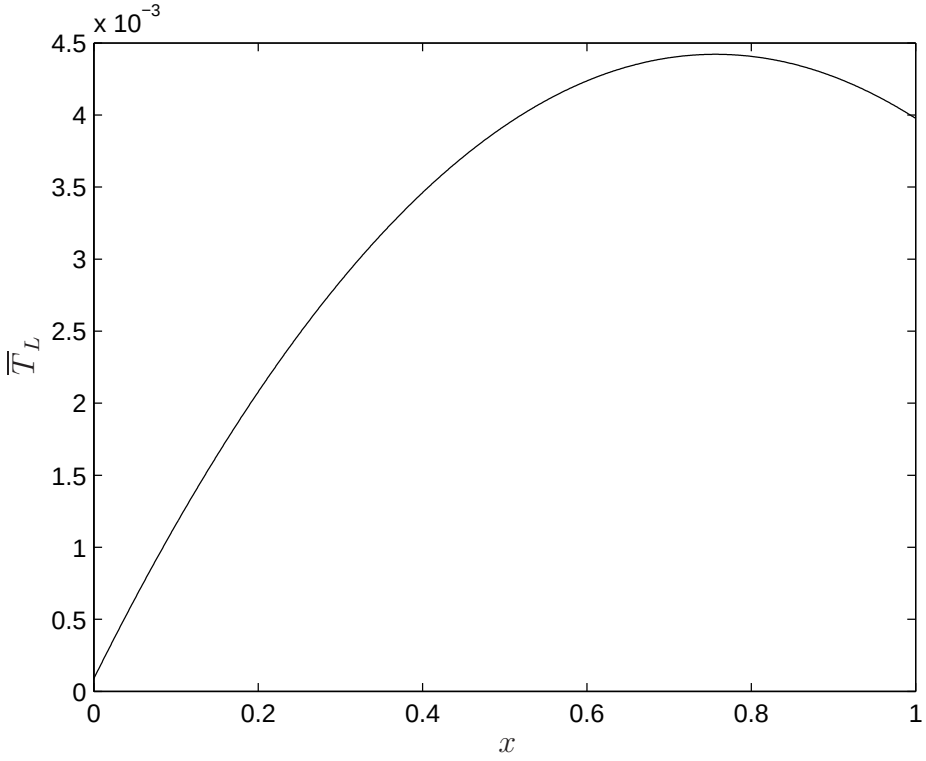

Figure 5.5. Two-temperature model; non-dimensional lattice temperature distribution.

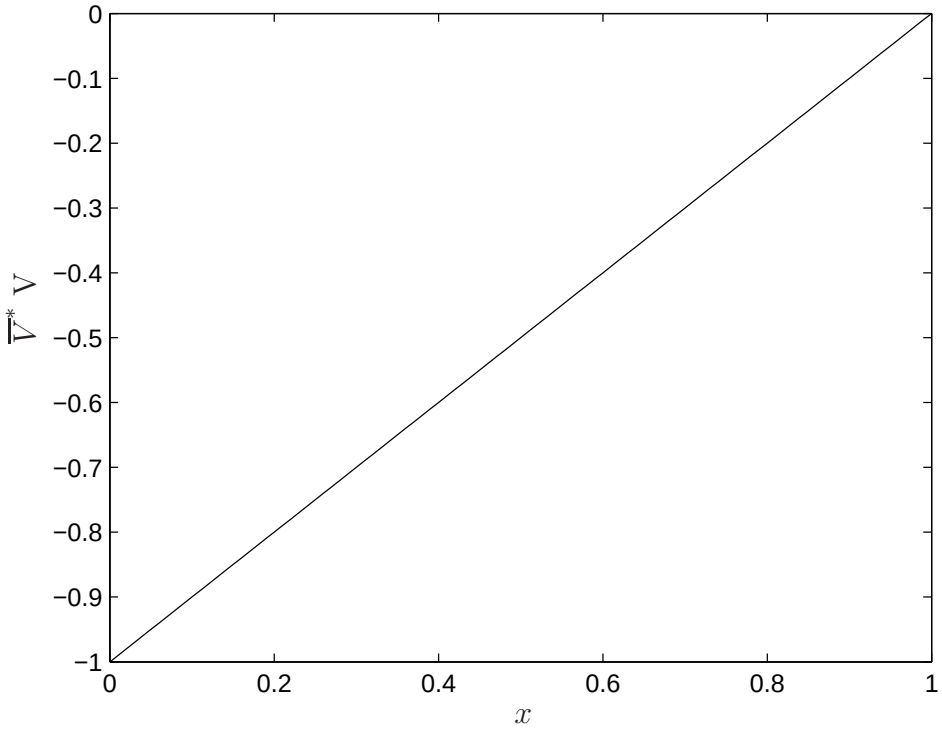

Figure 5.6. Two-temperature model; voltage distribution.

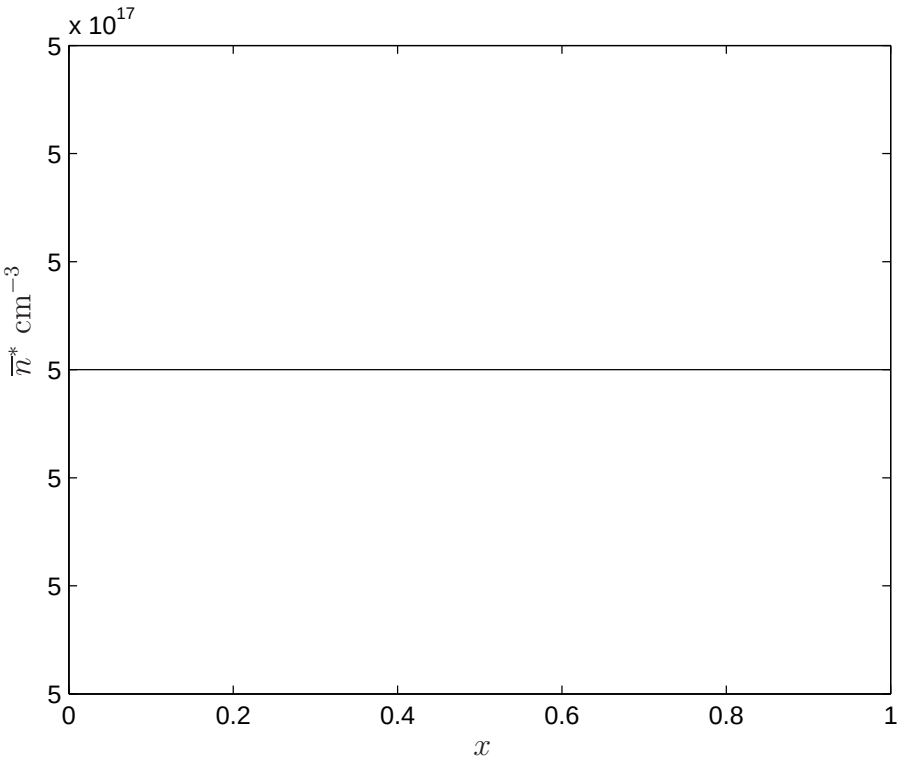

Figure 5.7. Two-temperature model; electron density distribution.

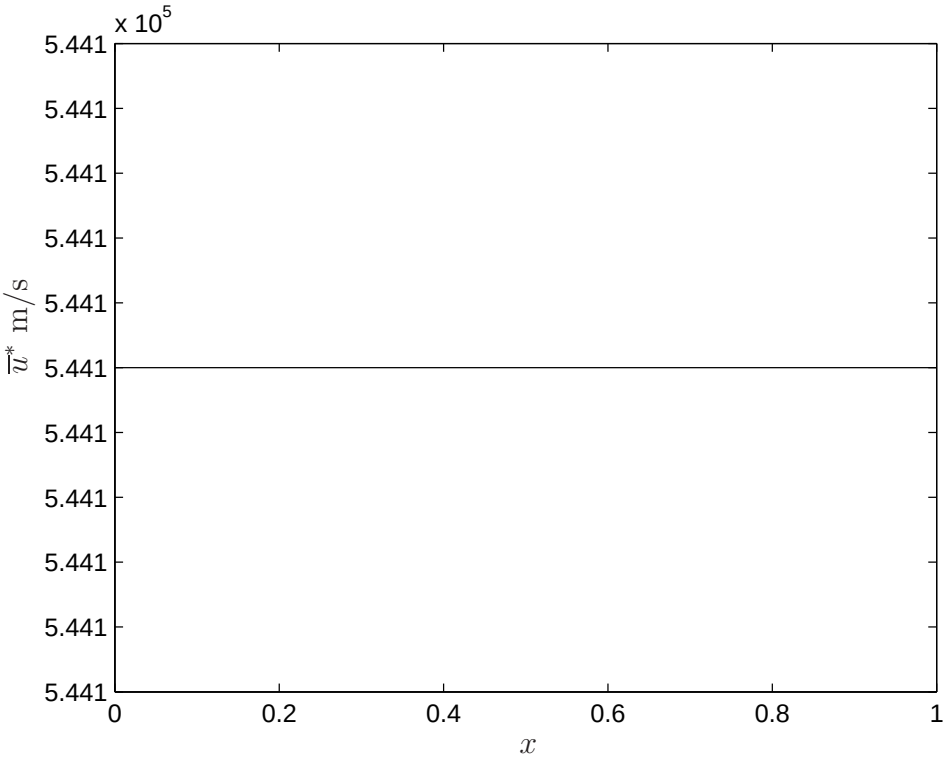

Figure 5.8. Two-temperature model; electron velocity distribution.

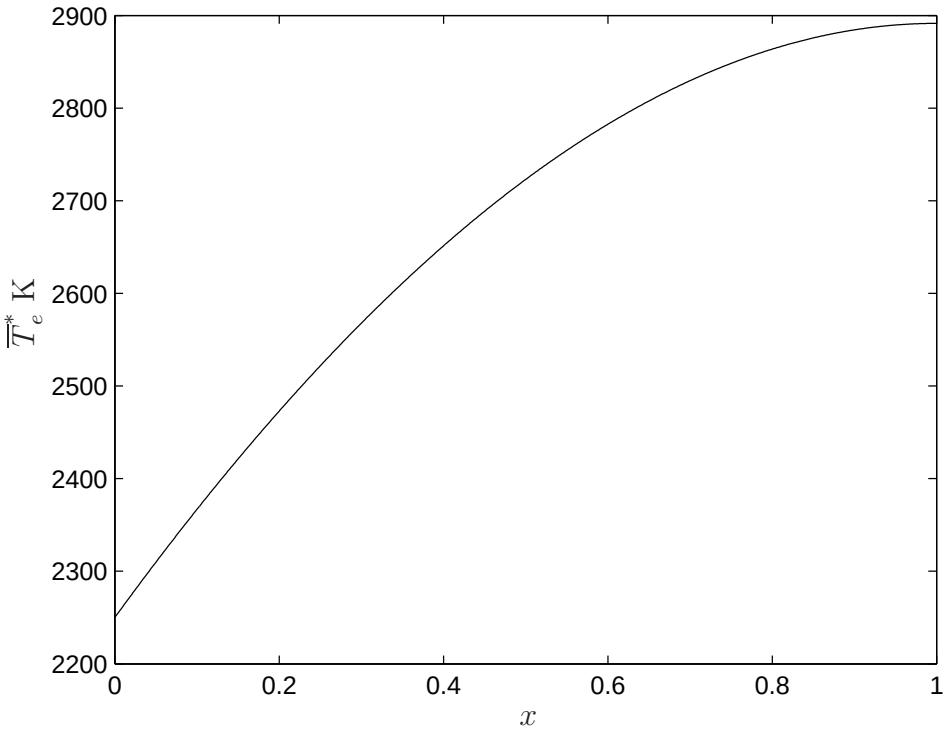

Figure 5.9. Two-temperature model; electron temperature distribution.

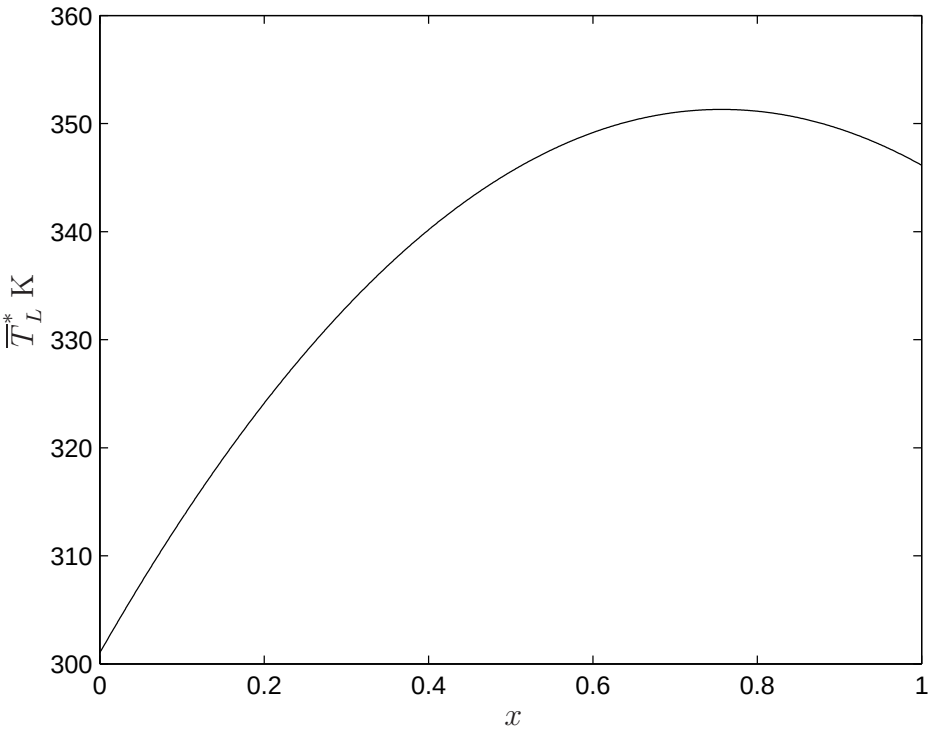

Figure 5.10. Two-temperature model; lattice temperature distribution.

Based on the values in Table 5.1, the electron velocity is $\overline{u}^* = 5.441 \cdot 10^5$ m/s. The electron temperature, T_e, is always growing in the direction of the electron flow as shown in Fig. 5.4. However, the lattice temperature, T_L, reaches its maximum value about the middle of the right half (drain side) of the semiconductor as shown in Fig. 5.5.

5.3.5 Linear stability analysis

We are interested in studying if the steady-state solution, known in the hydrodynamic stability literature as base flow, is stable or unstable. To do that, we introduce small perturbations to the steady-state solution of the form

$$V = \overline{V}(x) + V'(x,t), \quad n = \overline{n}(x) + n'(x,t), \quad u = \overline{u}(x) + u'(x,t),$$
$$T_e = \overline{T}_e(x) + T'_e(x,t), \quad T_L = \overline{T}_L(x) + T'_L(x,t), \tag{5.8}$$

where $'$ denotes the perturbed variable.

Substituting Eqs. (5.8) into the system of Eqs. (5.3) and linearizing, we get the following perturbed system of equations

$$\frac{\partial^2 V'}{\partial x^2} - \alpha n' = 0, \tag{5.9a}$$

$$\frac{\partial n'}{\partial t} + \overline{u}\frac{\partial n'}{\partial x} + \frac{\partial u'}{\partial x} = 0, \tag{5.9b}$$

$$(\beta + \overline{T}_L)\frac{\partial u'}{\partial t} + \left(\frac{\overline{u}\sqrt{\alpha}}{\gamma_{pn}}\right) T'_e + \left(\frac{\sqrt{\alpha}\beta}{\gamma_{pn}} + \frac{\sqrt{\alpha}\overline{T}_e}{\gamma_{pn}}\right) u'$$
$$+ \left(\beta^2 + \beta\overline{T}_e + \beta\overline{T}_L + \overline{T}_e\overline{T}_L\right)\frac{\partial n'}{\partial x}$$

$$+\left(\beta+\overline{T}_L\right)\frac{\partial T_e'}{\partial x}+\left(-1+\frac{d\overline{T}_e}{dx}\right)T_L'$$
$$+\left(-\beta+\frac{\overline{u}\sqrt{\alpha}\beta}{\gamma_{pn}}+\frac{\overline{u}\sqrt{\alpha\overline{T}_e}}{\gamma_{pn}}-\overline{T}_L+\beta\frac{d\overline{T}_e}{dx}+\overline{T}_L\frac{d\overline{T}_e}{dx}\right)n'$$
$$+\left(\overline{u}\beta+\overline{u}\overline{T}_L\right)\frac{\partial u'}{\partial x}-\left(\beta+\overline{T}_L\right)\frac{\partial V'}{\partial x}=0, \tag{5.9c}$$

$$(\beta+\overline{T}_L)\frac{\partial T_e'}{\partial t}+\left(\frac{\sqrt{\alpha}\beta}{\gamma_E}-\frac{2\overline{u}^2\sqrt{\alpha}}{3\gamma_{pn}}+\frac{\sqrt{\alpha\overline{T}_L}}{\gamma_E}\right)T_e'+\left(\overline{u}\beta+\overline{u}\overline{T}_L\right)\frac{\partial T_e'}{\partial x}$$
$$+\left(\frac{2\overline{u}\sqrt{\alpha}\beta}{3\gamma_E}-\frac{4\overline{u}\sqrt{\alpha}\beta}{3\gamma_{pn}}-\frac{4\overline{u}\sqrt{\alpha\overline{T}_e}}{3\gamma_{pn}}+\frac{2\overline{u}\sqrt{\alpha\overline{T}_L}}{3\gamma_E}+\beta\frac{d\overline{T}_e}{dx}+\overline{T}_L\frac{d\overline{T}_e}{dx}\right)u'$$
$$+\left(\frac{\overline{u}^2\sqrt{\alpha}\beta}{3\gamma_E}-\frac{2\overline{u}^2\sqrt{\alpha}\beta}{3\gamma_{pn}}+\frac{\sqrt{\alpha}\beta\overline{T}_e}{\gamma_E}-\frac{2\overline{u}^2\sqrt{\alpha\overline{T}_e}}{3\gamma_{pn}}+\frac{\overline{u}^2\sqrt{\alpha\overline{T}_L}}{3\gamma_E}\right)n'$$
$$-\left(\frac{\sqrt{\alpha}\beta\overline{T}_L}{\gamma_E}+\frac{\sqrt{\alpha\overline{T}_e\overline{T}_L}}{\gamma_E}-\frac{\sqrt{\alpha\overline{T}_L^2}}{\gamma_E}+\overline{u}\beta\frac{d\overline{T}_e}{dx}+\overline{u}\overline{T}_L\frac{d\overline{T}_e}{dx}\right)n'$$
$$+\left(\frac{2}{3}\beta^2+\frac{2}{3}\beta\overline{T}_e+\frac{2}{3}\beta\overline{T}_L+\frac{2}{3}\overline{T}_e\overline{T}_L\right)\frac{\partial u'}{\partial x}-\frac{2}{3}\left(\beta\sigma+\frac{2}{3}\sigma\overline{T}_L\right)\frac{\partial^2 T_e'}{\partial x^2}$$
$$+\left(\frac{\overline{u}^2\sqrt{\alpha}}{3\gamma_E}-\frac{\sqrt{\alpha}\beta}{\gamma_E}+\frac{\sqrt{\alpha\overline{T}_e}}{\gamma_E}-\frac{2\sqrt{\alpha\overline{T}_L}}{\gamma_E}+\overline{u}\frac{d\overline{T}_e}{dx}-\frac{2}{3}\sigma\frac{d^2\overline{T}_e}{dx^2}\right)T_L'=0, \tag{5.9d}$$

$$\frac{\partial T_L'}{\partial t}-\theta_2 T_e'+\theta_2 T_L'+\left(-\frac{\overline{u}^2\theta_2}{3}-\theta_2\overline{T}_e+\theta_2\overline{T}_L\right)n'-\frac{2}{3}\overline{u}\theta_2 u'-\theta_1\frac{\partial^2 T_L'}{\partial x^2}=0. \tag{5.9e}$$

Since the system (5.9) has variable coefficients in space derivatives, to do the linear stability analysis of the steady-state solution we use normal modes of the form

$$\left\{\begin{array}{c}V'\\ n'\\ u'\\ T_e'\\ T_L'\end{array}\right\}=\left\{\begin{array}{c}\widehat{V}(x)\\ \widehat{n}(x)\\ \widehat{u}(x)\\ \widehat{T}_e(x)\\ \widehat{T}_L(x)\end{array}\right\}e^{\omega t},$$

where the frequency ω and the amplitudes denoted by $\widehat{\ }$ are all complex. Thus, we get a system of differential equations with variable coefficients. This is

$$A_1(x)\frac{d^2\widehat{V}}{dx^2} + A_2(x)\widehat{n} = 0, \tag{5.10a}$$

$$B_1(x)\widehat{n} + B_2(x)\frac{d\widehat{n}}{dx} + B_3(x)\frac{d\widehat{u}}{dx} = 0, \tag{5.10b}$$

$$C_1(x)\widehat{T}_e + C_2(x)\widehat{u} + C_3(x)\frac{d\widehat{n}}{dx} + C_4(x)\frac{d\widehat{T}_e}{dx} + C_5(x)\widehat{T}_L + C_6(x)\widehat{n} + C_7(x)\frac{d\widehat{u}}{dx} + C_8(x)\frac{d\widehat{V}}{dx} = 0, \tag{5.10c}$$

$$D_1(x)\widehat{T}_e + D_2(x)\frac{d\widehat{T}_e}{dx} + D_3(x)\widehat{u} + D_4(x)\widehat{n} + D_5(x)\frac{d\widehat{u}}{dx} + D_6(x)\frac{d^2\widehat{T}_e}{dx^2} + D_7(x)\widehat{T}_L = 0, \tag{5.10d}$$

$$E_1(x)\widehat{T}_e + E_2(x)\widehat{T}_L + E_3(x)\widehat{n} + E_4(x)\widehat{u} + E_5(x)\frac{d^2\widehat{T}_L}{dx^2} = 0, \tag{5.10e}$$

where the coefficients are defined as

$$A_1(x) = 1, \quad A_2(x) = -\alpha,$$

$$B_1(x) = \omega, \quad B_2(x) = \overline{u}, \quad B_3(x) = \overline{n} = 1,$$

$$C_1(x) = \frac{\overline{u}\sqrt{\alpha}}{\gamma_{pn}}, \quad C_2(x) = \frac{\sqrt{\alpha}\beta}{\gamma_{pn}} + \beta\omega + \frac{\sqrt{\alpha}\overline{T}_e}{\gamma_{pn}} + \omega\overline{T}_L,$$

$$C_3(x) = \beta^2 + \beta\overline{T}_e + \beta\overline{T}_L + \overline{T}_e\overline{T}_L,$$

$$C_4(x) = \beta + \overline{T}_L, \quad C_5(x) = -1 + \frac{d\overline{T}_e}{dx},$$

$$C_6(x) = -\beta + \frac{\overline{u}\sqrt{\alpha}\beta}{\gamma_{pn}} + \frac{\overline{u}\sqrt{\alpha}\overline{T}_e}{\gamma_{pn}} - \overline{T}_L + \beta\frac{d\overline{T}_e}{dx} + \overline{T}_L\frac{d\overline{T}_e}{dx},$$

$$C_7(x) = \overline{u}\beta + \overline{u}\overline{T}_L, \quad C_8(x) = -\beta - \overline{T}_L,$$

$$D_1(x) = \frac{\sqrt{\alpha}\beta}{\gamma_E} - \frac{2\overline{u}^2\sqrt{\alpha}}{3\gamma_{pn}} + \beta\omega + \frac{\sqrt{\alpha}\overline{T}_L}{\gamma_E} + \omega\overline{T}_L,$$

$$D_2(x) = \overline{u}\beta + \overline{u}\overline{T}_L,$$

$$D_3(x) = \frac{2\overline{u}\sqrt{\alpha}\beta}{3\gamma_E} - \frac{4\overline{u}\sqrt{\alpha}\beta}{3\gamma_{pn}} - \frac{4\overline{u}\sqrt{\alpha}\overline{T}_e}{3\gamma_{pn}} + \frac{2\overline{u}\sqrt{\alpha}\overline{T}_L}{3\gamma_E} + \beta\frac{d\overline{T}_e}{dx} + \overline{T}_L\frac{d\overline{T}_e}{dx},$$

$$D_4(x) = \frac{\overline{u}^2\sqrt{\alpha}\beta}{3\gamma_E} - \frac{2\overline{u}^2\sqrt{\alpha}\beta}{3\gamma_{pn}} + \frac{\sqrt{\alpha}\beta\overline{T}_e}{\gamma_E} - \frac{2\overline{u}^2\sqrt{\alpha}\overline{T}_e}{3\gamma_{pn}} + \frac{\overline{u}^2\sqrt{\alpha}\overline{T}_L}{3\gamma_E}$$
$$-\frac{\sqrt{\alpha}\beta\overline{T}_L}{\gamma_E} + \frac{\sqrt{\alpha}\overline{T}_e\overline{T}_L}{\gamma_E} - \frac{\sqrt{\alpha}\overline{T}_L^2}{\gamma_E} + \overline{u}\beta\frac{d\overline{T}_e}{dx} + \overline{u}\overline{T}_L\frac{d\overline{T}_e}{dx},$$

$$D_5(x) = \frac{2}{3}\beta^2 + \frac{2}{3}\beta\overline{T}_e + \frac{2}{3}\beta\overline{T}_L + \frac{2}{3}\overline{T}_e\overline{T}_L,$$

$$D_6(x) = -\frac{2}{3}\left(\beta\sigma + \sigma\overline{T}_L\right),$$

$$D_7(x) = \frac{\overline{u}^2\sqrt{\alpha}}{3\gamma_E} - \frac{\sqrt{\alpha}\beta}{\gamma_E} + \frac{\sqrt{\alpha}\overline{T}_e}{\gamma_E} - \frac{2\sqrt{\alpha}\overline{T}_L}{\gamma_E} + \overline{u}\frac{d\overline{T}_e}{dx} - \frac{2}{3}\sigma\frac{d^2\overline{T}_e}{dx^2},$$

$$E_1(x) = -\theta_2, \quad E_2(x) = \theta_2 + \omega,$$

$$E_3(x) = -\frac{\overline{u}^2\theta_2}{3} - \theta_2\overline{T}_e + \theta_2\overline{T}_L,$$

$$E_4(x) = -\frac{2}{3}\overline{u}\theta_2, \quad E_5(x) = -\theta_1.$$

Following this form, the boundary conditions are

$$\widehat{V}(0) = 0, \quad \widehat{V}(1) = 0, \quad \widehat{n}(0) = 0, \quad \frac{d\widehat{V}}{dx}(0) = \frac{d\widehat{V}}{dx}(1), \tag{5.12a}$$

$$\widehat{T}_e(0) = 0, \quad \frac{d\widehat{T}_e}{dx}(1) = 0, \quad \widehat{T}_L(0) = 0, \quad \widehat{T}_L(1) = 0. \tag{5.12b}$$

5.3.6 Temporal eigenmodes

Our interest is to find unstable eigenmodes in time. The system of Eqs. (5.10) can be rewritten as a system of first-order differential equations as

$$\frac{d\widehat{V}}{dx} = -\widehat{E}, \tag{5.13a}$$

$$\frac{d\widehat{E}}{dx} = \frac{A_2(x)}{A_1(x)}\widehat{n}, \tag{5.13b}$$

$$B_2(x)\frac{d\widehat{n}}{dx} + B_3(x)\frac{d\widehat{u}}{dx} = -B_1(x)\widehat{n}, \tag{5.13c}$$

$$C_8(x)\frac{d\widehat{V}}{dx} + C_3(x)\frac{d\widehat{n}}{dx} + C_7(x)\frac{d\widehat{u}}{dx} + C_4(x)\frac{d\widehat{T}_e}{dx} = -C_6(x)\widehat{n} - C_2(x)\widehat{u} - C_1(x)\widehat{T}_e, \tag{5.13d}$$

$$\frac{d\widehat{T}_e}{dx} = \widehat{q}_e, \tag{5.13e}$$

$$D_5(x)\frac{d\widehat{u}}{dx} + D_2(x)\frac{d\widehat{T}_e}{dx} + D_6(x)\frac{d\widehat{q}_e}{dx} = -D_4(x)\widehat{n} - D_3(x)\widehat{u} - D_1(x)\widehat{T}_e, \tag{5.13f}$$

$$\frac{d\widehat{T}_L}{dx} = \widehat{q}_L, \tag{5.13g}$$

$$E_5(x)\frac{d\widehat{q}_L}{d} = -E_2(x)\widehat{T}_L. \tag{5.13h}$$

By defining

$$Y = \left\{ \begin{array}{c} \widehat{V} \\ \widehat{E} \\ \widehat{n} \\ \widehat{u} \\ \widehat{T}_e \\ \widehat{q}_e \\ \widehat{T}_L \\ \widehat{q}_L \end{array} \right\},$$

$$\mathbf{J} = \begin{bmatrix} 1 & 0 & 0 & 0 & 0 & 0 & 0 & 0 \\ 0 & 1 & 0 & 0 & 0 & 0 & 0 & 0 \\ 0 & 0 & B_2(x) & B_3(x) & 0 & 0 & 0 & 0 \\ C_8(x) & 0 & C_3(x) & C_7(x) & C_4(x) & 0 & 0 & 0 \\ 0 & 0 & 0 & 0 & 1 & 0 & 0 & 0 \\ 0 & 0 & 0 & D_5(x) & D_2(x) & D_6(x) & 0 & 0 \\ 0 & 0 & 0 & 0 & 0 & 0 & 1 & 0 \\ 0 & 0 & 0 & 0 & 0 & 0 & 0 & E_5(x) \end{bmatrix},$$

$$\mathbf{P} = \begin{bmatrix} 0 & -1 & 0 & 0 & 0 & 0 & 0 & 0 \\ 0 & 0 & A_2(x)/A_1(x) & 0 & 0 & 0 & 0 & 0 \\ 0 & 0 & -B_1(x) & 0 & 0 & 0 & 0 & 0 \\ 0 & 0 & -C_6(x) & -C_2(x) & -C_1(x) & 0 & -C_5(x) & 0 \\ 0 & 0 & 0 & 0 & 0 & 1 & 0 & 0 \\ 0 & 0 & -D_4(x) & -D_3(x) & -D_1(x) & 0 & D_7(x) & 0 \\ 0 & 0 & 0 & 0 & 0 & 0 & 0 & 1 \\ 0 & 0 & -E_3(x) & -E_4(x) & -E_1(x) & 0 & -E_2(x) & 0 \end{bmatrix},$$

the system of equations (5.13) can be written as

$$\frac{d\mathbf{Y}}{dx} = \mathbf{J}^{-1}\mathbf{P}\mathbf{Y}, \tag{5.14}$$

where $\mathbf{J}^{-1}\mathbf{P}$ is a square matrix which depends on the eigenmode in time ω and

the position x. The boundary conditions (5.12) for Eq. (5.14) are

$$\mathbf{Y}(0) = \left\{ \begin{array}{c} 0 \\ E_0 \\ 0 \\ u_0 \\ 0 \\ q_{e0} \\ 0 \\ q_{L0} \end{array} \right\}, \quad \mathbf{Y}(1) = \left\{ \begin{array}{c} 0 \\ E_0 \\ \widehat{n}(1) \\ \widehat{u}(1) \\ \widehat{T}_e(1) \\ 0 \\ 0 \\ \widehat{q}_L(1) \end{array} \right\}.$$

The relation between $\mathbf{Y} = \mathbf{Y}_0$ at $x = 0$ and $\mathbf{Y} = \mathbf{Y}_1$ at $x = 1$ can be defined to be of the form

$$\mathbf{Y}_1 = \mathbf{A}\mathbf{Y}_0, \tag{5.15}$$

where $\mathbf{A}$ is the transfer matrix which depends only on ω and not on the boundary conditions. The allowed values of ω are determined by the boundary conditions. For a given value of ω, the differential equation (5.14) can be integrated from $x = 0$ to $x = 1$ using as Y_0 the orthonormal vectors $[1,0,0,0,0,0,0,0]^T$, $[0,1,0,0,0,0,0,0]^T$, $[0,0,1,0,0,0,0,0]^T$, $[0,0,0,1,0,0,0,0]^T$, $[0,0,0,0,1,0,0,0]^T$, $[0,0,0,0,0,1,0,0]^T$, $[0,0,0,0,0,0,1,0]^T$, $[0,0,0,0,0,0,0,1]^T$ in turn to get the columns of the transfer matrix $\mathbf{A}$ [96]. A fourth-order Runge-Kutta method was used with 100 integration steps.

Once we have the transfer matrix $\mathbf{A}$, a non-trivial solution is required to be satisfied for the system of four algebraic equations in terms of E_0, u_0, q_{e0} and q_{L0} (see $\mathbf{Y}(0)$) that contains the boundary conditions at $x = 1$, with $\mathbf{Y}_0 = \mathbf{Y}(0)$.

Thus

$$\begin{bmatrix} a_{12} & a_{14} & a_{16} & a_{18} \\ a_{22}-1 & a_{24} & a_{26} & a_{28} \\ a_{62} & a_{64} & a_{66} & a_{68} \\ a_{72} & a_{74} & a_{76} & a_{78} \end{bmatrix} \begin{Bmatrix} E_0 \\ u_0 \\ q_{e0} \\ q_{L0} \end{Bmatrix} = \begin{Bmatrix} 0 \\ 0 \\ 0 \\ 0 \end{Bmatrix}, \tag{5.16}$$

where a_{ij} are the coefficients (i, j) of the matrix $\mathbf{A}$.

By applying Muller's method to find the roots of the determinant of the matrix that contains the boundary conditions, we get the eigenmodes in time ω around the origin. The Muller method is an extension of the secant method, where a second-degree polynomial is used to interpolate three points, instead of a linear polynomial [97, 98]; and its order of convergence is almost quadratic. The purpose of this is to find the closest unstable eigenmode in time to the origin. The first five eigenmodes in time are shown in Table 5.3. Unstable eigenmodes in time (positive real part) were not found using the procedure described before. Also, oscillatory eigenmodes (with imaginary part) were not found, even though oscillatory eigenmodes were used to start the iteration process in Muller's method. It is important to emphasize that Muller's method requires that starting values be neighbors to the value of our interest.

According to the eigenmodes in Table 5.3, the system is stable and without an oscillatory component. The main difference between the mathematical model described in this Chapter and the others in Chapters 3 and 4 is the thermal coupling. In this analysis we are considering conduction effects in the electron transport in the semiconductor. Effects such as scattering by the lattice and heat generation are included in the model and can be responsible for the stability or instability of the electron flow.

TABLE 5.3

TEMPORAL EIGENMODES

ω_1	-0.00295023
ω_2	-0.0118009
ω_3	-0.0265521
ω_4	-0.0472039
ω_5	-0.0737565

5.4 One-temperature approximation with collision

The model takes into account several effects that determine the electron flow in the semiconductor. With the purpose of exploring which effect contributes to the stability of system, in this section we study a simplified model in which we assume that $T_e = T_L$ and neglect the heat conduction of the electrons, i.e., $k_e \to 0$.

5.4.1 Governing equations and steady-state solution

$$\frac{\partial^2 V}{\partial x^2} = \alpha\,(n-1)\,, \tag{5.17a}$$

$$\frac{\partial n}{\partial t} + \frac{\partial (un)}{\partial x} = 0, \tag{5.17b}$$

$$\frac{\partial u}{\partial t} + u\frac{\partial u}{\partial x} = \frac{\partial V}{\partial x} - \frac{\beta}{n}\frac{\partial n}{\partial x} - \frac{\partial T_e}{\partial x} - \frac{T_e}{n}\frac{\partial n}{\partial x} - \frac{\sqrt{\alpha}}{\gamma_{pn}}u, \tag{5.17c}$$

$$\frac{\partial T_e}{\partial t} + u\frac{\partial T_e}{\partial x} = -\frac{2}{3}\beta\frac{\partial u}{\partial x} - \frac{2}{3}T_e\frac{\partial u}{\partial x} - \frac{\sqrt{\alpha}}{3}\left(\frac{1}{\gamma_E} - \frac{2}{\gamma_{pn}}\right)u^2. \tag{5.17d}$$

The new energy conservation equation Eq. (5.17d) considers only the terms for energy advection, work done by the electron pressure and a part of the collision term [22]. $T_e = T_L$ implies that (5.3e) is uncoupled and does not provide information about the dependent variables. The boundary conditions for Eqs. (5.17) are Eqs. (5.4a) and Eq. (5.4b) with $T_1 = T_{room}$. This last condition imposes that the electron temperature at the source must be constant and equal to the room temperature T_{room}. The steady-state solution for Eqs. (5.17) is

$$\overline{V}(x) = x - 1, \quad \overline{n}(x) = 1, \quad \overline{u}(x) = \frac{1}{\frac{5}{3}\frac{\sqrt{\alpha}}{\gamma_{pn}} - \frac{1}{3}\frac{\sqrt{\alpha}}{\gamma_E}}, \quad \overline{T}_e(x) = \left(\frac{\frac{2}{3}\frac{\sqrt{\alpha}}{\gamma_{pn}} - \frac{1}{3}\frac{\sqrt{\alpha}}{\gamma_E}}{\frac{5}{3}\frac{\sqrt{\alpha}}{\gamma_{pn}} - \frac{1}{3}\frac{\sqrt{\alpha}}{\gamma_E}} \right) x.$$

The only dependent variable that varies along the semiconductor is $\overline{T}_e$.

5.4.2 Linear stability analysis

To do the linear stability analysis of the steady-state solution we introduce small perturbations for V, n, u and T_e of the form shown in Eq. (5.8). Substituting the perturbations into the system (5.17) and linearizing, we get

$$\frac{\partial^2 V'}{\partial x^2} - \alpha n' = 0, \tag{5.18a}$$

$$\frac{\partial n'}{\partial t} + \overline{u}\frac{\partial n'}{\partial x} + \frac{\partial u'}{\partial x} = 0, \tag{5.18b}$$

$$\frac{\partial u'}{\partial t} + \overline{u}\frac{\partial u'}{\partial x} - \frac{\partial V'}{\partial x} + \beta\frac{\partial n'}{\partial x} + \frac{\partial T_e'}{\partial x} + \overline{T}_e\frac{\partial n'}{\partial x} + \frac{\sqrt{\alpha}}{\gamma_{pn}}u' = 0, \tag{5.18c}$$

$$\frac{\partial T_e'}{\partial t} + \overline{u}\frac{\partial T_e'}{\partial x} + \frac{2}{3}\beta\frac{\partial u'}{\partial x} + \frac{2}{3}\overline{T}_e\frac{\partial u'}{\partial x} + \frac{2}{3}\sqrt{\alpha}\left(\frac{1}{\gamma_E} - \frac{2}{\gamma_{pn}}\right)\overline{u}u' = 0. \tag{5.18d}$$

The boundary conditions take the form

$$V'(0,t)=0, \quad V'(1,t)=0, \quad n'(0,t)=0, \quad \frac{\partial V'}{\partial x}(0,t)=\frac{\partial V'}{\partial x}(1,t), \quad T_e'(0,t)=0. \tag{5.19}$$

Since the system (5.18) has variable coefficients in spatial derivatives we use normal modes of the form

$$\begin{Bmatrix} V' \\ n' \\ u' \\ T_e' \end{Bmatrix} = \begin{Bmatrix} \widehat{V}(x) \\ \widehat{n}(x) \\ \widehat{u}(x) \\ \widehat{T}_e(x) \end{Bmatrix} e^{\omega t}.$$

The system in Eqs. (5.18) can be rewritten as

$$\frac{d\mathbf{Y}}{dx} = \mathbf{J}_s^{-1}\mathbf{P}_s\mathbf{Y}, \tag{5.20}$$

where $\mathbf{Y} = \left\{\widehat{V}, \widehat{E}, \widehat{n}, \widehat{u}, \widehat{T}_e\right\}^T$,

$$\mathbf{J}_s(\omega,x) = \begin{bmatrix} 1 & 0 & 0 & 0 & 0 \\ 0 & 1 & 0 & 0 & 0 \\ 0 & 0 & \overline{u} & 1 & 0 \\ 0 & 0 & \beta+\overline{T}_e & \overline{u} & 1 \\ 0 & 0 & 0 & \frac{2}{3}\left(\beta+\overline{T}_e\right) & \overline{u} \end{bmatrix},$$

$$\mathbf{P}_s(\omega, x) = \begin{bmatrix} 0 & -1 & 0 & 0 & 0 \\ 0 & 0 & -\alpha & 0 & 0 \\ 0 & 0 & -\omega & 0 & 0 \\ 0 & -1 & 0 & -\left(\omega + \frac{\sqrt{\alpha}}{\gamma_{pn}}\right) & 0 \\ 0 & 0 & 0 & -\frac{2}{3}\sqrt{\alpha}\left(\frac{1}{\gamma_E} - \frac{2}{\gamma_{pn}}\right)\overline{u} & -\omega \end{bmatrix},$$

$\mathbf{J}_s^{-1}\mathbf{P}_s$ is a square matrix. This is also a boundary-value problem where the boundary conditions for Eq. (5.20) are $\mathbf{Y}(0) = \{0, E_0, 0, u_0, 0\}^T$ and $\mathbf{Y}(1) = \left\{0, E_0, \widehat{n}(1), \widehat{u}(1), \widehat{T}_e(1)\right\}^T$. The same numerical procedure described before was used to satisfy the boundary conditions and get the eigenfrequencies ω. We take the non-dimensional parameters $\alpha = 7.072$ and $\beta = 0.026$ from Table 5.2 and explore the necessary condition between γ_E and γ_{pn} to make the system in Eqs. (5.17) unstable.

The steady-state electron velocity must be greater than zero. That implies the condition

$$\frac{\gamma_{pn}}{\gamma_E} < 5. \tag{5.21}$$

The closest eigenfrequencies to the origin when γ_{pn}/γ_E varies are shown in Fig. 5.11 for different values of applied voltage V_0. The relation is linear and shows that the system is more unstable when γ_E decreases with respect to γ_{pn}. There is a critical value $\gamma_{pn}/\gamma_E = 3.5$ that defines a transition of the eigenfrequency from stable to unstable. Choosing $\gamma_E = \gamma_{pn}/4$, the system is unstable and some eigenfrequencies are shown in Table 5.4. If we imposed this critical value, the collision term (last term in Eq. (5.17d)) is rewritten as

$$-\frac{1}{2}\frac{\sqrt{\alpha}}{\gamma_{pn}}u^2. \tag{5.22}$$

TABLE 5.4

TEMPORAL EIGENMODES OF ONE-TEMPERATURE APPROXIMATION WITH COLLISION $\gamma_E = \gamma_{pn}/4$

ω_1	0.118627
ω_2	417.697
ω_3	940.637
ω_4	1607.64
ω_5	1887.8

Physically, this means that the electrons are loosing energy due to collisions. Also, the critical value implies $\overline{u} = 2\gamma_{pn}/\sqrt{\alpha}$ and $\overline{T}_e = -x$. The magnitude of the collision term also depends on α. When the applied voltage V_0 increases, α decreases and the energy loss due to collisions also decreases. In conclusion, the condition

$$3.5 < \frac{\gamma_{pn}}{\gamma_E} < 5 \tag{5.23}$$

guaranties that the system is unstable. In terms of electron velocity and temperature Eq. (5.23) implies that

$$\overline{u} > 2\frac{\gamma_{pn}}{\sqrt{\alpha}}, \quad \frac{d\overline{T}_e}{dx} < -1.$$

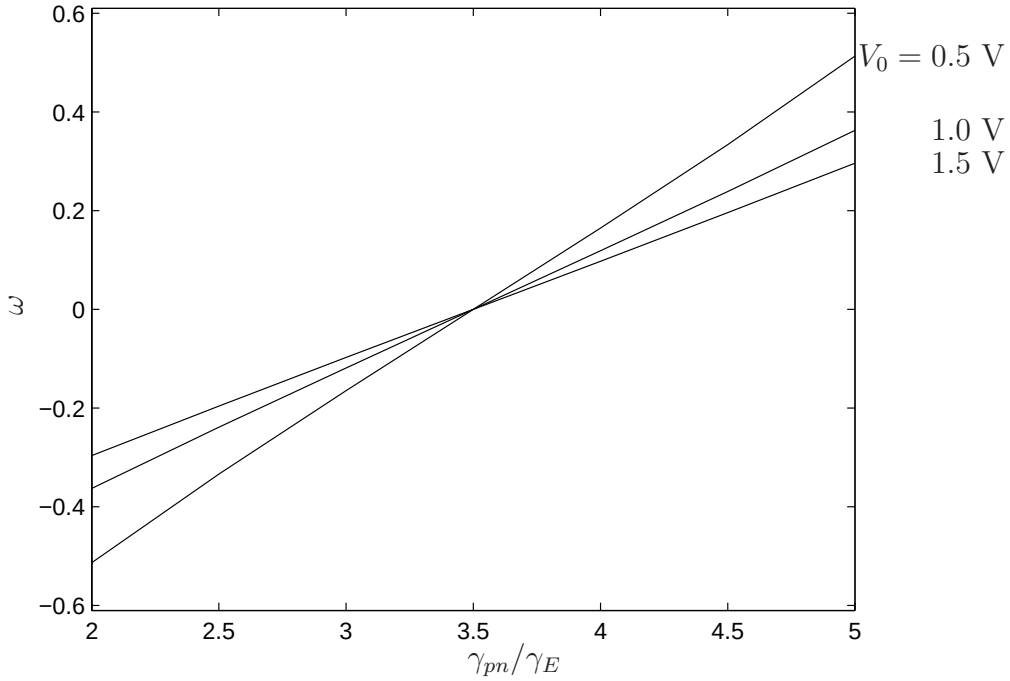

Figure 5.11. One-temperature approximation with collision; closest eigenfrequency to the origin at $T_{room} = 300$ K.

5.5 One-temperature approximation without collision

In the uncoupled model the electron and lattice temperatures were neglected. That implies that the system is totally independent of these temperatures. This model assumes that the electron scattering events are few and just affect the momentum conservation; there is no heat conduction and energy loss for the electrons and the lattice, and the electron temperature remains constant. Energy balances were not considered for electrons and the lattice.

5.5.1 Governing equations and steady-state solution

To understand if the effects of heat conduction and energy loss due to scattering are responsible for the stability of the system, we study the model in the limit when these effects are neglected. We neglect the last four terms in the electron energy equation, Eq. (5.3d), where the first is the heat conduction term and the last three are the collision terms. We consider a very large energy relaxation time τ_E, very small electronic k_e and lattice k_L thermal conductivities, and assume that the electrons are not losing energy due to collisions. Thermal equilibrium between the lattice and the electrons is also required. Based on this, the system of Eqs. (5.3) is rewritten as follows,

$$\frac{\partial^2 V}{\partial x^2} - \alpha\,(n-1) = 0, \tag{5.24a}$$

$$\frac{\partial n}{\partial t} + \frac{\partial (un)}{\partial x} = 0, \tag{5.24b}$$

$$\frac{\partial u}{\partial t} + u\frac{\partial u}{\partial x} - \frac{\partial V}{\partial x} + \frac{\beta}{n}\frac{\partial n}{\partial x} + \frac{\partial T_e}{\partial x} + \frac{T_e}{n}\frac{\partial n}{\partial x} + \frac{\sqrt{\alpha}}{\gamma_{pn}}u = 0, \tag{5.24c}$$

$$\frac{\partial T_e}{\partial t} + u\frac{\partial T_e}{\partial x} + \frac{2}{3}\beta\frac{\partial u}{\partial x} + \frac{2}{3}T_e\frac{\partial u}{\partial x} = 0. \tag{5.24d}$$

The new energy conservation equation Eq. (5.24d) considers just the terms for energy advection and work done by the electron pressure. Since we assumed $k_L \to 0$ and $\tau_E \to \infty$, we have $\theta_1 \to 0$ and $\theta_2 \to 0$, that implies that Eq. (5.3e) vanishes. The boundary conditions for Eqs. (5.24) are in Eqs. (5.4a) and Eq. (5.4b) with $T_1 = T_{room}$. This last condition imposes that the electron temperature at the source must be constant and equal to the room temperature T_{room}. The steady-state solution for Eqs. (5.24) is

$$\overline{V}(x) = x - 1, \tag{5.25a}$$

$$\overline{n}(x) = 1, \tag{5.25b}$$

$$\overline{u}(x) = \frac{\gamma_{pn}}{\sqrt{\alpha}}, \tag{5.25c}$$

$$\overline{T}_e(x) = 0. \tag{5.25d}$$

5.5.2 Linear stability analysis

As before, to do the linear stability analysis of the steady-state solution we introduce small perturbations of the form

$$\begin{aligned} V &= \overline{V}(x) + V'(x,t), \quad n = \overline{n}(x) + n'(x,t), \\ u &= \overline{u}(x) + u'(x,t), \quad T_e = \overline{T}_e(x) + T'_e(x,t), \end{aligned} \tag{5.26}$$

where $'$ denotes the perturbations. Substituting the perturbations into the system (5.24) and linearizing, we get the following system of equations

$$\frac{\partial^2 V'}{\partial x^2} - \alpha n' = 0, \tag{5.27a}$$

$$\frac{\partial n'}{\partial t} + \overline{u}\frac{\partial n'}{\partial x} + \frac{\partial u'}{\partial x} = 0, \tag{5.27b}$$

$$\frac{\partial u'}{\partial t} + \overline{u}\frac{\partial u'}{\partial x} - \frac{\partial V'}{\partial x} + \beta\frac{\partial n'}{\partial x} + \frac{\partial T_e'}{\partial x} + \frac{\sqrt{\alpha}}{\gamma_{pn}}u' = 0, \tag{5.27c}$$

$$\frac{\partial T_e'}{\partial t} + \overline{u}\frac{\partial T_e'}{\partial x} + \frac{2}{3}\beta\frac{\partial u'}{\partial x} = 0. \tag{5.27d}$$

The boundary conditions take the form

$$V'(0,t) = 0, \quad V'(1,t) = 0, \quad n'(0,t) = 0, \quad \frac{\partial V'}{\partial x}(0,t) = \frac{\partial V'}{\partial x}(1,t), \tag{5.28a}$$

$$T_e'(0,t) = 0. \tag{5.28b}$$

The system (5.27) has constant coefficients in space derivatives. This allows us to do the linear stability analysis of the steady-state solution using the normal modes

$$\begin{Bmatrix} V' \\ n' \\ u' \\ T_e \\ T_L \end{Bmatrix} = \begin{Bmatrix} \widehat{V} \\ \widehat{n} \\ \widehat{u} \\ \widehat{T}_e \\ \widehat{T}_L \end{Bmatrix} e^{kx+\omega t},$$

where the frequency ω, the wavevector k, and the amplitudes denoted by $\widehat{\ }$ are all complex and constant. Thus, we can rewrite the system of Eqs. (5.27) as the following matrix,

$$\begin{bmatrix} k^2 & -\alpha & 0 & 0 \\ 0 & \omega + k\overline{u} & k & 0 \\ -k & k\beta & \omega + k\overline{u} + \frac{\sqrt{\alpha}}{\gamma_{pn}} & k \\ 0 & 0 & \frac{2}{3}k\beta & \omega + k\overline{u} \end{bmatrix} \begin{Bmatrix} \widehat{V} \\ \widehat{n} \\ \widehat{u} \\ \widehat{T}_e \end{Bmatrix} = \begin{Bmatrix} 0 \\ 0 \\ 0 \\ 0 \end{Bmatrix}. \tag{5.29}$$

By imposing a non-trivial solution, we get the characteristic equation,

$$\begin{aligned} &k^5\left(\overline{u}^3-\frac{5\overline{u}\beta}{3}\right)+k^4\left(\frac{\overline{u}^2\sqrt{\alpha}}{\gamma_{pn}}+3\overline{u}^2\omega-\frac{5\beta\omega}{3}\right)\\ &+k^3\left(\overline{u}\alpha+\frac{2\overline{u}\sqrt{\alpha}\omega}{\gamma_{pn}}+3\overline{u}\omega^2\right)+k^2\left(\alpha\omega+\frac{\sqrt{\alpha}\omega^2}{\gamma_{pn}}+\omega^3\right)=0, \end{aligned} \tag{5.30}$$

whose solutions in terms of k are

$$k_1=0, \tag{5.31a}$$

$$k_2=0, \tag{5.31b}$$

$$k_3=-\frac{\omega}{\overline{u}}, \tag{5.31c}$$

$$k_4=\frac{-3\overline{u}\left(\sqrt{\alpha}+2\gamma_{pn}\omega\right)-\sqrt{9\overline{u}^2\alpha\left(1-4\gamma_{pn}^2\right)+60\beta\gamma_{pn}\left(\alpha\gamma_{pn}+\sqrt{\alpha}\omega+\gamma_{pn}\omega^2\right)}}{2\left(3\overline{u}^2-5\beta\right)\gamma_{pn}}, \tag{5.31d}$$

$$k_5=\frac{-3\overline{u}\left(\sqrt{\alpha}+2\gamma_{pn}\omega\right)+\sqrt{9\overline{u}^2\alpha\left(1-4\gamma_{pn}^2\right)+60\beta\gamma_{pn}\left(\alpha\gamma_{pn}+\sqrt{\alpha}\omega+\gamma_{pn}\omega^2\right)}}{2\left(3\overline{u}^2-5\beta\right)\gamma_{pn}}. \tag{5.31e}$$

Therefore, the solutions for V', n', u' and T_e' can be written as

$$V'(x,t)=\left(Z_1+Z_2x+Z_3e^{k_3x}+Z_4e^{k_4x}+Z_5e^{k_5x}\right)e^{\omega t}, \tag{5.32a}$$

$$n'(x,t)=\frac{1}{\alpha}\left(Z_3k_3^2e^{k_3x}+Z_4k_4^2e^{k_4x}+Z_5k_5e^{k_5x}\right)e^{\omega t}, \tag{5.32b}$$

$$u'(x,t)=\frac{-1}{\alpha}\left(Z_3k_3(k_3\overline{u}+\omega)e^{k_3x}+Z_4k_4(k_4\overline{u}+\omega)e^{k_4x}+Z_5k_5(k_5\overline{u}+\omega)e^{k_5x}\right)e^{\omega t}, \tag{5.32c}$$

$$T_e'(x,t)=-\frac{e^{\omega t}}{3\alpha\gamma_{pn}\omega}\left(3Z_2\overline{u}\alpha\gamma_{pn}+Z_3e^{k_3x}k_3\left(k_3^2\phi_1+3\phi_2+k_3\phi_3\right)\right)$$

$$-\frac{e^{\omega t}}{3\alpha\gamma_{pn}\omega}\left(Z_4 e^{k_4 x}k_4\left(k_4^2\phi_1+3\phi_2+k_4\phi_3\right)+Z_5 e^{k_5 x}k_5\left(k_5^2\phi_1+3\phi_2+k_5\phi_3\right)\right) \tag{5.32d}$$

where $[Z_1, Z_2, Z_3, Z_4, Z_5]^T$ is the vector of the constant coefficients, $\phi_1 = \overline{u}(3\overline{u}^2 - 5\beta)\gamma_{pn}$, $\phi_2 = \overline{u}(\alpha\gamma_{pn} + \sqrt{\alpha}\omega + \gamma_{pn}\omega^2)$ and $\phi_3 = -2\beta\gamma_{pn}\omega + 3\overline{u}^2(\sqrt{\alpha} + 2\gamma_{pn}\omega)$.

By applying the boundary conditions in Eqs. (5.28) to Eqs. (5.32), we get the following matrix equation

$$\begin{bmatrix} 1 & 0 & 1 & 1 & 1 \\ 1 & 1 & e^{k_3} & e^{k_4} & e^{k_5} \\ 0 & 0 & \frac{k_3^2}{\alpha} & \frac{k_4^2}{\alpha} & \frac{k_5^2}{\alpha} \\ 0 & 0 & k_3(1-e^{k_3}) & k_4(1-e^{k_4}) & k_5(1-e^{k_5}) \\ 0 & 3\overline{u}\alpha\gamma_{pn} & k_3\eta_1 & k_4\eta_2 & k_5\eta_3 \end{bmatrix} \begin{Bmatrix} Z_1 \\ Z_2 \\ Z_3 \\ Z_4 \\ Z_5 \end{Bmatrix} = \begin{Bmatrix} 0 \\ 0 \\ 0 \\ 0 \\ 0 \end{Bmatrix}. \tag{5.33}$$

where $\eta_1 = k_3^2\phi_1 + 3\phi_2 + k_3\phi_3$, $\eta_2 = k_4^2\phi_1 + 3\phi_2 + k_4\phi_3$ and $\eta_3 = k_5^2\phi_1 + 3\phi_2 + k_5\phi_3$. By imposing a non-trivial solution to Eq. (5.33), we get the characteristic equation

$$\begin{aligned} &3\left(-1+e^{k_3}\right)k_4k_5\left\{\left(-1+e^{k_5}\right)k_4+k_5-e^{k_4}k_5\right\}\overline{u}\alpha\gamma_{pn} \\ &+k_3\left[3\left(-1+e^{k_3}\right)\left(-1+e^{k_4}\right)k_5^2\overline{u}\alpha\gamma_{pn}+k_4k_5^2\left\{\left(-1+e^{k_4}\right)\eta_1+\eta_2-e^{k_3}\eta_2\right\}\right] \\ &-k_3\left[k_4^2\left\{3\left(-1+e^{k_3}\right)\left(-1+e^{k_5}\right)\overline{u}\alpha\gamma_{pn}+k_5\left(\left(-1+e^{k_5}\right)\eta_1+\eta_3-e^{k_3}\eta_3\right)\right\}\right] \\ &+k_3^2\left\{-3\left(-1+e^{k_4}\right)\left(-1+e^{k_5}\right)k_5\overline{u}\alpha\gamma_{pn}\right\} \\ &+k_3^2\left[k_4\left\{3\left(-1+e^{k_4}\right)\left(-1+e^{k_5}\right)\overline{u}\alpha\gamma_{pn}+k_5\left(\left(-1+e^{k_5}\right)\eta_2+\eta_3-e^{k_4}\eta_3\right)\right\}\right]=0. \end{aligned} \tag{5.34}$$

5.5.3 Temporal eigenmodes

Two of the solutions of Eq. (5.34) in terms of ω are

$$\omega_1 = \frac{-20\sqrt{\alpha}\beta - \sqrt{400\alpha\beta^2 - 80\beta\gamma_{pn}\left(3\gamma_{pn} + 20\alpha\beta\gamma_{pn} - 12\gamma_{pn}^3\right)}}{40\beta\gamma_{pn}}, \tag{5.35}$$

$$\omega_2 = \frac{-20\sqrt{\alpha}\beta + \sqrt{400\alpha\beta^2 - 80\beta\gamma_{pn}\left(3\gamma_{pn} + 20\alpha\beta\gamma_{pn} - 12\gamma_{pn}^3\right)}}{40\beta\gamma_{pn}}. \tag{5.36}$$

We are interested in finding unstable temporal eigenmodes. That means, values of ω with positive real part. The real part of ω_1 is always negative and the real part of ω_2 can be positive depending on the values of α, β and γ_{pn} . If we impose $\omega_2 > 0$ we get the condition

$$\gamma_{pn} > \frac{1}{2}, \quad \alpha < \frac{12\gamma_{pn}^2 - 3}{20\beta}. \tag{5.37}$$

Taking $\gamma_{pn} = 7.331$ and $\beta = 0.026$ from Table 5.2, we need $\alpha < 1234.47$ to have at least one unstable eigenmode. With $\alpha = 7.072$ we get $\omega_2 = 34.8533$, which is unstable. By using the definitions of the non-dimensional groups α, β and γ_{pn}, the condition in Eq. (5.37) can be rewritten in terms of the applied voltage at the source as $V_0 > L\sqrt{20N_D k_B T_{room}/(12m_e\mu_{no}^2 N_D - 3\epsilon_s)}$.

The eigenmodes in time in Eqs. (5.35) and (5.36) depend on α, β and γ_{pn}. ω_1 and ω_2 are constant and independent of the value of α when β and γ take a fixed value as shown in Fig. 5.12. ω_1 remains stable and ω_2 unstable. ω_1 turns out to be more stable and ω_2 more unstable when β decreases with α and γ constant as shown in Fig. 5.13. Besides, ω_1 turns to be more stable and ω_2 more unstable when γ_{pn} goes to zero or gets a high value as shown in Figs. 5.14, 5.15 and 5.16. The applied voltage at the source, V_0, and the room temperature T_{room} are part of

the tunable parameters of the system. They can be specified locally what makes them easy to impose and vary at the source and the drain. α and β cannot vary independently if just V_0 varies. Figs. 5.14, 5.15 and 5.16 show the dependency of ω_1 and ω_2 with γ_{pn} for different applied voltages. ω_1 is more stable and ω_2 more unstable when the applied voltage is higher. The room temperature can vary by changing the value of β. Figs. 5.17, 5.18 and 5.19 show the dependency of ω_1 and ω_2 with the absolute value of the applied voltage at the source, V_0, for different room temperatures. ω_1 is more stable and ω_2 is more unstable when T_{room} is lower and the applied voltage varies. The value of T_{room} is the condition for the electron temperature at the source as shown in Eq. (5.4b) with $T_1 = T_{room}$.

5.6 Conclusions

The analysis of the thermal coupled model shows that heat conduction and energy loss contribute to the stability of the electron flow. If the heat conduction and energy loss due to scattering of the electrons are neglected in the model, it is possible to find an operating condition in terms of α, β and γ_{pn} to get an unstable eigenmode in time ω_2. The two-temperature and one-temperature models consider the electron temperature as a variable that can have perturbations and the thermally uncoupled model described in Chapters 3 and 4 does not consider the electron temperature as a variable. In both kinds of models, when α decreases the system becomes more unstable, that means the system gets more unstable when the applied voltage is increased.

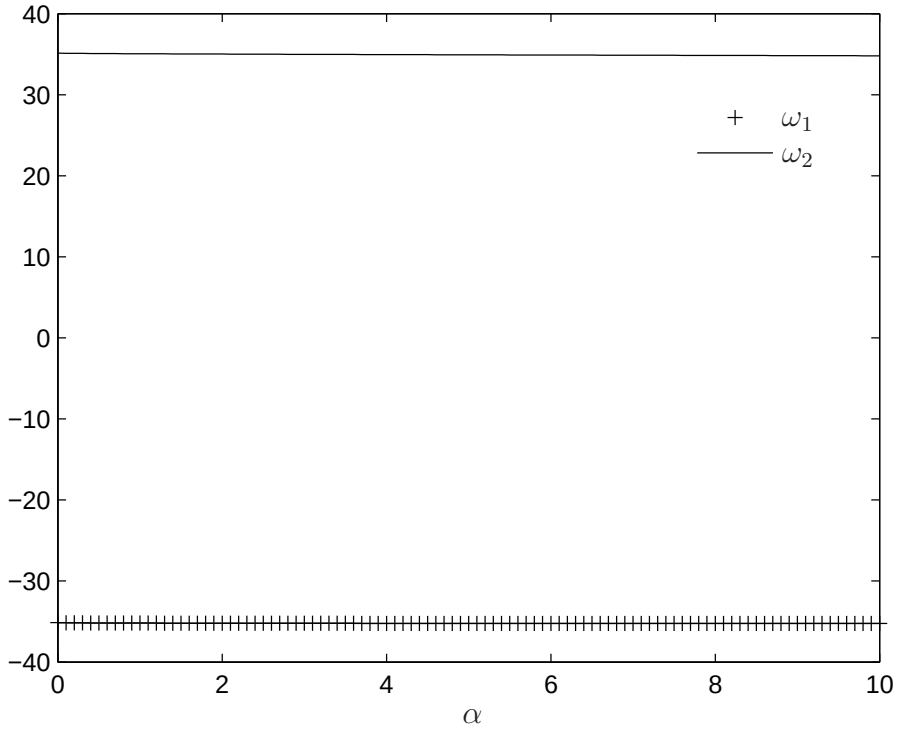

Figure 5.12. One-temperature approximation without collision; ω_1 and ω_2 eigenmodes as a function of α with $\gamma_{pn} = 7.331$ and $\beta = 0.026$.

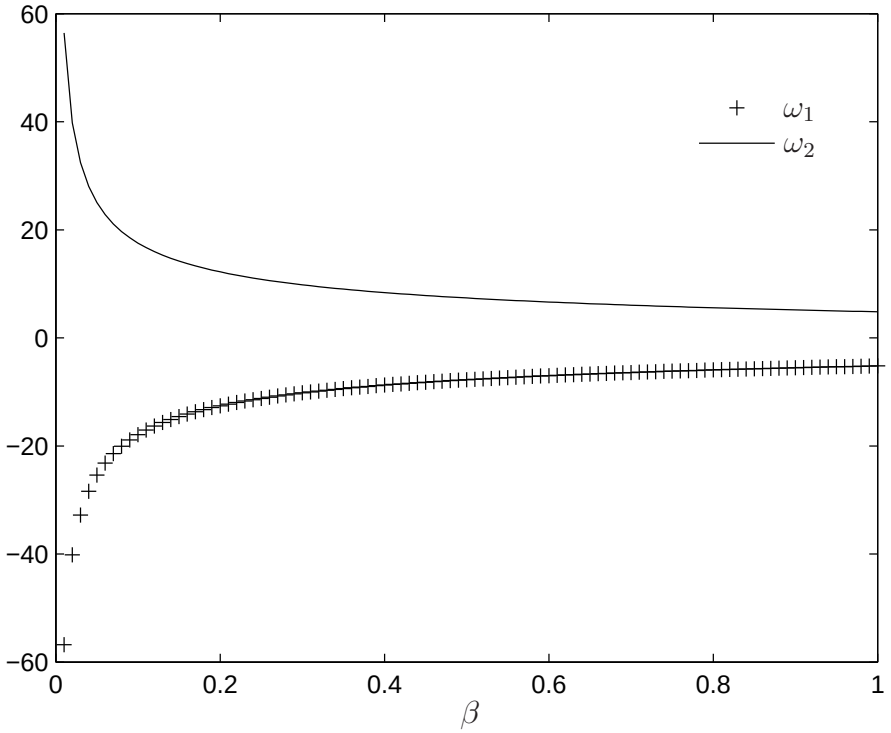

Figure 5.13. One-temperature approximation without collision; ω_1 and ω_2 eigenmodes as a function of β with $\alpha = 7.072$ and $\gamma_{pn} = 7.331$.

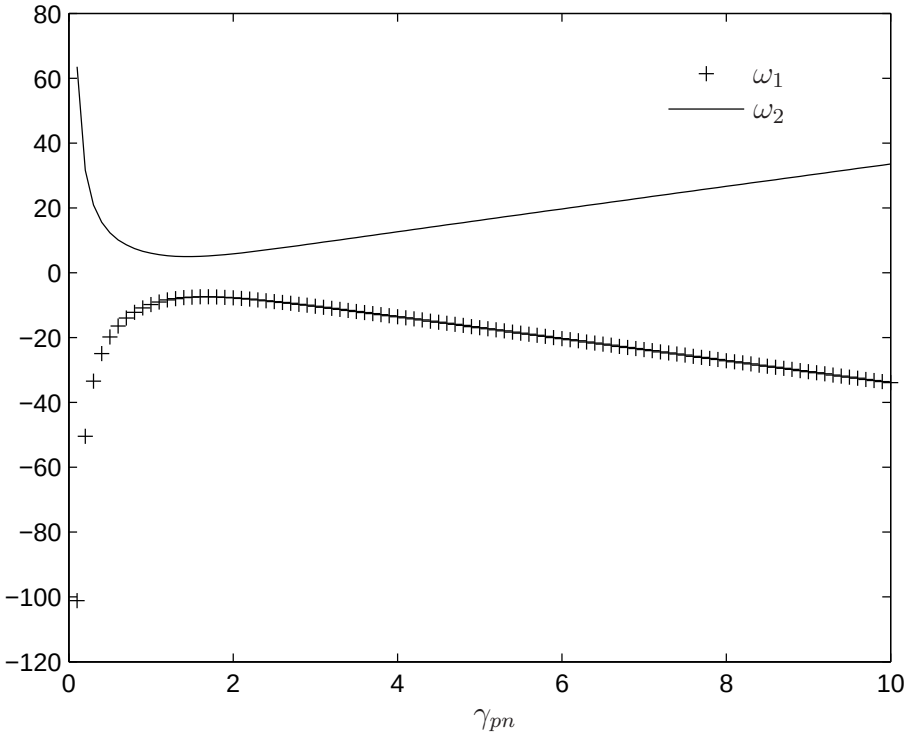

Figure 5.14. One-temperature approximation without collision; unstable eigenmode as a function of γ_{pn} with $\alpha = 14.144$ and $\beta = 0.052$ and $V_0 = 0.5$ V.

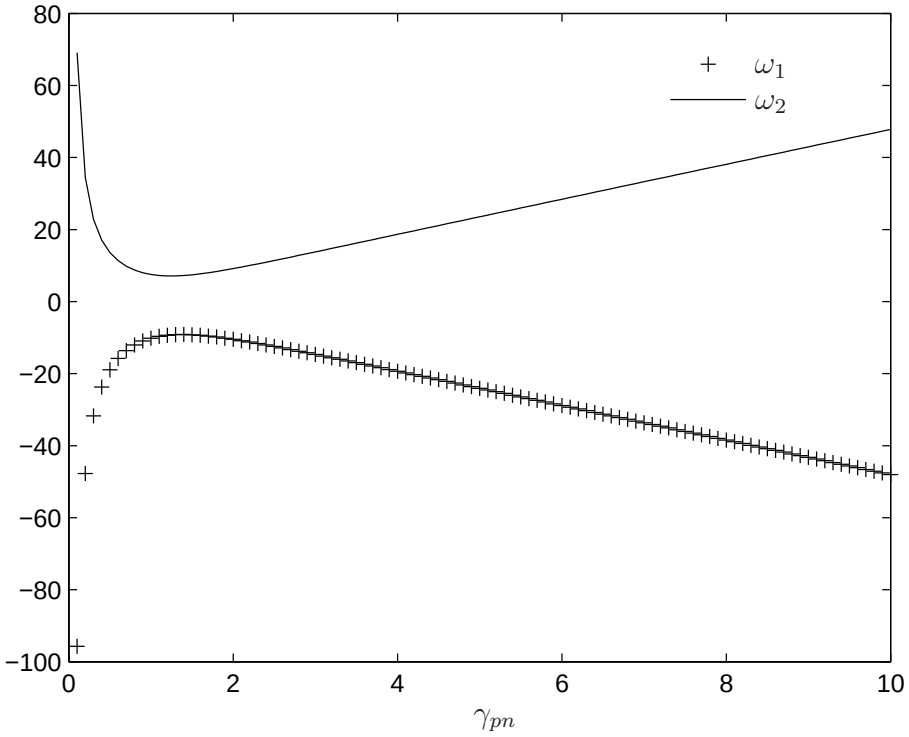

Figure 5.15. One-temperature approximation without collision; unstable eigenmode as a function of γ_{pn} with $\alpha = 7.072$ and $\beta = 0.026$ and $V_0 = 1.0$ V.

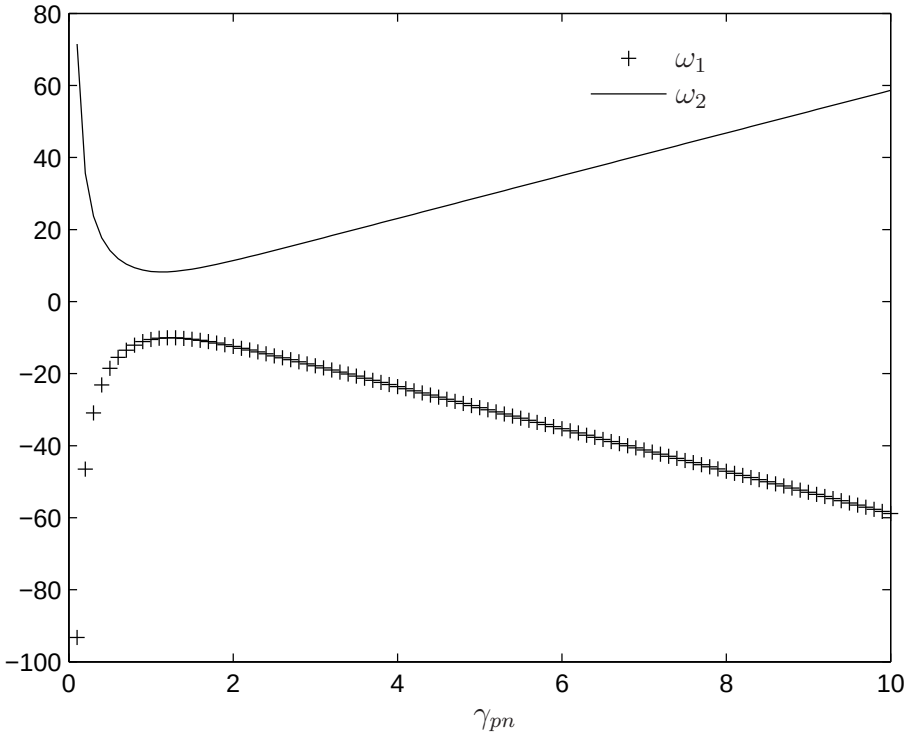

Figure 5.16. One-temperature approximation without collision; unstable eigenmode as a function of γ_{pn} with $\alpha = 4.7147$ and $\beta = 0.0173$ and $V_0 = 1.5$ V.

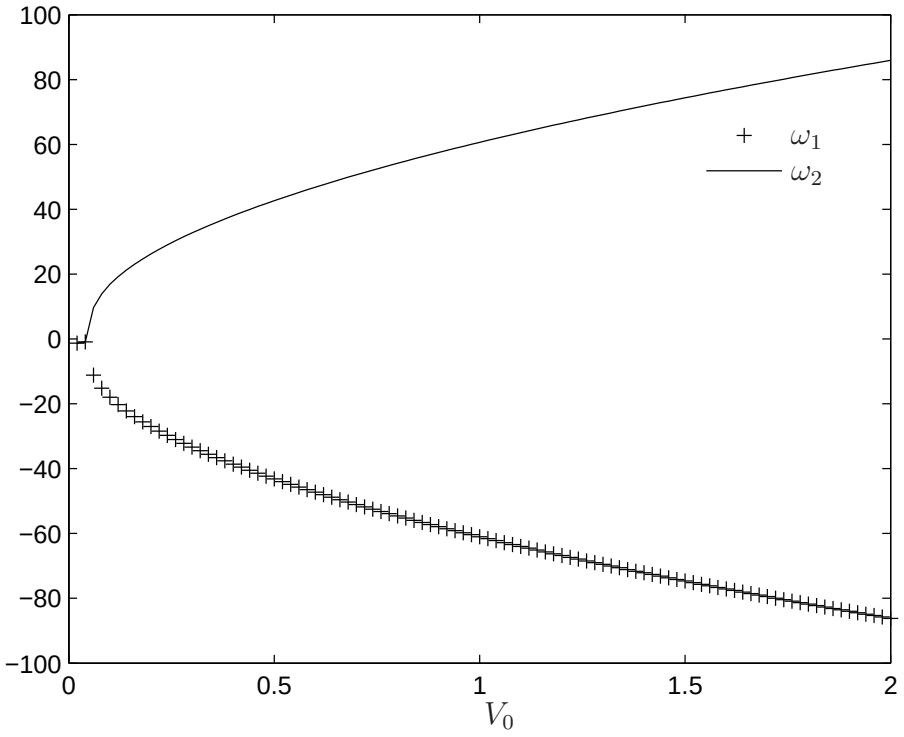

Figure 5.17. One-temperature approximation without collision; unstable eigenmode as a function of applied voltage V_0 with $T_{room} = 100$ K and $\gamma = 7.331$.

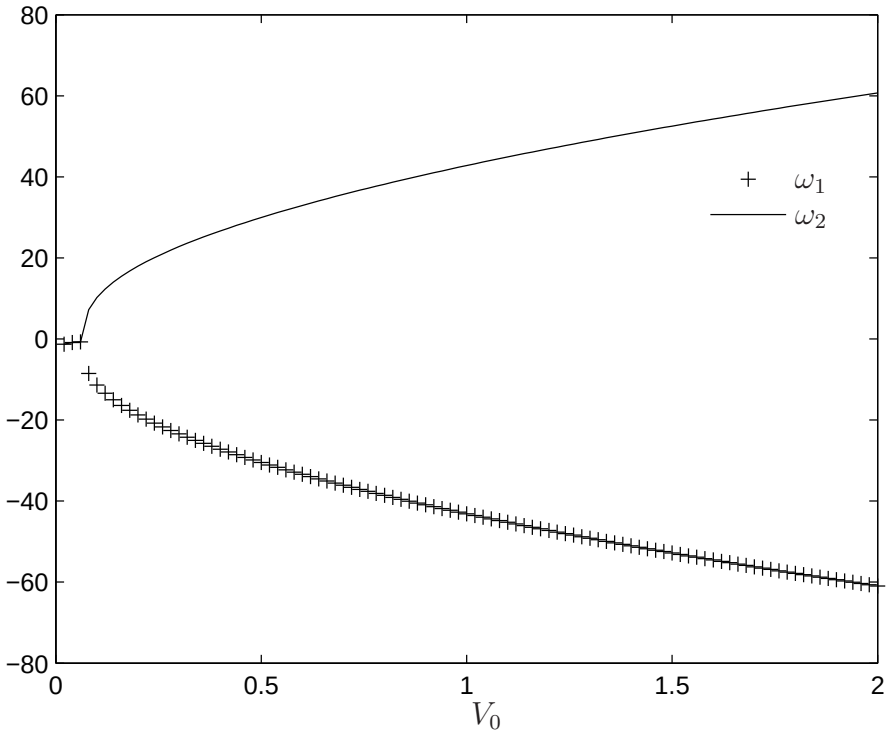

Figure 5.18. One-temperature approximation without collision; unstable eigenmode as a function of applied voltage V_0 with $T_{room} = 200$ K and $\gamma = 7.331$.

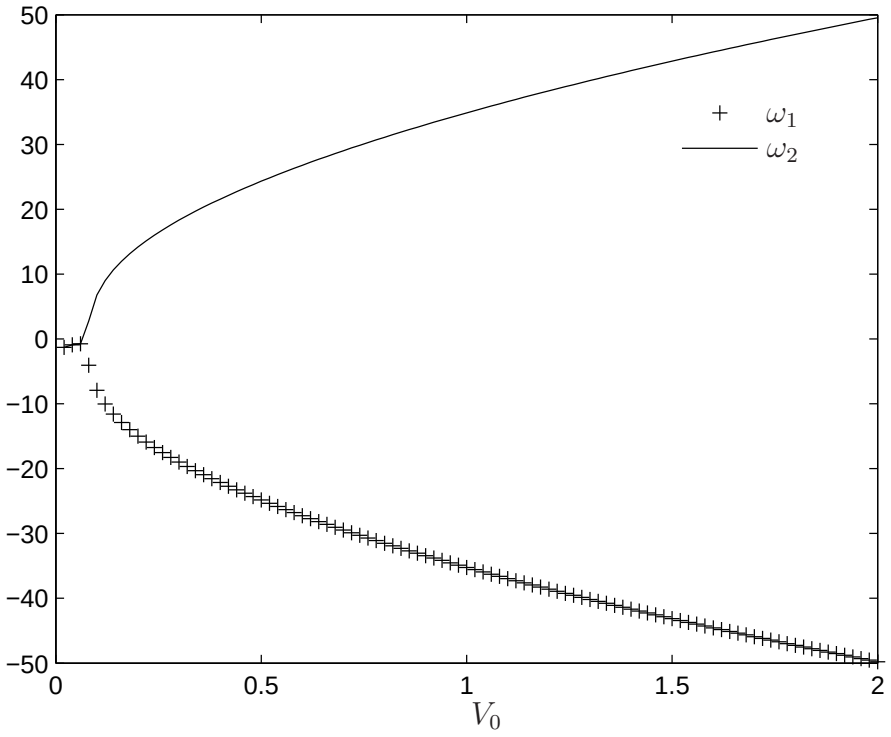

Figure 5.19. One-temperature approximation without collision; unstable eigenmode as a function of applied voltage V_0 with $T_{room} = 300$ K and $\gamma = 7.331$.

CHAPTER 6

CONCLUSIONS AND RECOMMENDATIONS

6.1 Conclusions

This work has presented the linear stability analysis of electron flow in ungated semiconductors by using a hydrodynamic model. The main contribution of this dissertation research was to provide an analysis of the instabilities of electron flow in an ungated semiconductor. The purpose of this work was to study the instabilities of electron flow in semiconductors and their dependency on the operating conditions, by making the electron flow more unstable or more stable. The motivation was the knowledge of the mechanisms to generate instabilities that can be useful for the use of semiconductors as a source of terahertz radiation.

In Chapters 3 and 4 was applied a thermally-uncoupled model to study the one-dimensional and two-dimensional configurations. Electron and lattice temperatures were not considered in the model. That analysis showed that the electron flow can be unstable depending on the operating conditions and the semiconductor physical properties. For the one-dimensional problem, the spectrum of eigenmodes in time was determined by using an analytical procedure. It was described by an out of phase Lambert W-function. Also, an important part of the spectrum in the two-dimensional configuration was determined analytically. That includes the spectra obtained in the one-dimensional configuration and also an infinite set of unstable and stable oscillatory modes.

In Chapter 5 was studied a one-dimensional configuration with three thermally-coupled models: two-temperature, one-temperature with collision and one-temperature without collision. A part of the spectrum of eigenmodes in time for the two-temperature model was determined by using numerical methods. These eigenmodes were found to be stable and without oscillatory components. In the one-temperature model without collision, no heat conduction of the electrons and equal electron and lattice temperatures were assumed. In the one-temperature model without collision no energy loss term due to electron scattering was also assumed. The purpose was to get an unstable spectrum in a model where the electron temperature was not being neglected. These models showed the conditions to be satisfied to have at least one unstable eigenmode in time, whose magnitude was determined by the operating conditions.

In summary, the study of electron flow in ungated semiconductors by using a hydrodynamic model showed that the flow can be unstable by specifying an operating regime through the applied voltage and room temperature, and physical properties of the semiconductor such as doping density. To make the electron flow unstable, heat conduction and energy transfer from the electrons to the lattice through collisions needed to be neglected since energy transfer to the lattice stabilizes the system.

6.2 Recommendations

As a consequence of this dissertation research, there are some aspects that would contribute and complement the results and conclusions presented in this work.

1. *Study of the transport and stability of holes in semiconductors.* The hy-

drodynamic model applied in this work can be modified and extended to study the transport of holes in semiconductors and its applications in quantum wells [99–101], P-N junctions and solar cells [102].

2. *Study of electron flow in heterostructures.* Modeling of parallel and serial electron flow in heterostructures by using hydrodynamic models to investigate the interactions present and how they can affect the instabilities that were analyzed in Chapter 3. Also, this can be extended to semiconductor devices with a linearly graded doping distribution [103].

3. *Thermal instabilities in the Dyakonov and Shur model [64, 72] for gated semiconductors and two-dimensional electron layers.* Study of the instabilities when the energy balance of the electrons is taken into account in the model. This would be very useful to understand the effect of a perturbed electron temperature in the temporal eigenmodes.

4. *Numerical simulations of one-dimensional model.* Implementation of an explicit finite difference method to solve the transient regime of the two-temperature model.

5. *Weakly nonlinear stability analysis.* Study of the nonlinear uncoupled one-dimensional model to find the amplitudes of the oscillations and determine the saturated behavior of the system.

6. *Study of periodic solutions.* Estimate the amplitude and frequencies of the limit cycles that are present in the uncoupled one-dimensional system by using averaging methods used in nonlinear differential equations such as the harmonic balance [104].

APPENDIX A

HYDRODYNAMIC EQUATIONS FROM MOMENTS OF BOLTZMANN'S EQUATION

The distribution function $f(t, x_i, v_i)$ that represents the number of particles in the six-dimensional phase space $dx_1 dx_2 dx_3 dv_1 dv_2 dv_3$ at time t obeys Boltzmann's equation:

$$\frac{\partial f}{\partial t} + v_i \frac{\partial f}{\partial x_i} + F_i \frac{\partial f}{\partial v_i} = \left(\frac{\partial f}{\partial t}\right)_{coll}, \tag{A.1}$$

where x_i corresponds to the spatial coordinates, v_i corresponds to the velocities coordinates, F_i represents to the external forces (per unit mass) and the right-hand-side term represents the particle collisions.

A.1 Continuity equation

Integrating equation (A.1) over the velocity space, the following result is obtained,

$$\int_{-\infty}^{+\infty}\int_{-\infty}^{+\infty}\int_{-\infty}^{+\infty} \frac{\partial f}{\partial t}\, dv_1 dv_2 dv_3 + \int_{-\infty}^{+\infty}\int_{-\infty}^{+\infty}\int_{-\infty}^{+\infty} v_i \frac{\partial f}{\partial x_i}\, dv_1 dv_2 dv_3 + \int_{-\infty}^{+\infty}\int_{-\infty}^{+\infty}\int_{-\infty}^{+\infty} F_i \frac{\partial f}{\partial v_i}\, dv_1 dv_2 dv_3$$

$$= \int_{-\infty}^{+\infty}\int_{-\infty}^{+\infty}\int_{-\infty}^{+\infty}\left(\frac{\partial f}{\partial t}\right)_{coll} dv_1 dv_2 dv_3.$$

Using integration by parts in the third term, this expression is equivalent to,

$$\begin{aligned}
&\frac{\partial}{\partial t}\int_{-\infty}^{+\infty}\int_{-\infty}^{+\infty}\int_{-\infty}^{+\infty} f\ dv_1 dv_2 dv_3 + \frac{\partial}{\partial x_i}\int_{-\infty}^{+\infty}\int_{-\infty}^{+\infty}\int_{-\infty}^{+\infty} v_i f\ dv_1 dv_2 dv_3 \\
&- \int_{-\infty}^{+\infty}\int_{-\infty}^{+\infty}\int_{-\infty}^{+\infty} \frac{\partial v_i}{\partial x_i} f\ dv_1 dv_2 dv_3 + \int_{-\infty}^{+\infty}\int_{-\infty}^{+\infty} (F_1 f)|_0^0\ dv_2 dv_3 \\
&- \int_{-\infty}^{+\infty}\int_{-\infty}^{+\infty}\int_{-\infty}^{+\infty} f\frac{\partial F_1}{\partial v_1}\ dv_1 dv_2 dv_3 + \int_{-\infty}^{+\infty}\int_{-\infty}^{+\infty} (F_2 f)|_0^0\ dv_1 dv_3 \\
&- \int_{-\infty}^{+\infty}\int_{-\infty}^{+\infty}\int_{-\infty}^{+\infty} f\frac{\partial F_2}{\partial v_2}\ dv_1 dv_2 dv_3 + \int_{-\infty}^{+\infty}\int_{-\infty}^{+\infty} (F_3 f)|_0^0\ dv_1 dv_2 \\
&- \int_{-\infty}^{+\infty}\int_{-\infty}^{+\infty}\int_{-\infty}^{+\infty} f\frac{\partial F_3}{\partial v_3}\ dv_1 dv_2 dv_3 \\
&= \left(\frac{\partial}{\partial t}\int_{-\infty}^{+\infty}\int_{-\infty}^{+\infty}\int_{-\infty}^{+\infty} f\ dv_1 dv_2 dv_3\right)_{coll} \\
&= \left(\frac{\partial n}{\partial t}\right)_{coll},
\end{aligned}$$

where the fact that $f = 0$ or $f \to 0$ as $v_i \to \pm\infty$ has been used. Assuming that F_i is independent of v_i, this expression can be written as

$$\begin{aligned}
&\frac{\partial}{\partial t}\int_{-\infty}^{+\infty}\int_{-\infty}^{+\infty}\int_{-\infty}^{+\infty} f\ dv_1 dv_2 dv_3 + \frac{\partial}{\partial x_i}\int_{-\infty}^{+\infty}\int_{-\infty}^{+\infty}\int_{-\infty}^{+\infty} v_i f\ dv_1 dv_2 dv_3 \\
&- \int_{-\infty}^{+\infty}\int_{-\infty}^{+\infty}\int_{-\infty}^{+\infty} \frac{\partial v_i}{\partial x_i} f\ dv_1 dv_2 dv_3 \\
&= \left(\frac{\partial}{\partial t}\int_{-\infty}^{+\infty}\int_{-\infty}^{+\infty}\int_{-\infty}^{+\infty} f dv_1 dv_2 dv_3\right)_{coll} \\
&= \left(\frac{\partial n}{\partial t}\right)_{coll},
\end{aligned}$$

where n corresponds to the number of particles in the three-dimensional space $dx_1 dx_2 dx_3$ at time t. Since v_i is independent of x_i, $\partial v_i/\partial x_i = 0$. Also, it is

necessary to consider the drift and thermal component of the velocity, $v_i = v_i^d + v_i^{th}$ and the fact that the average of the thermal velocity over the velocity space is zero ($\langle v_i^{th} \rangle = 0$) since these are vectors pointing in random directions with the same magnitude. This velocity follows the Maxwellian theory of gas dynamics and its average magnitude is much larger than the drift velocity. Therefore, the expression is

$$\frac{\partial n}{\partial t} + \frac{\partial (v_i^d n)}{\partial x_i} = \left(\frac{\partial n}{\partial t} \right)_{coll}. \tag{A.2}$$

This equation corresponds to the continuity equation. Using $v_i = v_i^d$, we get

$$\frac{\partial n}{\partial t} + \frac{\partial (v_i n)}{\partial x_i} = \left(\frac{\partial n}{\partial t} \right)_{coll}. \tag{A.3}$$

The collision term $(\partial n/\partial t)_{coll}$ represents the rate of the recombination-generation process.

A.2 Momentum equation

In order to get the momentum equation, it is necessary to multiply the equation (A.1) by the momentum $p_j = m_e v_j$ and integrate it over the velocity space. The following expression is obtained:

$$\begin{aligned}
&\int_{-\infty}^{+\infty}\int_{-\infty}^{+\infty}\int_{-\infty}^{+\infty} \frac{\partial f}{\partial t} m_e v_j \; dv_1 dv_2 dv_3 + \int_{-\infty}^{+\infty}\int_{-\infty}^{+\infty}\int_{-\infty}^{+\infty} v_i \frac{\partial f}{\partial x_i} m_e v_j \; dv_1 dv_2 dv_3 \\
&+ \int_{-\infty}^{+\infty}\int_{-\infty}^{+\infty}\int_{-\infty}^{+\infty} F_i \frac{\partial f}{\partial v_i} m_e v_j \; dv_1 dv_2 dv_3 \\
&= \int_{-\infty}^{+\infty}\int_{-\infty}^{+\infty}\int_{-\infty}^{+\infty} \left(\frac{\partial f}{\partial t} \right)_{coll} m_e v_j \; dv_1 dv_2 dv_3.
\end{aligned}$$

Since,

$$\begin{aligned}
&\int_{-\infty}^{+\infty}\int_{-\infty}^{+\infty}\int_{-\infty}^{+\infty}\frac{\partial f}{\partial t}m_e v_j\ dv_1dv_2dv_3\\
&=\frac{\partial}{\partial t}\int_{-\infty}^{+\infty}\int_{-\infty}^{+\infty}\int_{-\infty}^{+\infty}fm_e v_j\ dv_1dv_2dv_3\\
&=\frac{\partial(nm_e v_j^d)}{\partial t},
\end{aligned}$$

$$\begin{aligned}
&\int_{-\infty}^{+\infty}\int_{-\infty}^{+\infty}\int_{-\infty}^{+\infty}v_i\frac{\partial f}{\partial x_i}m_e v_j\ dv_1dv_2dv_3\\
&=\frac{\partial}{\partial x_i}\int_{-\infty}^{+\infty}\int_{-\infty}^{+\infty}\int_{-\infty}^{+\infty}v_i fm_e v_j\ dv_1dv_2dv_3\\
&=\frac{\partial}{\partial x_i}\int_{-\infty}^{+\infty}\int_{-\infty}^{+\infty}\int_{-\infty}^{+\infty}(v_i^d+v_i^{th})fm_e(v_j^d+v_j^{th})\ dv_1dv_2dv_3,
\end{aligned}$$

$$\begin{aligned}
&\int_{-\infty}^{+\infty}\int_{-\infty}^{+\infty}\int_{-\infty}^{+\infty}F_i\frac{\partial f}{\partial v_i}m_e v_j\ dv_1dv_2dv_3\\
&=\int_{-\infty}^{+\infty}\int_{-\infty}^{+\infty}\int_{0}^{0}d(F_1fm_e v_j)dv_2dv_3+\int_{-\infty}^{+\infty}\int_{-\infty}^{+\infty}\int_{0}^{0}d(F_2fm_e v_j)dv_1dv_3\\
&+\int_{-\infty}^{+\infty}\int_{-\infty}^{+\infty}\int_{0}^{0}d(F_3fm_e v_j)dv_1dv_2-\int_{-\infty}^{+\infty}\int_{-\infty}^{+\infty}\int_{-\infty}^{+\infty}f\frac{\partial(F_i m_e v_j)}{\partial v_i}\ dv_1dv_2dv_3,
\end{aligned}$$

$$\begin{aligned}
&\int_{-\infty}^{+\infty}\int_{-\infty}^{+\infty}\int_{-\infty}^{+\infty}\left(\frac{\partial f}{\partial t}\right)_{coll}m_e v_j\ dv_1dv_2dv_3\\
&=\left(\frac{\partial}{\partial t}\int_{-\infty}^{+\infty}\int_{-\infty}^{+\infty}\int_{-\infty}^{+\infty}fm_e v_j\ dv_1dv_2dv_3\right)_{coll}\\
&=\left(\frac{\partial(nm_e v_j^d)}{\partial t}\right)_{coll},
\end{aligned}$$

So, since the term $m_e v_j$ depends only in v_j (it is independent of x_i and t), $\langle v_j^{th} \rangle = 0$, and $\langle v_j^d \rangle = v_j^d$, we get

$$\begin{aligned}
&\frac{\partial (n m_e v_j^d)}{\partial t} + \frac{\partial}{\partial x_i} \int_{-\infty}^{+\infty} \int_{-\infty}^{+\infty} \int_{-\infty}^{+\infty} (v_i^d + v_i^{th}) f m_e (v_j^d + v_j^{th}) \, dv_1 dv_2 dv_3 \\
&- \int_{-\infty}^{+\infty} \int_{-\infty}^{+\infty} \int_{-\infty}^{+\infty} f \frac{\partial (F_i m_e v_j)}{\partial v_i} \, dv_1 dv_2 dv_3 \\
&= \left(\frac{\partial (n m_e v_j^d)}{\partial t} \right)_{coll}.
\end{aligned}$$

This expression is equivalent to

$$\begin{aligned}
&\frac{\partial (n m_e v_j^d)}{\partial t} + \frac{\partial}{\partial x_i} \int_{-\infty}^{+\infty} \int_{-\infty}^{+\infty} \int_{-\infty}^{+\infty} f m_e (v_i^d v_j^d + v_i^d v_j^{th} + v_i^{th} v_j^d + v_i^{th} v_j^{th}) \, dv_1 dv_2 dv_3 \\
&- \int_{-\infty}^{+\infty} \int_{-\infty}^{+\infty} \int_{-\infty}^{+\infty} f \frac{\partial (F_i m_e v_j)}{\partial v_i} \, dv_1 dv_2 dv_3 \\
&= \left(\frac{\partial (n m_e v_j^d)}{\partial t} \right)_{coll}.
\end{aligned}$$

Since $\langle v_i^d v_j^{th} \rangle = v_i^d \langle v_j^{th} \rangle = 0$, we have

$$\begin{aligned}
&\frac{\partial (n m_e v_j^d)}{\partial t} + \frac{\partial}{\partial x_i} (\langle n m_e v_i^d v_j^d \rangle + n m_e \langle v_i^{th} v_j^{th} \rangle) \\
&- \int_{-\infty}^{+\infty} \int_{-\infty}^{+\infty} \int_{-\infty}^{+\infty} f \frac{\partial (F_i m_e v_j)}{\partial v_i} \, dv_1 dv_2 dv_3 \\
&= \left(\frac{\partial (n m_e v_j^d)}{\partial t} \right)_{coll}.
\end{aligned}$$

The thermal energy can be related to the carrier temperature through $\frac{3}{2} n k_B T = \frac{1}{2} n m_e \langle v_j^{th} v_j^{th} \rangle$. Due to the lack of correlation, the off-diagonal components of this tensor are equal to zero. Therefore, the thermal energy for each degree of freedom k_d is $\frac{1}{2} n k_B T = \frac{1}{2} n m_e \langle v_{k_d}^{th} v_{k_d}^{th} \rangle$. Using the momentum density $p_{nj} = n m_e v_j^d =$

$nm_e v_j$, we get

$$\frac{\partial p_{nj}}{\partial t} + \frac{\partial (v_i p_{nj})}{\partial x_i} + \frac{\partial (nk_B T_e)}{\partial x_j} - \int_{-\infty}^{+\infty}\int_{-\infty}^{+\infty}\int_{-\infty}^{+\infty} f \frac{\partial (F_i m_e v_j)}{\partial v_i}\, dv_1 dv_2 dv_3 = \left(\frac{\partial p_{nj}}{\partial t}\right)_{coll}.$$

Since $\partial v_j / \partial v_i = \delta_{ij}$, we get,

$$\frac{\partial p_{nj}}{\partial t} + \frac{\partial (v_i p_{nj})}{\partial x_i} + \frac{\partial (nk_B T_e)}{\partial x_j} - F_j n m_e = \left(\frac{\partial p_{nj}}{\partial t}\right)_{coll},$$

where F corresponds to the external force per unit mass over each particle. Using the expression for the Lorentz force per unit mass, $F_j^{tot} = -e\frac{1}{m_e}(\mathcal{E}_j + \varepsilon_{ikj} v_i^d B_k)$, we have

$$\frac{\partial p_{nj}}{\partial t} + \frac{\partial (v_i p_{nj})}{\partial x_i} = -ne(\mathcal{E}_j + \varepsilon_{ikj} v_i B_k) - \frac{\partial (nk_B T_e)}{\partial x_j} + \left(\frac{\partial p_{nj}}{\partial t}\right)_{coll},$$

which corresponds to the momentum equation.

Substituting $p_{nj} = nm_e v_j$, we get,

$$nm_e \frac{\partial v_j}{\partial t} + m_e v_j \frac{\partial n}{\partial t} + nm_e v_i \frac{\partial v_j}{\partial x_i} + m_e v_j \frac{\partial (nv_i)}{\partial x_i} = -ne(\mathcal{E}_j + \varepsilon_{ikj} v_i B_k) - \frac{\partial (nk_B T_e)}{\partial x_j} + nm_e \left(\frac{\partial v_j}{\partial t}\right)_{coll} + m_e v_j \left(\frac{\partial n}{\partial t}\right)_{coll}.$$

Reorganizing terms

$$m_e v_j \left[\frac{\partial n}{\partial t} + \frac{\partial (nv_i)}{\partial x_i} - \left(\frac{\partial n}{\partial t}\right)_{coll}\right] + nm_e \frac{\partial v_j}{\partial t} + nm_e v_i \frac{\partial v_j}{\partial x_i} = -ne(\mathcal{E}_j + \varepsilon_{ikj} v_i B_k) - \frac{\partial (nk_B T_e)}{\partial x_j} + nm_e \left(\frac{\partial v_j}{\partial t}\right)_{coll},$$

the first term is the continuity equation (A.3), so we get the momentum equation in terms of velocity (drift),

$$\frac{\partial v_j}{\partial t} + v_i \frac{\partial v_j}{\partial x_i} = -\frac{e}{m_e}(\mathcal{E}_j + \varepsilon_{ikj} v_i B_k) - \frac{1}{n m_e}\frac{\partial (n k_B T_e)}{\partial x_j} + \left(\frac{\partial v_j}{\partial t}\right)_{coll}. \qquad (A.4)$$

The collision term $(\partial v_j/\partial t)_{coll}$ can be approximated by $-v_j/\tau_p$ [22], where τ_p corresponds to the momentum relaxation time. Therefore, the momentum equation in terms of velocity is:

$$\frac{\partial v_j}{\partial t} + v_i \frac{\partial v_j}{\partial x_i} = -\frac{e}{m_e}(\mathcal{E}_j + \varepsilon_{ikj} v_i B_k) - \frac{1}{n m_e}\frac{\partial (n k_B T_e)}{\partial x_j} - \frac{v_j}{\tau_p}. \qquad (A.5)$$

A.3 Energy equation

Multiplying Eq. (A.1) by the energy $E = \frac{1}{2} m_e v_j v_j$, where $v_j = v_j^d + v_j^{th}$, and integrating over the velocity space, the following expression is obtained,

$$\begin{aligned}
&\int_{-\infty}^{+\infty}\int_{-\infty}^{+\infty}\int_{-\infty}^{+\infty} \frac{\partial f}{\partial t} E \; dv_1 dv_2 dv_3 + \int_{-\infty}^{+\infty}\int_{-\infty}^{+\infty}\int_{-\infty}^{+\infty} v_i \frac{\partial f}{\partial x_i} E \; dv_1 dv_2 dv_3 \\
&+ \int_{-\infty}^{+\infty}\int_{-\infty}^{+\infty}\int_{-\infty}^{+\infty} F_i \frac{\partial f}{\partial v_i} E \; dv_1 dv_2 dv_3 \\
&= \int_{-\infty}^{+\infty}\int_{-\infty}^{+\infty}\int_{-\infty}^{+\infty} \left(\frac{\partial f}{\partial t}\right)_{coll} E \; dv_1 dv_2 dv_3.
\end{aligned}$$

Since,

$$\begin{aligned}
&\int_{-\infty}^{+\infty}\int_{-\infty}^{+\infty}\int_{-\infty}^{+\infty} \frac{\partial f}{\partial t} E \; dv_1 dv_2 dv_3 \\
&= \frac{\partial}{\partial t}\int_{-\infty}^{+\infty}\int_{-\infty}^{+\infty}\int_{-\infty}^{+\infty} f E \; dv_1 dv_2 dv_3 \\
&= \frac{\partial n\langle E\rangle}{\partial t},
\end{aligned}$$

$$
\begin{aligned}
&\int_{-\infty}^{+\infty}\int_{-\infty}^{+\infty}\int_{-\infty}^{+\infty} v_i\frac{\partial f}{\partial x_i}E\ dv_1dv_2dv_3\\
&=\frac{\partial}{\partial x_i}\int_{-\infty}^{+\infty}\int_{-\infty}^{+\infty}\int_{-\infty}^{+\infty} v_i f E\ dv_1dv_2dv_3\\
&=\frac{\partial}{\partial x_i}\int_{-\infty}^{+\infty}\int_{-\infty}^{+\infty}\int_{-\infty}^{+\infty} (v_i^d+v_i^{th})f\frac{1}{2}m_e(v_j^d+v_j^{th})(v_j^d+v_j^{th})dv_1dv_2dv_3,
\end{aligned}
$$

$$
\begin{aligned}
&\int_{-\infty}^{+\infty}\int_{-\infty}^{+\infty}\int_{-\infty}^{+\infty} F_i\frac{\partial f}{\partial v_i}E\ dv_1dv_2dv_3\\
&=\int_{-\infty}^{+\infty}\int_{-\infty}^{+\infty}\int_{0}^{0} d(F_1fE)dv_2dv_3+\int_{-\infty}^{+\infty}\int_{-\infty}^{+\infty}\int_{0}^{0} d(F_2fE)dv_1dv_3\\
&+\int_{-\infty}^{+\infty}\int_{-\infty}^{+\infty}\int_{0}^{0} d(F_3fE)dv_1dv_2-\int_{-\infty}^{+\infty}\int_{-\infty}^{+\infty}\int_{-\infty}^{+\infty} f\frac{\partial F_iE}{\partial v_i}\ dv_1dv_2dv_3,
\end{aligned}
$$

$$
\begin{aligned}
&\int_{-\infty}^{+\infty}\int_{-\infty}^{+\infty}\int_{-\infty}^{+\infty}\left(\frac{\partial f}{\partial t}\right)_{coll}E\ dv_1dv_2dv_3\\
&=\left(\frac{\partial}{\partial t}\int_{-\infty}^{+\infty}\int_{-\infty}^{+\infty}\int_{-\infty}^{+\infty} fE\ dv_1dv_2dv_3\right)_{coll}\\
&=\left(\frac{\partial n\langle E\rangle}{\partial t}\right)_{coll},
\end{aligned}
$$

where $\langle E\rangle$ denotes the average energy in the velocity space. Using $E_n = n\langle E\rangle$ and reorganizing terms, we get

$$
\begin{aligned}
&\frac{\partial E_n}{\partial t}+\frac{\partial}{\partial x_i}\int_{-\infty}^{+\infty}\int_{-\infty}^{+\infty}\int_{-\infty}^{+\infty}(v_i^d+v_i^{th})f\frac{1}{2}m_e(v_j^d+v_j^{th})(v_j^d+v_j^{th})dv_1dv_2dv_3\\
&-\int_{-\infty}^{+\infty}\int_{-\infty}^{+\infty}\int_{-\infty}^{+\infty} f\frac{\partial F_iE}{\partial v_i}dv_1dv_2dv_3\\
&=\left(\frac{\partial E_n}{\partial t}\right)_{coll}.
\end{aligned}
$$

This expression is equivalent to

$$\begin{aligned}
&\frac{\partial E_n}{\partial t} + \frac{\partial}{\partial x_i}\int_{-\infty}^{+\infty}\int_{-\infty}^{+\infty}\int_{-\infty}^{+\infty} v_i^d f E dv_1 dv_2 dv_3 \\
&+\frac{\partial}{\partial x_i}\int_{-\infty}^{+\infty}\int_{-\infty}^{+\infty}\int_{-\infty}^{+\infty} f\frac{1}{2}m_e(v_j^d v_j^d v_i^{th} + 2v_j^d v_j^{th} v_i^{th} + v_j^{th} v_j^{th} v_i^{th})\; dv_1 dv_2 dv_3 \\
&-\int_{-\infty}^{+\infty}\int_{-\infty}^{+\infty}\int_{-\infty}^{+\infty} f\frac{1}{2}m_e\frac{\partial F_i v_j v_j}{\partial v_i} dv_1 dv_2 dv_3 \\
&=\left(\frac{\partial E_n}{\partial t}\right)_{coll}.
\end{aligned}$$

Since $\langle v_j^d v_j^d v^{th}\rangle = v_j^d v_j^d \langle v_i^{th}\rangle = 0$, we have

$$\begin{aligned}
&\frac{\partial E_n}{\partial t} + \frac{\partial (v_i^d E_n)}{\partial x_i} + \frac{1}{2}\left[2\frac{\partial n m_e \langle v_j^d v_j^{th} v_i^{th}\rangle}{\partial x_i} + \frac{\partial n m_e \langle v_j^{th} v_j^{th} v_i^{th}\rangle}{\partial x_i}\right] \\
&-\int_{-\infty}^{+\infty}\int_{-\infty}^{+\infty}\int_{-\infty}^{+\infty} f\frac{1}{2}m_e\frac{\partial F_i v_j v_j}{\partial v_i}\; dv_1 dv_2 dv_3 \\
&=\left(\frac{\partial E_n}{\partial t}\right)_{coll},
\end{aligned}$$

where $2\langle v_j^d v_j^{th} v_i^{th}\rangle = 2v_j^d\langle v_i^{th} v_j^{th}\rangle = 2\frac{v_i^d}{m_e}k_B T_e$ (the off-diagonal components of the tensor are equal to zero) and the heat flux $q_i = \frac{1}{2}n m_e \langle v_j^{th} v_j^{th} v_i^{th}\rangle$. Using the expression for the Lorentz force per unit mass, $F_j^{tot} = -e\frac{1}{m_e}(\mathcal{E}_j + \varepsilon_{ikj} v_i^d B_k)$, we get the energy equation and reorganizing terms, we get

$$\frac{\partial E_n}{\partial t} + \frac{\partial (v_i^d E_n)}{\partial x_i} + \frac{\partial (n k_B T_e v_i^d)}{\partial x_i} + \frac{\partial q_i}{\partial x_i} + ne(\mathcal{E}_j + \varepsilon_{ikj} v_i^d B_k) v_j^d = \left(\frac{\partial E_n}{\partial t}\right)_{coll}.$$

Using $v_i = v_i^d$,

$$\frac{\partial E_n}{\partial t} + \frac{\partial (v_i E_n)}{\partial x_i} + \frac{\partial (n k_B T_e v_i)}{\partial x_i} + \frac{\partial q_i}{\partial x_i} + ne(\mathcal{E}_j + \varepsilon_{ikj} v_i B_k) v_j = \left(\frac{\partial E_n}{\partial t}\right)_{coll}. \quad \text{(A.6)}$$

Using $E_n = \frac{1}{2}nm_e v_j v_j + \frac{3}{2}nk_B T_e$, we get

$$\begin{aligned}
&nm_e v_j \frac{\partial v_j}{\partial t} + \frac{E_n}{n}\frac{\partial n}{\partial t} + \frac{3}{2}nk_B \frac{\partial T_e}{\partial t} + E_n \frac{\partial v_i}{\partial x_i} \\
&+\frac{E_n}{n} v_i \frac{\partial n}{\partial x_i} + nm_e v_j v_i \frac{\partial v_j}{\partial x_i} + \frac{3}{2}nk_B v_i \frac{\partial T_e}{\partial x_i} \\
&= -\frac{\partial (nk_B T_e v_i)}{\partial x_i} - \frac{\partial q_i}{\partial x_i} - ne(\mathcal{E}_j + \varepsilon_{ikj} v_i B_k) v_j + nm_e v_j \left(\frac{\partial v_j}{\partial t}\right)_{coll} \\
&+\frac{E_n}{n}\left(\frac{\partial n}{\partial t}\right)_{coll} + \frac{3}{2}nk_B \left(\frac{\partial T_e}{\partial t}\right)_{coll}.
\end{aligned}$$

Multiplying by n and reorganizing terms,

$$\begin{aligned}
&n^2 m_e v_j \left[\frac{\partial v_j}{\partial t} + v_i \frac{\partial v_j}{\partial x_i} + \frac{1}{nm_e}\frac{\partial (nk_B T_e)}{\partial x_j} - \left(\frac{\partial v_j}{\partial t}\right)_{coll} + \frac{e}{m_e}(\mathcal{E}_j + \varepsilon_{ikj} v_i B_k)\right] \\
&+E_n \left[\frac{\partial n}{\partial t} + \frac{\partial (nv_i)}{\partial x_i} - \left(\frac{\partial n}{\partial t}\right)_{coll}\right] + \frac{3}{2}n^2 k_B \frac{\partial T_e}{\partial t} + \frac{3}{2}n^2 k_B v_i \frac{\partial T_e}{\partial x_i} \\
&= -n^2 k_B T_e \frac{\partial v_i}{\partial x_i} - n\frac{\partial q_i}{\partial x_i} + \frac{3}{2}n^2 k_B \left(\frac{\partial T_e}{\partial t}\right)_{coll}.
\end{aligned}$$

The first term contains the momentum equation (A.4) in terms of the drift velocity and the second term contains the continuity equation (A.3). So we get

$$\frac{3}{2}n^2 k_B \left[\frac{\partial T_e}{\partial t} + v_i \frac{\partial T_e}{\partial x_i}\right] = \frac{3}{2}n^2 k_B \left[-\frac{2}{3}T_e \frac{\partial v_i}{\partial x_i} - \frac{2}{3nk_B}\frac{\partial q_i}{\partial x_i} + \left(\frac{\partial T_e}{\partial t}\right)_{coll}\right],$$

which corresponds to the energy equation in terms of the carrier temperature. Using the Fourier's Law $q_i = -k_e \partial T_e / \partial x_i$ we get

$$\frac{\partial T_e}{\partial t} + v_i \frac{\partial T_e}{\partial x_i} = -\frac{2}{3}T_e \frac{\partial v_i}{\partial x_i} + \frac{2}{3nk_B}\frac{\partial}{\partial x_i}\left(k_e \frac{\partial T_e}{\partial x_i}\right) + \left(\frac{\partial T_e}{\partial t}\right)_{coll}. \tag{A.7}$$

The collision term $(\partial T_e/\partial t)_{coll}$ can be approximated by $-(T_e - T_L)/\tau_E + 2m_e(v_i^2)(1 - \tau_p/2\tau_E)/3k_B\tau_p$ [22], where T_L is the lattice temperature, τ_E is the energy relaxation

time and τ_p is the momentum relaxation time. Therefore, the energy equation in terms of the carrier temperature is:

$$\frac{\partial T_e}{\partial t} + v_i \frac{\partial T_e}{\partial x_i} = -\frac{2}{3} T_e \frac{\partial v_i}{\partial x_i} + \frac{2}{3nk_B} \frac{\partial}{\partial x_i} \left(k_e \frac{\partial T_e}{\partial x_i} \right) \\ -\frac{T_e - T_L}{\tau_E} + \frac{2m_e(v_i v_i)}{3k_B \tau_p} \left(1 - \frac{\tau_p}{2\tau_E} \right). \tag{A.8}$$

A.4 Equations for longitudinal optical and acoustic phonons

The constitutive relation that relates the change of energy of the longitudinal optical phonons due to their interaction with electrons and acoustic phonons can be expressed through the following energy balance,

$$\frac{\partial E_{LO}}{\partial t} = -\left(\frac{\partial E_e}{\partial t} \right)_{coll} + \left(\frac{\partial E_{LO}}{\partial t} \right)_{coll}, \tag{A.9}$$

where E_{LO} and E_e are the longitudinal optical phonon and electron energies per unit volume respectively.

Equation (A.9) is equivalent to

$$C_{LO} \frac{\partial T_{LO}}{\partial t} = -\left(\frac{\frac{3}{2} n k_B T_{LO} - \frac{3}{2} n k_B T_e - \frac{1}{2} n m_e v_i v_i}{\tau_{e-LO}} \right) - C_{LO} \frac{T_{LO} - T_A}{\tau_{LO-A}}, \tag{A.10}$$

where τ_{e-LO} is the electron energy relaxation time for the electron-longitudinal optical phonon scattering, τ_{LO-A} is the energy relaxation time for the longitudinal optical-acoustic phonon scattering, and C_{LO} is the heat capacity for longitudinal optical phonons.

Following the same idea for acoustic phonons, the constitutive relation between the change of energy of the acoustic phonons due to their interaction with longitudinal optical phonons and the lattice itself can be expressed through the

following energy balance,

$$\frac{\partial E_A}{\partial t} = -\left(\frac{\partial E_{LO}}{\partial t}\right)_{coll} - \frac{\partial q_{Ai}}{\partial x_i}, \tag{A.11}$$

where E_A is the energy of acoustic phonons and $\partial q_{Ai}/\partial x_i$ is the energy loss of the acoustic phonons by heat transfer ($q_{Ai} = -k_A \partial T_A/\partial x_i$).

Equation (A.11) is equivalent to

$$C_A \frac{\partial T_A}{\partial t} = \frac{\partial}{\partial x_i}\left(k_A \frac{\partial T_A}{\partial x_i}\right) + C_{LO}\left(\frac{T_{LO} - T_A}{\tau_{LO-A}}\right), \tag{A.12}$$

where C_A is the heat capacity for acoustic phonons.

A.5 Lattice energy constitutive equation

The energy that the lattice gets finally is the energy loss from electrons due to scattering. Therefore, the constitutive relation of the change of energy in the lattice due to interaction with electrons can be expressed through the following energy balance,

$$C_L \frac{\partial T_L}{\partial t} = \frac{\partial}{\partial x_i}\left(k_L \frac{\partial T_L}{\partial x_i}\right) + \frac{3}{2} n k_B \left(\frac{T_e - T_L}{\tau_E}\right) + \frac{1}{2\tau_E} n m_e v_i v_i, \tag{A.13}$$

where C_L is the heat capacity for the lattice, T_L is the lattice temperature, and τ_E is the energy relaxation time for electron-lattice scattering.

Since T_A is the lattice temperature, and assuming that C_{LO} is very small, $T_{LO} \approx T_L$ and $\tau_E \approx \tau_{e-LO}$, from Eq. (A.10) we get the following approximation

$$C_{LO}\left(\frac{T_{LO} - T_A}{\tau_{LO-A}}\right) \approx \frac{3}{2} n k_B \left(\frac{T_e - T_L}{\tau_E}\right) + \frac{1}{2\tau_E} n m_e v_i v_i, \tag{A.14}$$

and by substituting Eq. (A.14) into Eq. (A.12) we get Eq. (A.13).

APPENDIX B

HYDRODYNAMIC EQUATIONS FROM DIFFERENTIAL CONTROL VOLUME FIXED IN SPACE

Considering a fixed differential control volume $dV = dx_1 dx_2 dx_3$ in space as shown in Fig. B.1 that represents an infinitesimal box in three-dimensional space at the position (x_1, x_2, x_3), the continuity, momentum, and energy equations are as follows.

B.1 Continuity equation

The rate of increase of mass inside dV is equal to the rate of mass in minus the rate of mass out. Considering the mass as $M = nm_e dV$, this can be written as

$$\begin{aligned}\frac{\partial M}{\partial t} &= nm_e v_1|_{x_1} dx_2 dx_3 - nm_e v_1|_{x_1+dx_1} dx_2 dx_3 + nm_e v_2|_{x_2} dx_1 dx_3 \\ &- nm_e v_2|_{x_2+dx_2} dx_1 dx_3 + nm_e v_3|_{x_3} dx_1 dx_2 - nm_e v_3|_{x_3+dx_3} dx_1 dx_2.\end{aligned} \tag{B.1}$$

By using a Taylor series approximation

$$nm_e v_j|_{x_j+dx_j} dx_i dx_k = nm_e v_j|_{x_j} dx_i dx_k + \frac{\partial (nm_e v_j)}{\partial x_j} dx_j dx_i dx_k,$$

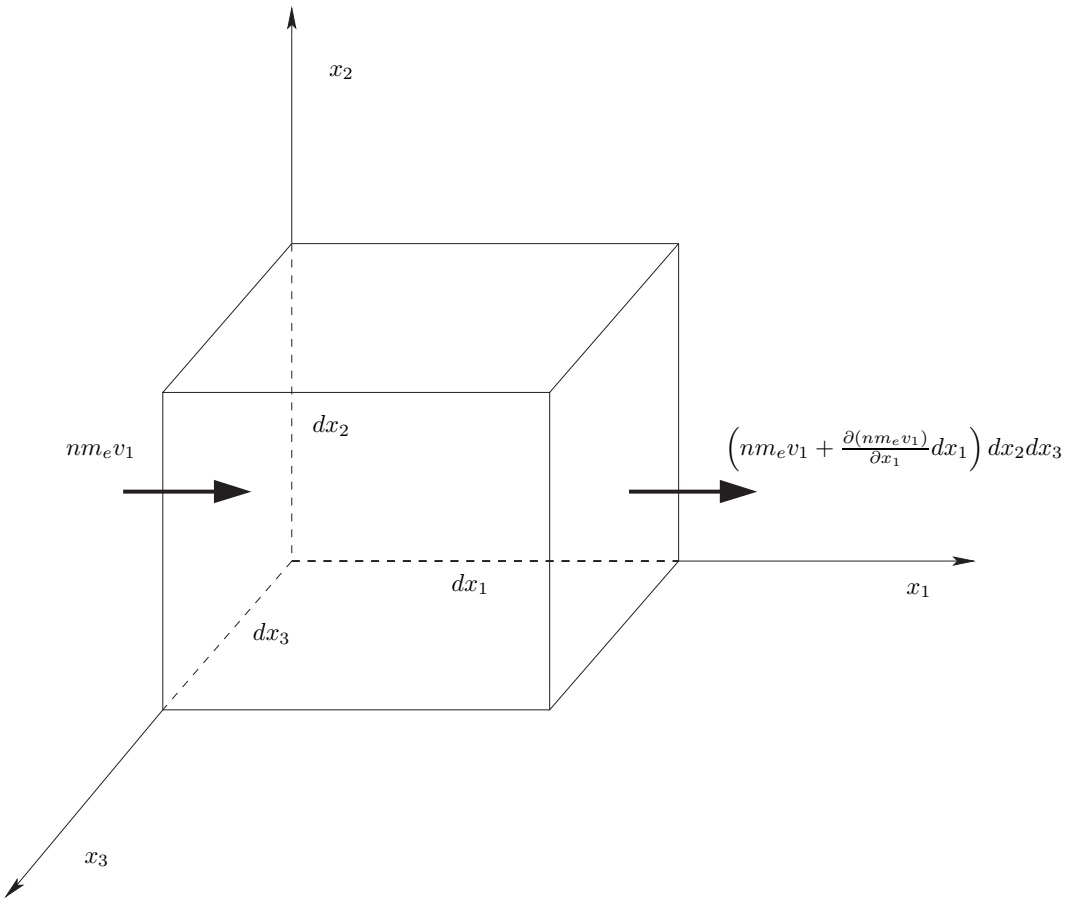

Figure B.1. Infinitesimal fixed control volume. Model used for the derivation of the mass balance in x-direction.

then Eq. (B.1) can be written as

$$\frac{\partial n m_e dV}{\partial t} = -\frac{\partial (n m_e v_i)}{\partial x_i} dV,$$

which is equivalent to

$$\frac{\partial n}{\partial t} + \frac{\partial (n v_i)}{\partial x_i} = 0. \tag{B.2}$$

This is Eq. (A.3) without the collision term.

B.2 Momentum equation

The rate of increase of momentum inside dV is equal to the rate of momentum in minus the rate of momentum out, by momentum advection and molecular transport, plus external forces on the fluid. Considering the momentum as $\vec{p} = M\vec{v}$, this can be written as

$$\begin{aligned}
\frac{\partial \vec{p}}{\partial t} &= n m_e \vec{v} v_1|_{x_1} dx_2 dx_3 - n m_e \vec{v} v_1|_{x_1+dx_1} dx_2 dx_3 \\
&+ n m_e \vec{v} v_2|_{x_2} dx_1 dx_3 - n m_e \vec{v} v_2|_{x_2+dx_2} dx_1 dx_3 + n m_e \vec{v} v_3|_{x_3} dx_1 dx_2 \\
&- n m_e \vec{v} v_3|_{x_3+dx_3} dx_1 dx_2 + n k_B T_e|_{x_1} dx_2 dx_3 - n k_B T_e|_{x_1+dx_1} dx_2 dx_3 \\
&+ n k_B T_e|_{x_2} dx_1 dx_3 - n k_B T_e|_{x_2+dx_2} dx_1 dx_3 + n k_B T_e|_{x_3} dx_1 dx_2 \\
&- n k_B T_e|_{x_3+dx_3} dx_1 dx_2 - ne(\vec{\mathcal{E}} + \vec{v} \times \vec{B}) dV.
\end{aligned} \tag{B.3}$$

By using a Taylor series approximation

$$n m_e \vec{v} v_j|_{x_j+dx_j} dx_i dx_k = n m_e \vec{v} v_j|_{x_j} dx_i dx_k + \frac{\partial (n m_e \vec{v} v_j)}{\partial x_j} dx_j dx_i dx_k,$$

$$nk_BT_e|_{x_j+dx_j}dx_idx_k = nk_BT_e|_{x_j}dx_idx_k + \frac{\partial(nk_BT_e)}{\partial x_j}dx_jdx_idx_k,$$

then Eq. (B.3) can be written as

$$\vec{v}\frac{\partial n}{\partial t}m_edV + n\frac{\partial \vec{v}}{\partial t}m_edV = -ne(\vec{\mathcal{E}} + \vec{v}\times\vec{B})dV - \frac{\partial(nm_e\vec{v}v_i)}{\partial x_i}dV - \nabla(nk_BT_e)dV.$$

By using Eq. (B.2), we get

$$-\vec{v}\frac{\partial(nv_i)}{\partial x_i} + n\frac{\partial\vec{v}}{\partial t} = -\frac{n}{m_e}e(\vec{\mathcal{E}} + \vec{v}\times\vec{B}) - \frac{\partial(nv_i)}{\partial x_i}\vec{v} - \frac{\partial\vec{v}}{\partial x_i}nv_i - \frac{1}{m_e}\frac{\partial(nk_BT_e)}{\partial x_j},$$

which is equivalent to

$$\frac{\partial v_j}{\partial t} + v_i\frac{\partial v_j}{\partial x_i} = -\frac{e}{m_e}(\vec{\mathcal{E}}_j + \varepsilon_{ikj}v_iB_k) - \frac{1}{nm_e}\frac{\partial(nk_BT_e)}{\partial x_j}. \tag{B.4}$$

This is Eq. (A.4) without the collision term.

B.3 Energy equation

The rate of increase of energy inside dV is equal to the rate of energy in minus the energy out as result of energy advection, work done by pressure by the surroundings and external forces, and heat transfer. Considering the energy as $EdV = (\frac{1}{2}nm_ev_iv_i + \frac{3}{2}nk_BT_e)dV$, this can be written as

$$\begin{aligned}\frac{\partial E}{\partial t}dV &= Ev_1|_{x_1}dx_2dx_3 - Ev_1|_{x_1+dx_1}dx_2dx_3 + Ev_2|_{x_2}dx_1dx_3\\ &- Ev_2|_{x_2+dx_2}dx_1dx_3 + Ev_3|_{x_3}dx_1dx_2 - Ev_3|_{x_3+dx_3}dx_1dx_2\\ &+ nk_BT_ev_1|_{x_1}dx_2dx_3 - nk_BT_ev_1|_{x_1+dx_1}dx_2dx_3 + nk_BT_ev_2|_{x_2}dx_1dx_3\end{aligned}$$

$$
\begin{aligned}
&- nk_BT_ev_2|_{x_2+dx_2}dx_1dx_3 + nk_BT_ev_3|_{x_3}dx_1dx_2 - nk_BT_ev_3|_{x_3+dx_3}dx_1dx_2 \\
&- ne(\vec{\mathcal{E}} + \vec{v} \times \vec{B})_1 v_1 dV - ne(\vec{\mathcal{E}} + \vec{v} \times \vec{B})_2 v_2 dV - ne(\vec{\mathcal{E}} + \vec{v} \times \vec{B})_3 v_3 dV \\
&+ q_1|_{x_1}dx_2dx_3 - q_1|_{x_1+dx_1}dx_2dx_3 + q_2|_{x_2}dx_1dx_3 - q_2|_{x_2+dx_2}dx_1dx_3 \\
&+ q_3|_{x_3}dx_1dx_2 - q_3|_{x_3+dx_3}dx_1dx_2. \qquad \text{(B.5)}
\end{aligned}
$$

By using a Taylor series approximation as follows

$$Ev_j|_{x_j+dx_j}dx_idx_k = Ev_j|_{x_j}dx_idx_k + \frac{\partial(Ev_j)}{\partial x_j}dx_jdx_idx_k, \qquad \text{(B.6)}$$

$$nk_BT_ev_j|_{x_j+dx_j}dx_idx_k = nk_BT_ev_j|_{x_j}dx_idx_k + \frac{\partial(nk_BT_ev_j)}{\partial x_j}dx_jdx_idx_k, \qquad \text{(B.7)}$$

$$q_j|_{x_j+dx_j}dx_idx_k = q_j|_{x_j}dx_idx_k + \frac{\partial(q_j)}{\partial x_j}dx_jdx_idx_k, \qquad \text{(B.8)}$$

then Eq. (B.5) can be written as

$$\frac{\partial E}{\partial t}dV = -\frac{\partial(Ev_i)}{\partial x_i}dV - \frac{\partial(nk_BT_ev_i)}{\partial x_i}dV - ne\vec{\mathcal{E}} \cdot \vec{v}dV - \frac{\partial(q_i)}{\partial x_i}dV,$$

which is equivalent to

$$\frac{\partial E}{\partial t} + \frac{\partial(Ev_i)}{\partial x_i} + \frac{\partial(nk_BT_ev_i)}{\partial x_i} + ne\vec{\mathcal{E}} \cdot \vec{v} + \frac{\partial(q_i)}{\partial x_i} = 0. \qquad \text{(B.9)}$$

This is Eq. (A.6) without the collision term.

BIBLIOGRAPHY

1. G.B. Schubauer and H.K. Skramstad. Laminar-boundary-layer oscillations and transition on a flat plate. *National Advisory Committee for Aeronautics*, Report No. 909:327–357, 1943.

2. P.G. Drazin. *Introduction to Hydrodynamic Stability*. Cambridge University Press, Cambridge, UK, 2002.

3. R. Betchov and W.O. Criminale. *Stability of Parallel Flows*. Academic Press, New York, 1967.

4. S. Chandrasekhar. *Hydrodynamic and Hydromagnetic Stability*. Oxford University Press, Oxford, UK, 1961.

5. L. Zommer, B. Lesiak, A. Jablonski, G. Gergely, M. Menyhard, A. Sulyok, and S. Gurban. Determination of the inelastic mean free path of electrons in GaAs and InP after surface cleaning by ion bombardment using elastic peak electron spectroscopy. *Journal of Electron Spectroscopy and Related Phenomena*, 87(3):177–185, 1998.

6. J. Roig, D. Flores, J. Urresti, S. Hidalgo, and J. Rebollo. Modeling of non-uniform heat generation in LDMOS transistors. *Solid State Electronics*, 49(1):77–84, 2005.

7. D. Li, S. Huxtable, A. Abramson, and A. Majumdar. Thermal transport in nanostructured solid-state cooling devices. *Journal of Heat Transfer*, 127:108–114, 2005.

8. P.G. Sverdrup, S. Sinha, M. Ashegui, S. Uma, and K.E. Goodson. Measurement of ballistic phonon conduction near hotspots in silicon. *Applied Physics Letters*, 78(21):3331–3333, 2001.

9. S. Sinha, P.K. Schelling, S.R. Phillpot, and K.E. Goodson. Scattering of g-process longitudinal optical phonons at hotspots in silicon. *Journal of Applied Physics*, 97:023702–1–023702–9, 2005.

10. A. Majumdar, K. Fushinobu, and K. Hijikata. Effect of gate voltage on hot-electron and hot-phonon interaction and transport in a submicrometer transistor. *Journal of Applied Physics*, 77(12):6686–6694, 1995.

11. J. Lai and A. Majumdar. Concurrent thermal and electrical modeling of sub-micrometer silicon devices. *Journal of Applied Physics*, 79(9):7353–7361, 1996.

12. A. Raman, D.G. Walker, and T.S. Fisher. Simulation of nonequilibrium thermal effects in power LDMOS transistors. *Solid-State Electronics*, 47:1265–1273, 2003.

13. A.W. Smith and K.F. Brennan. Hydrodynamic simulation of semiconductor devices. *Progress in Quantum Electronics*, 21(4):293–360, 1998.

14. A. Rangel-Huerta and R.M. Velasco. Kinetic model of thermotransport in semiconductors. *Physica A*, 308:161–178, 2002.

15. L. Ballestra, S. Micheletti, and R. Sacco. Semiconductor device simulation using a viscous-hydrodynamic model. *Computer Methods in Applied Mechanics Engineering*, 191:5447–5466, 2002.

16. A. Aste and R. Vahldieck. Time-domain simulation of the full hydrodynamic model. *International Journal of Numerical Modelling: Electronic Networks, Devices and Fields*, 16:161–174, 2003.

17. L. Ballestra and R. Sacco. Numerical problems in semiconductor simulation using the hydrodynamic model: a second-order finite difference scheme. *Journal of Computational Physics*, 195:320–340, 2004.

18. A. Rangel-Huerta, R.M. Velasco, and M.A. Rodríguez-Meza. Kinetic theory of thermotransport of degenerate polar semiconductor electrons. *Physica A*, 349:202–220, 2005.

19. A. Aste, R. Vahldieck, and M. Rohner. Full hydrodynamic simulation of GaAs MESFETs. *International Journal of Numerical Modelling: Electronic Networks, Devices and Fields*, 17:43–59, 2004.

20. J.C. Cao and X.L. Lei. Hydrodynamic balance-equation analysis of spatiotemporal domains and negative differential conductance in a voltage-biased GaAs superlattice. *Physical Review B*, 59(3):2199–2206, 1999.

21. X.L. Lei and H.L. Cui. Suppression of absolute instability by elastic scattering in semiconductor superlattices. *Journal of Physics: Condensed Matter*, 9(23):4853–4861, 1997.

22. K. Blotekjaer. Transport equations for electrons in two-valley semiconductors. *IEEE Transactions on Electron Devices*, 17(1):38–47, 1970.

23. K. Fushinobu, A. Majumdar, and K. Hijikata. Heat generation and transport in submicron semiconductor devices. *Journal of Heat Transfer*, 117:25–31, 1995.

24. S. Mazumder and A. Majumdar. Monte Carlo study of phonon transport in solid thin films including dispersion and polarization. *Journal of Heat Transfer*, 123:749–759, 2001.

25. A. Abramson, C. Tien, and A. Majumdar. Interface and strain effects on the thermal conductivity of heterostructures: A molecular dynamics study. *Journal of Heat Transfer*, 124:963–970, 2002.

26. J.Y. Murthy and S.R. Mathur. Computation of sub-micron thermal transport using an unstructured finite volume method. *Journal of Heat Transfer*, 124:1176–1181, 2002.

27. A. Majumdar. Thermal microscopy and heat generation in electronic devices. *Microelectronics Reliability*, 38(4):559–565, 1998.

28. G.D. Mahan and F. Claro. Nonlocal theory of thermal conductivity. *Physical Review B*, 38(3):1963–1969, 1988.

29. F. Claro and G.D. Mahan. Transient heat transport in solids. *Journal of Applied Physics*, 66(9):4213–4217, 1989.

30. M. Galler and F. Schürrer. A direct multigroup-WENO solver for the 2D non-stationary Boltzmann-Poisson system for GaAs devices: GaAs-MESFET. *Journal of Computational Physics*, 212:778–797, 2006.

31. S. Yang and Y. Yu. Temperature dependence of the conductivity of an electronic crystal. *Physical Review B*, 69:233307–1–233307–3, 2004.

32. K. Bertilsson, C. Harris, and H. Nilsson. Calculation of lattice heating in SiC RF power devices. *Solid-State Electronics*, 48:2103–2107, 2004.

33. Z. Ikonic, R.W. Kelsall, and P. Harrison. Monte Carlo simulations of hole dynamics in SiGe/Si terahertz quantum-cascade structures. *Physical Review B*, 69:235308–1–235308–9, 2004.

34. M.S. Kushwaha and P. Vasilopoulos. Current instability in field-effect transistors: influence of magnetic field and collisions. *Journal of Physics:Condensed Matter*, 13(44):10105–10116, 2001.

35. M.S. Kushwaha and P. Vasilopoulos. Influence of a magnetic field on the current instability in a ballistic field-effect transistor. *Physical Review B*, 64(12):125320–1–125320–5, 2001.

36. M.S. Kushwaha. Resonant response of a field-effect transistor to an alternate current signal. *Applied Physics Letters*, 85(6):1048–1050, 2004.

37. Frank J. Blatt. *Physics of Electronic Conduction in Solids*. McGraw-Hill, New York, 1968.

38. C.L. Collins and P.Y. Yu. Generation of nonequilibrium optical phonons in GaAs and their application in studying intervalley electron-phonon scattering. *Physical Review B*, 30(8):4501–4514, 1984.

39. L.G.C. Rego and A.C.S. Algarte. Mechanism for LO-phonon temperature overshoot in GaAs. *Physical Review B*, 49(11):7257–7261, 1994.

40. C.-L. Tien, A. Majumdar, and F.M. Gerner. *Microscale Energy Transport*. Taylor & Francis, Washington, DC, 1998.

41. E. Pop, S. Sinha, and K.E. Goodson. Monte Carlo modeling of heat generation in electronic nanostructures. In *ASME International Mechanical Engineering Congress and Exposition*, pages 1–6, November 2002.

42. Y. Li and S. Yu. A parallel adaptive finite volume method for nanoscale double-gate MOSFETs simulation. *Journal of Computational and Applied Mathematics*, 175(1):87–99, 2005.

43. S. Ren, W. Cheng, and P. Yu. Microscopic investigation of phonon modes in SiGe alloy nanocrystals. *Physical Review B*, 69:235327–1–235327–8, 2004.

44. Y.S. Ju and K.E. Goodson. Phonon scattering in silicon films with thickness of order 100nm. *Applied Physics Letters*, 74(20):3005–3007, 1999.

45. Y. Chen, D. Li, J.R. Lukes, and A. Majumdar. Monte Carlo simulation of silicon nanowire thermal conductivity. *Journal of Heat Transfer*, 127:1129–1137, 2005.

46. A. Majumdar and P. Reddy. Role of electron-phonon coupling in thermal conductance of metal-nonmetal interfaces. *Applied Physics Letters*, 84(23):4768–4770, 2004.

47. N. Mingo, L. Yang, D. Li, and A. Majumdar. Predicting the thermal conductivity of Si and Ge nanowires. *Nano Letters*, 3(12):1713–1716, 2003.

48. D.G. Cahill, W.K. Ford, K.E. Goodson, G.D. Mahan, A. Majumdar, H.J. Maris, R. Merlin, and S.R. Phillpot. Nanoscale thermal transport. *Journal of Applied Physics*, 93(2):793–818, 2003.

49. S. Sinha and K.E. Goodson. Review: Multiscale thermal modeling in nanoelectronics. *International Journal for Multiscale Computational Engineering*, 3(1):107–133, 2005.

50. L.-M. Yeh. Well-posedness of the hydrodynamic model for semiconductors. *Mathematical Methods in the Applied Sciences*, 19:1489–1507, 1996.

51. L.-M. Yeh. Subsonic solutions of hydrodynamic model for semiconductors. *Mathematical Methods in the Applied Sciences*, 20:1389–1410, 1997.

52. W. Fang and K. Ito. Steady-state solutions of a one-dimensional hydrodynamic model for semiconductors. *Journal of Differential Equations*, 133:224–244, 1997.

53. P. Amster, M.P. Beccar Varela, A. Jungel, and M.C. Mariani. Subsonic solutions to a one-dimensional non-isentropic hydrodynamic model for semiconductors. *Journal of Mathematical Analysis and Applications*, 258:52–62, 2001.

54. Y. Li. Asymptotic profile in a one-dimensional steady-state nonisentropic hydrodynamic model for semiconductors. *Journal of Mathematical Analysis and Applications*, 325(2):949–967, 2007.

55. K. Mohseni, A. Shakouri, R.J. Ranm, and M.C. Abraham. Electron vortices in semiconductors devices. *Physics of Fluids*, 17(10):100602–1–100602–7, 2005.

56. C.L. Gardner. Numerical simulation of a steady-state electron shock wave in a submicrometer semiconductor device. *IEEE Transactions on Electron Devices*, 38(2):392–398, 1991.

57. C.L. Gardner, J.W. Jerome, and D.J. Rose. Numerical methods for the hydrodynamic device model: subsonic flow. *IEEE Transactions on Computer-Aided Design*, 8(5):501–507, 1989.

58. R. D'Agosta and M.Di Ventra. Hydrodynamic approach to transport and turbulence in nanoscale conductors. *Journal of Physics Condensed Matter*, 18:11059–11065, 2006.

59. Boris M. Smirnov. *Physics of Ionized Gases*. John Wiley & Sons, New York, 2001.

60. W.B. Colson, E.D. Johnson, M.J. Kelly, and A.H. Schwettman. Putting free-electron lasers to work. *Physics Today*, 55(1):35–41, 2002.

61. G.L. Carr, M.C. Martin, W.R. McKinney, K. Jordan, G.R. Neil, and G.P. Williams. High-power terahertz radiation from relativistic electrons. *Nature*, 420:153–156, 2002.

62. R. Köhler, A. Tredicucci, F. Beltram, H.E. Beere, E.H. Linfield, A.G. Davies, D.A. Ritchie, R.C. Iotti, and F. Rossi. Terahertz semiconductor-heterostructure laser. *Nature*, 417:156–159, 2002.

63. M. Rodwell, M. Urteaga, Y. Betser, T. Mathew, P. Krishnan, D. Scott, S. Jaganathan, D. Mensa, J. Guthrie, R. Pullela, Q. Lee, B. Agarwal, U. Bhattacharya, and S. Long. Scaling of InGaAsInAlAs HBTs for high speed mixed-signal and mm-wave ICs. *International Journal of High Speed Electronics and Systems*, 11(1):159–216, 2001.

64. M. Dyakonov and M.S. Shur. Shallow water analogy for a ballistic field effect transistor: New mechanism of plasma wave generation by dc current. *Physical Review Letters*, 71(15):2465–2468, 1993.

65. F.J. Crowne. Contact boundary conditions and the Dyakonov-Shur instability in high electron mobility transistors. *Journal of Applied Physics*, 82(3):1242–1254, 1997.

66. F.J. Crowne. Dyakonov-Shur plasma excitations in the channel of a real high-electron mobility transistor. *Journal of Applied Physics*, 87(11):8056–8063, 2000.

67. F.J. Crowne. Microwave response of a high electron mobility transistor in the presence of a Dyakonov-Shur instability. *Journal of Applied Physics*, 91(8):5377–5383, 2002.

68. W. Calderón-Muñoz, M. Sen, and D. Jena. Hydrodynamic instability of one-dimensional electron flow in ungated semiconductors. *Journal of Applied Physics*, 102(2):023703–1–023703–8, 2007.

69. P. Bakshi and K. Kempa. Current driven plasma instabilities in lower dimensional systems. *Superlattices and Microstructures*, 17(4):363–372, 1995.

70. M. Dyakonov and M.S. Shur. Choking of electron flow: A mechanism of current saturation in field-effect transistors. *Physical Review B*, 51(20):14 341–14 345, 1995.

71. A.P. Dmitriev, A.S. Furman, V.Yu. Kachorovskii, G.G. Samsonidze, and Ge.G. Samsonidze. Numerical study of the current instability in a two-dimensional electron fluid. *Physical Review B*, 55(16):10 319–10 325, 1997.

72. M. Dyakonov and M.S. Shur. Current instability and plasma waves generation in ungated two-dimensional electron layers. *Applied Physical Letters*, 87(11):111501, 2005.

73. M.I. Dyakonov. Boundary instability of a two-dimensional electron fluid. *Semiconductors*, 42(8):984–988, 2008.

74. S. Rudin, G. Samsonidze, and F. Crowne. Nonlinear response of two-dimensional electron plasmas in the conduction channels of field effect transistor structures. *Journal of Applied Physics*, 86(4):2083–2088, 1999.

75. V. Ryzhii, A. Satou, and M.S. Shur. Transit-time mechanism of plasma instability in high electron mobility transistors. *Physica Status Solidi A*, 202(10):R113–R115, 2005.

76. V.V. Popov, O.V. Polischuk, and M.S. Shur. Resonant excitation of plasma oscillations in a partially gated two-dimensional electron layer. *Journal of Applied Physics*, 98(3):033510, 2005.

77. A. Dmitriev and M.S. Shur. Plasma oscillations of two-dimensional electron stripe. *Applied Physics Letters*, 87(24):243514, 2005.

78. A.V. Gorbatyuk and F.J. Niedernostheide. Spatial current-density instabilities in multilayered semiconductor structures. *Physical Review B*, 65(24):245318, 2002.

79. A.A. Bulgakov and O.V. Shramkova. Instability of drift waves in two-component solid-state plasma. *Electronic and Optical Properties of Semiconductors*, 39(9):1007–1012, 2005.

80. S. Hoffmann, X. Luo, and M. Hofmann. Bandwidth limitations of two-colour diode lasers for direct terahertz emission. *Electronics Letters*, 42(12), 2006.

81. W. Knap, F. Teppe, Y. Meziani, N. Dyakonova, J. Lusakowski, F. Boeuf, T. Skotnicki, D. Maude, S. Rumyantsev, and M.S. Shur. Plasma wave detection of sub-terahertz and terahertz radiation by silicon field effect transistors. *Applied Physics Letters*, 85(4):675–677, 2004.

82. J. Lusakowski, F. Teppe, N. Dyakonova, Y. Meziani, W. Knap, T. Parenty, S. Bollaert, A. Cappy, V. Popov, and M.S. Shur. Terahertz generation by plasma waves in nanometer gate high electron mobility transistors. *Physica Status Solidi A*, 202(4):656–659, 2005.

83. N. Pala, E. Teppe, D. Veksler, Y. Deng, M.S. Shur, and R. Gaska. Nonresonant detection of terahertz radiation by silicon-on-insulator MOSFETs. *Electronics Letters*, 41(7), 2005.

84. D. Veksler, F. Teppe, A. Dmitriev, V.Yu. Kachorovski, W. Knap, and M.S. Shur. Detection of terahertz radiation in gated two-dimensional structures governed by dc current. *Physical Review B*, 73(12):125328–1–125328–10, 2006.

85. J. Lusakowski, W. Knap, N. Dyakonova, L. Varani, J. Mateos, T. Gonzalez, Y. Roelens, S. Bollaert, A. Cappy, and K. Karpierz. Voltage tuneable terahertz emission from a ballistic nanometer InGaAs/InAlAs transistor. *Journal of Applied Physics*, 97(6):064307, 2005.

86. N. Dyakonova, A. Fatimy, J. Lusakowski, W. Knap, M.I. Dyakonov, M.-A. Poisson, E. Morvan, S. Bollaert, A. Shchepetov, Y. Roelens, Ch. Gaquiere, D. Theron, and A. Cappy. Room-temperature terahertz emission from nanometer field-effect transistors. *Applied Physics Letters*, 88(14):141906, 2006.

87. Y.Q. Deng, R. Kersting, V. Roytburd, J.Z. Xu, R. Ascazubi, K. Liu, X.C. Zhang, and M.S. Shur. Spectrum determination of terahertz sources using Fabry-Perot interferometer and bolometer detector. *International Journal of Infrared and Millimeter Waves*, 25(2):215–228, 2004.

88. J. Callaway. Model for lattice thermal conductivity at low temperatures. *Physical Review*, 113(4):1046–1051, 1959.

89. M.G. Holland. Analysis of lattice thermal conductivity. *Physical Review*, 132(6):2461–2471, 1963.

90. J.S. Dugdale and D.K.C. MacDonald. Lattice thermal conductivity. *Physical Review*, 98(6):1751–1752, 1955.

91. G. Baccarani and M.R. Wordeman. An investigation of steady-state velocity overshoot in silicon. *Solid-State Electronics*, 28(4):407–416, 1985.

92. R.M. Corless, G.H. Gonnet, D.E.G. Hare, D.J. Jeffrey, and D.E. Knuth. On the Lambert W function. *Advances in Computational Mathematics*, 5(4):329–359, 1996.

93. R.M. Corless, D.J. Jeffrey, and D.E. Knuth. A sequence of series for the Lambert W function. *Proceedings of International Symposium on Algorithms and Computation*, pages 197–204, 1997.

94. O. Vatel and M. Tanimoto. Kelvin probe force microscopy for potential distribution measurement of semiconductor devices. *Journal of Applied Physics*, 77(6):2358–2362, 1995.

95. D.S.H. Charrier, M. Kemerink, B.E. Smalbrugge, T. de Vries, and R.A.J. Janssen. Real versus measured surface potentials in scanning Kelvin probe microscopy. *American Chemical Society NANO*, 2(4):622–626, 2008.

96. F.J. Solorio and M. Sen. Linear stability of a cylindrical falling film. *Journal of Fluid Mechanics*, 183:365–377, 1987.

97. A. Quarteroni, R. Sacco, and F. Saleri. *Numerical Mathematics.* Springer, New York, 2000.

98. W.J. Minkowycz, E.M. Sparrow, G.E. Schneider, and R.H. Pletcher. *Handbook of Numerical Heat Transfer.* John Wiley & Sons, Inc., New York, 1988.

99. R. A. Höpfel, J. Shah, P. A. Wolff, and A. C. Gossard. Negative absolute mobility of minority electrons in GaAs quantum wells. *Physical Review Letters*, 56(25):2736–2739, 1986.

100. R. M. Abrarov, E. Ya. Sherman, and J.E. Sipe. Hydrodynamic model for relaxation of optically injected currents in quantum wells. *Applied Physics Letters*, 91(23):232113–1–232113–3, 2007.

101. E. Ta. Sherman, R. M. Abrarov, and J.E. Sipe. Dynamics of optically injected two-dimensional currents. *Journal of Applied Physics*, 104(10):103701–1–103701–11, 2008.

102. J. Nelson. *The Physics of Solar Cells.* Imperial College Press, London, 2003.

103. J. He, M. Chan X. Xi, C. Hu, Y. Li, Z. Xing, and R. Huang. Linearly graded doping drift region: a novel lateral voltage-sustaining layer used for improvement of RESURF LDMOS transistor performances. *Semiconductor Science and Technology*, 17(7):721–727, 2002.

104. D. W. Jordan and P. Smith. *Nonlinear Ordinary Differential Equations. An Introduction to Dynamical Systems.* Oxford University Press, New York, 1999.

This document was prepared & typeset with LaTeX 2ε*, and formatted with* NDdiss2ε *classfile (v3.0[2005/07/27]) provided by Sameer Vijay.*